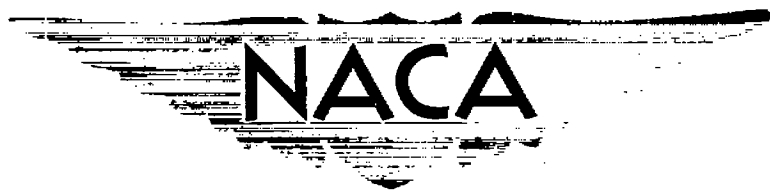


~~CONFIDENTIAL~~

Copy fi

RM A54F18



# RESEARCH MEMORANDUM

A COMPARISON OF THE LONGITUDINAL AERODYNAMIC  
CHARACTERISTICS AT MACH NUMBERS UP TO 0.94  
OF SWEPTBACK WINGS HAVING NACA 4-DIGIT  
OR NACA 64A THICKNESS DISTRIBUTIONS

By Fred B. Sutton and Jerald K. Dickson

**Ames Aeronautical Laboratory  
Moffett Field, Calif.**

**CLASSIFICATION CHANGED**

**UNCLASSIFIED**

卷之三

Atlas of the U.S.A.

LANGLEY AERONAUTICAL LABORATORY  
LIBRARY - 4454  
LANGLEY FIELD, VIRGINIA

By authority of R N-116 Date June 20, 1957  
7-2-57

CLASSIFIED DOCUMENT

This material contains information affecting the National Defense of the United States within the meaning of the espionage laws, Title 18, U.S.C. & Secs. 793 and 794, the transmission of which in any manner to an unauthorized person is prohibited by law.

# NATIONAL ADVISORY COMMITTEE FOR AERONAUTICS

## **WASHINGTON**

August 23, 1954

~~CONFIDENTIAL~~

## NATIONAL ADVISORY COMMITTEE FOR AERONAUTICS

RESEARCH MEMORANDUM

A COMPARISON OF THE LONGITUDINAL AERODYNAMIC  
CHARACTERISTICS AT MACH NUMBERS UP TO 0.94  
OF SWEPTBACK WINGS HAVING NACA 4-DIGIT  
OR NACA 64A THICKNESS DISTRIBUTIONS

By Fred B. Sutton and Jerald K. Dickson

SUMMARY

A wind-tunnel investigation has been conducted on two series of twisted and cambered wings, which were identical in all respects except wing section, to compare the effects of NACA 4-digit and NACA 64A chordwise distributions of thickness upon the longitudinal aerodynamic characteristics of the wings. The wings were tested at angles of sweepback of  $40^\circ$ ,  $45^\circ$ , and  $50^\circ$ . With a sweepback angle of  $40^\circ$ , the wings had geometric aspect ratios of 7; with  $45^\circ$  and  $50^\circ$  of sweepback, the aspect ratios were approximately 6 and 5, respectively. The tests were conducted through an angle-of-attack range at Reynolds numbers up to 10 million at a Mach number of 0.25, and at Mach numbers varying from 0.25 to 0.94 at a Reynolds number of 2 million.

At low speeds, the lift coefficient at which static longitudinal instability first became manifest was higher for the wings with 4-digit sections than for the wings with 64A sections. This effect of section was inconsistent with increasing Mach number. For Mach numbers near 0.80 and a wing sweepback of  $40^\circ$ , the lift coefficient for static instability was higher for the wing with 64A sections than for the wing with 4-digit sections. Increasing the angle of wing sweepback resulted in decreases in the lift coefficient at which the abrupt longitudinal instability occurred. At high Mach numbers this effect was larger for the wings with 64A sections than for the wings with 4-digit sections.

The wings with 4-digit sections had higher lift-curve slopes at lift coefficients greater than about 0.4 and higher maximum lifts than the corresponding wings with 64A sections. At subcritical speeds and at lift coefficients corresponding to the low-drag range for the 64A section, the wings employing these sections usually had less drag and higher lift-drag ratios than the wings with 4-digit sections. However, at higher lift coefficients and at supercritical speeds, the wings with 4-digit sections generally had less drag.

## INTRODUCTION

Commercial and military needs for long-range airplanes capable of relatively high subsonic speeds have stimulated much research aimed toward the development of suitable airframe configurations. Indications are that these performance requirements can be met best by airplanes with sweptback wings of relatively high aspect ratio.

A wing of this type has recently been investigated in the Ames 12-foot pressure wind tunnel and the results are presented in reference 1. In an effort to obtain good stability characteristics, the reference wing used NACA 4-digit sections in combination with moderate amounts of camber and twist. However, the data in references 2 and 3 indicate that in two-dimensional flow at speeds below the Mach number for drag divergence and at the lift coefficients required for cruising flight of long-range airplanes, cambered NACA 6-series wing sections (of laminar-flow type) have less drag than cambered NACA 4-digit sections. The two-dimensional data also show about equal drags for the two types of section at supercritical speeds and about equal Mach numbers for drag divergence.

In order to assess the anticipated drag penalties at subcritical speeds as well as the probable gains in stability resulting from the use of 4-digit wing sections with sweptback wings of relatively high aspect ratio, the present investigation was undertaken in the Ames 12-foot pressure wind tunnel. Two series of twisted and cambered wings, identical in all respects except the thickness distributions of the wing sections, were tested. One series employed NACA 4-digit sections and the other NACA 64A sections. The sweepback angle of the wings was varied from  $40^\circ$  to  $50^\circ$  to determine if the Mach number of drag divergence could be raised by increasing sweepback without introducing severe stability problems.

The experimental data include longitudinal aerodynamic characteristics for both series at sweepback angles of  $40^\circ$ ,  $45^\circ$ , and  $50^\circ$ . The tests covered a range of Mach numbers up to 0.94 at a constant Reynolds number of 2 million and a range of Reynolds numbers up to 10 million at low speeds.

## NOTATION

- A aspect ratio,  $\frac{b^2}{2S}$
- a mean line designation, fraction of chord over which design load is uniform
- b<sub>2</sub> wing semispan perpendicular to the plane of symmetry

$C_D$	drag coefficient, $\frac{\text{drag}}{qS}$
$C_{D_0}$	drag coefficient at zero lift
$C_{D_p}$	profile drag coefficient assuming elliptical span load distribution, $C_D = \frac{C_L^2}{\pi A}$
$C_L$	lift coefficient, $\frac{\text{lift}}{qS}$
$C_{L_i}$	inflection lift coefficient, lowest positive lift coefficient at which $\frac{dC_m}{dC_L} = 0$
$C_m$	pitching-moment coefficient about the quarter point of the wing mean aerodynamic chord, $\frac{\text{pitching moment}}{qSc}$
$c$	local wing chord parallel to the plane of symmetry
$c_{av}$	average wing chord, $\frac{2S}{b}$
$c'$	local wing chord perpendicular to the wing sweep axis
$\bar{c}$	mean aerodynamic chord, $\frac{\int_0^{b/2} c^2 dy}{\int_0^{b/2} c dy}$
$c_l$	section lift coefficient
$c_{l_i}$	design section lift coefficient
$\frac{L}{D}$	lift-drag ratio
$M$	free-stream Mach number
$q$	free-stream dynamic pressure
$R$	Reynolds number based on the mean aerodynamic chord
$S$	area of semispan wing
$t$	maximum thickness of section

- x distance from the intersection of the leading edges of the wings and the plane of symmetry to the moment center, measured parallel to free stream
- y lateral distance from the plane of symmetry
- $\alpha$  angle of attack, measured with respect to a reference plane through the leading edge and the root chord of the wing with  $40^\circ$  of sweepback  
(This reference plane was used for all wings.)
- $\Phi$  angle of twist, the angle between the local wing chord and a reference plane through the leading edge and the root chord of the wing with  $40^\circ$  of sweepback (positive for washin and measured in planes parallel to the plane of symmetry)
- $\eta$  fraction of semispan,  $\frac{y}{b/2}$
- $\Lambda$  angle of sweepback of the line through the quarter-chord points of the sections of the unswept wing panel
- $\lambda$  taper ratio,  $\frac{c_t}{c_r}$

#### Subscripts

- a additional
- b basic
- div divergence
- r wing root
- t wing tip

#### MODELS

The models used in this investigation consisted of two wings which differed only with respect to the basic thickness distributions used for the wing sections. One of the models used NACA 4-digit sections and the other employed NACA 64A sections. The basic thickness distributions were combined with an  $a = 0.8$  modified mean line having an ideal lift coefficient of 0.4 to form the sections perpendicular to the quarter-chord line of the unswept wing panels. The thickness-chord ratios of these sections varied from 14 percent at the root to 11 percent at the tip.

Dimensions of the wings are given in figure 1. The models were solid steel, and the surfaces were polished smooth. Their construction was such that the angle of sweepback could be adjusted to  $40^\circ$ ,  $45^\circ$ , or  $50^\circ$ . Interchangeable tip portions were used to maintain consistent tip shape and wing panel length. An aspect ratio of 7.0 was chosen for the wings with  $40^\circ$  of sweepback. This choice fixed the panel length of the wings and resulted in a structural aspect ratio ( $\frac{A_{geometric}}{\cos^2\Lambda}$ ) of 12. When the wings were swept to  $45^\circ$  and  $50^\circ$ , the panel length and structural aspect ratio were held constant and, consequently, the geometric aspect ratios decreased to approximately 6 and 5, respectively. To a first approximation, the wings with the various angles of sweepback may be regarded as having equal strength because of their identical structural aspect ratios. The models are regarded herein as six individual wings; the wings employing NACA 4-digit sections are hereinafter referred to as 4-digit wings and the wings using NACA 64A sections are called the 64A wings.

The wings had the same camber and spanwise distributions of twist and thickness ratio for the unswept panels as the wing of reference 1. These spanwise distributions of section twist and thickness ratio were selected to provide linear surface elements connecting points at equal percentages of the chords at all sections. Twist was introduced by rotating the streamwise sections of the wings with  $40^\circ$  of sweepback about the leading edges while maintaining the projected plan form. The variations of twist and thickness ratio along the semispan are shown in figure 1(b) for angles of sweepback of  $40^\circ$ ,  $45^\circ$ , and  $50^\circ$ . Basic and additional span load distributions, as calculated by the modified Falkner 1x19 method presented in reference 4, are presented in figure 2 for the three angles of sweepback. A photograph of one of the wings at  $50^\circ$  of sweepback is shown in figure 3.

#### CORRECTIONS TO DATA

The data have been corrected for constriction effects due to the presence of the tunnel walls, for tunnel-wall interference originating from lift on the wings, and for drag tares caused by aerodynamic forces on the turntable upon which the model was mounted.

The dynamic pressure was corrected for constriction effects due to the presence of the tunnel walls by the method of reference 5. These corrections and the corresponding corrections to the Mach number are listed in the following table:

Corrected Mach number	Uncorrected Mach number	$\frac{c_{corrected}}{c_{uncorrected}}$
0.165	0.165	1.001
.25	.250	1.001
.60	.599	1.002
.70	.699	1.002
.80	.798	1.003
.83	.827	1.004
.86	.856	1.005
.88	.875	1.006
.90	.895	1.007
.92	.913	1.008
.94	.929	1.009

Corrections for the effects of tunnel-wall interference originating from lift on the model were calculated by the method of reference 6. The corrections to the angle of attack and to the drag coefficient showed insignificant variations with Mach number. The corrections added to the data were as follows:

$$\Delta\alpha = 0.455 C_L$$

$$\Delta C_D = 0.00662 C_L^2$$

The correction to the pitching-moment coefficient had a significant variation with Mach number. The following corrections were added to the measured pitching-moment coefficients:

$$\Delta C_m = K C_L$$

where  $K$  is given in the following table:

Corrected Mach number	K
0.165	0.0025
.25	.0027
.60	.0038
.70	.0043
.80	.0049
.83	.0050
.86	.0053
.88	.0054
.90	.0056
.92	.0057
.94	.0059

Since the turntable upon which the model was mounted was directly connected to the balance system, a tare correction to drag was necessary. The drag force on the turntable with the model removed from the wind tunnel was measured and the tare correction was assumed to be equal to this measured drag.

Static loading of the wing of reference 1 indicated that the twist due to aeroelastic deformation was small. Since the wings used in the present investigation were stiffer than the reference wing due to their reduced aspect ratios and solid steel construction, it is believed that the effects of aeroelastic deformation are negligible. Hence, no corrections have been made to the data for these effects.

#### TESTS

The wings were investigated with sweepback angles of  $40^\circ$ ,  $45^\circ$ , and  $50^\circ$ . The lift, drag, and pitching moments were measured through an angle-of-attack range at Reynolds numbers from 2 million to 10 million at low Mach numbers and at Mach numbers from 0.25 to 0.94 at a Reynolds number of 2 million. Flow studies on the wings with  $40^\circ$  and  $50^\circ$  of sweepback were made through an angle-of-attack range at a Mach number of 0.165 and a Reynolds number of 8 million and at Mach numbers of 0.25, 0.80, and 0.90 at a Reynolds number of 2 million.

#### RESULTS AND DISCUSSION

Figures 4 to 24 compare the results of tests of the wings with  $40^\circ$ ,  $45^\circ$ , and  $50^\circ$  of sweepback. Figures 4 through 7 show the lift, drag, and pitching-moment coefficients, and the lift-drag ratios measured at low speed and at Reynolds numbers which varied from 2 million to 10 million. Summary plots showing the effects of Reynolds number on the characteristics of the wings at low speed are presented in figures 8 and 9.

Test results at Mach numbers from 0.25 to 0.94 at a constant Reynolds number of 2 million are presented in figures 10 through 13. The effects of Mach number on the longitudinal characteristics of the wings are summarized in figures 14 through 18.

Flow studies were made with tufts on the wings with  $40^\circ$  and  $50^\circ$  of sweepback. Interpretations of the flow studies are shown in figures 19 and 20. The effects of the tufts on the lift and pitching-moment characteristics of the wings are shown in figures 21 through 24.

Some of the data for the highest Mach numbers and angles of attack have been faired with dotted lines. This was done whenever the static

pressure on the tunnel wall opposite the upper surface of the wing indicated a local Mach number greater than 1.0. Under these conditions the wind tunnel may have been partially choked.

### Low-Speed Results

Lift.- The effects of wing section on the lift characteristics of the wings at low speeds are shown for several Reynolds numbers in figure 4. At most angles of sweepback and Reynolds numbers and at lift coefficients greater than about 0.4, the 4-digit wings had higher lift-curve slopes than the corresponding 64A wings. Higher maximum lift coefficients were indicated for 40° of sweepback for the 4-digit wing than for the 64A wing. Although maximum lift coefficient was not attained at higher angles of sweepback, the data indicate that this effect, although diminished, would also prevail at 45° and 50° of sweepback.

Pitching moment.- The effects of wing section on the pitching-moment characteristics of the wings at low speed are shown in figure 5. The inflection lift coefficients were usually higher for the 4-digit wings than for the 64A wings. (For convenience, the term, "inflection lift coefficient," is used to denote the lift coefficient at which static longitudinal instability first appeared. For the subject wings this was taken as the lowest lift coefficient at which  $dC_m/dC_L = 0$ .) This effect of section on the pitching-moment characteristics was relatively independent of wing sweepback. The superiority of the pitching-moment characteristics of the 4-digit wings at most angles of sweepback as compared to the 64A wings probably stems from the better lift characteristics of the 4-digit section in this speed range. It is believed that this was due to the comparatively large leading-edge radii of the 4-digit sections.

Figure 8 shows the variation with Reynolds number of the inflection lift coefficients for the wings at the various angles of sweepback. The inflection lift coefficients for all angles of sweepback increased with increasing Reynolds number; however, the effects of wing section on the variation of inflection lift coefficient with Reynolds number were small. Decreases in inflection lift coefficient as large as about 30 percent were indicated for the wings when the angle of sweepback was increased from 40° to 50°. It is interesting to apply simple sweep theory (ref. 7) to predict the onset of stalling over the outer portions of the wings and the consequent changes in inflection lift coefficients with increasing sweepback. The predicted values of inflection lift coefficient for the 45° and 50° wings

$$C_{L1}{}_{40^\circ} \frac{\cos^2 45^\circ}{\cos^2 40^\circ} \quad \text{and} \quad C_{L1}{}_{40^\circ} \frac{\cos^2 50^\circ}{\cos^2 40^\circ}$$

are in good agreement with the values measured at a Mach number of 0.25 and a Reynolds number of 8 million as may be seen from the results shown in the following table:

$\Lambda$	$C_{L_1}$			
	4-digit		64A	
	Measured	Predicted	Measured	Predicted
$40^\circ$	0.85	---	0.75	---
$45^\circ$	.76	0.72	.67	0.64
$50^\circ$	.61	.60	.53	.53

Drag and lift-drag ratios. - The effects of wing section on the drag characteristics of the wings at low speed are shown in figure 6 for several Reynolds numbers. At lift coefficients corresponding to the low-drag range for the 64A sections, the wings employing these sections usually had less drag for all the angles of sweepback than the wings using 4-digit sections. However, at the higher lift coefficients the 4-digit wings usually had less drag. These differences are best shown by figure 7 which presents the lift-drag ratios of the various wings as a function of lift coefficient. For lift coefficients between about 0.1 and 0.4, the lift-drag ratios of the 64A wings were usually higher than for the 4-digit wings. In the cases where this expected benefit is not achieved (fig. 7(c),  $R = 10$  million, for example), it is probable that the surface condition of the 64A wings had deteriorated to the extent that the expected chordwise extent of laminar flow was not realized. This is somewhat borne out by the shapes of the lift-drag-ratio curves which have considerably steeper peaks in those cases where substantial increments in maximum lift-drag ratios are achieved by the 64A wings. These data emphasize the importance of surface condition if the drag benefits of the 64A section are to be obtained.

The effects of Reynolds number on the drag due to lift,  $C_D - C_{D_0}$ , of the wings at the various angles of sweepback are shown in figure 9. Also shown in this figure are the theoretical induced drag coefficients,  $C_L^2/\pi A$ , for wings with elliptical span load distributions and having aspect ratios corresponding to those for the model wings. For most angles of wing sweepback and Reynolds numbers, the drag due to lift of the 4-digit wings compared more closely to the theoretical induced drag for elliptic loading than did the drag due to lift for the 64A wings. The drag due to lift for the wings compared less closely to the induced drag for elliptic loading when the angle of sweepback was increased. At a sweepback angle of  $40^\circ$  and a Reynolds number of 10 million, neither wing showed an abrupt increase in drag due to lift until lift coefficients greater than unity were attained. Increasing the sweepback angle from  $40^\circ$  to  $50^\circ$  at the same Reynolds number resulted in about a 25-percent reduction in the lift coefficient at which the abrupt increase in drag occurred. This effect of sweepback is merely another manifestation of the same separation phenomena

which caused the inflection lift coefficient to decrease with increasing sweepback. As was pointed out in the discussion of inflection lift coefficient, this effect can be predicted from application of simple sweep theory.

### High-Speed Results

The low-speed results which have just been discussed and the investigation reported in reference 8 have indicated the susceptibility of swept wings employing camber and twist to large effects of scale. It is likely that the test results at high speeds which are discussed in the following paragraphs may have been affected by the comparatively low Reynolds number (2 million) at which these data were obtained. While no prognostication is made herein as to the possible magnitude of this scale effect, caution should be exercised in applying these data to the prediction of the characteristics of full-scale wings.

Lift.- The lift characteristics of the wings at the various angles of sweepback are shown in figure 10 for Mach numbers ranging from 0.25 to 0.94 at a constant Reynolds number of 2 million. As was the case at low speed, higher lift-curve slopes at moderate lift coefficients were measured for the 4-digit wings than for the 64A wings. The effect of Mach number on the lift-curve slopes of the wings at lift coefficients of 0.2 and 0.4 is shown in figure 14. The inflection lift coefficient of the 64A wings was 0.4 or less over most of the range of Mach numbers at sweepback angles of 45° and 50°, indicating that flow separation had occurred on the outer portions of the wing spans. This flow separation was responsible for the low lift-curve slopes of these wings at the higher angles of sweepback and a lift coefficient of 0.4. The 4-digit wings usually reached slightly higher Mach numbers before abrupt losses of lift-curve slope occurred than did the 64A wings. The lift-curve slopes for both the 4-digit and the 64A wings decreased with increasing angle of sweepback. This was partly due to the accompanying reduction in aspect ratio.

Pitching moment.- Figure 11 shows the effect of wing section on the pitching-moment characteristics of the wings at Mach numbers from 0.25 to 0.94. The variations with Mach number of the inflection lift coefficients and the slopes of the pitching-moment curves are shown in figures 15 and 16, respectively. At the lower Mach numbers, higher inflection lift coefficients were obtained at all angles of sweepback for the 4-digit wings than for the 64A wings. With increasing Mach number and 40° or 45° of sweepback, the inflection lift coefficient gradually decreased for the 4-digit wings; whereas, for the 64A wing swept back 40° an over-all increase was indicated up to a Mach number of 0.80. At higher Mach numbers the inflection lift coefficients decreased. At Mach numbers near 0.80, the inflection lift coefficient for the 64A wing was higher than for the 4-digit wing but at higher speeds the effect was reversed. A similar

trend is shown for the 64A wing with  $45^\circ$  of sweepback except that the maximum inflection lift coefficient occurred at a Mach number of approximately 0.86 and equalled but never exceeded the inflection lift coefficient for the 4-digit wing. The effects of Mach number on the inflection lift coefficients of both wings when swept back  $50^\circ$  were comparatively small, the inflection lift coefficient for the 4-digit wing being considerably higher than that for the 64A wing throughout the range of Mach numbers. The flow studies presented in figure 19(c) indicate that the surprisingly high inflection lift coefficient for the 64A wing with  $40^\circ$  of sweepback at a Mach number of 0.80 was due to less flow separation on the 64A wing than on the 4-digit wing. This is also indicated by the more favorable lift and drag characteristics at this Mach number (0.80) for the 64A wing than for the 4-digit wing. Similar characteristics may be observed in the data for the wings with  $45^\circ$  of sweepback (fig. 11(b)) at Mach numbers of 0.83 and 0.86. These characteristics are barely discernible in the data for the wings with  $50^\circ$  of sweepback (fig. 11(c)) at Mach numbers of 0.90 and 0.92. The fact that the phenomena occurred at progressively higher Mach numbers as sweepback was increased indicates that it was probably connected with shock formation on the wing.

The data in figure 15 indicate that the decrease in inflection lift coefficient with increasing sweepback which was observed at low speeds occurred at all subcritical Mach numbers. However, the 64A wings were more affected in this respect than the 4-digit wings. This effect was greatest at a Mach number of 0.80 where decreases in inflection lift coefficient as large as 40 percent occurred when the angle of sweepback was increased from  $40^\circ$  to  $50^\circ$  for the 64A wings as compared to a decrease of approximately 12 percent for the 4-digit wings.

The effects of Mach number on the slopes of the pitching-moment curves (fig. 16) were small at low lift coefficients ( $C_L = 0.2$  or less) up to approximately the critical Mach number of the various configurations. At a lift coefficient of 0.4 and a sweepback angle of  $40^\circ$ , the effects of Mach number were similar for both wings; however, at the higher angles of sweepback and a lift coefficient of 0.4, the effects of Mach number became more pronounced and more varied for the 64A wings than for the 4-digit wings. This erratic behavior was mostly due to the low inflection lift coefficients (generally less than 0.4) of the 64A wings at these angles of sweepback. As previously mentioned, it is possible that the Reynolds number of these tests (2 million) was not high enough to preclude sizable dynamic scale effects in these results.

Drag and lift-drag ratios.— The drag characteristics of the wings with the various angles of sweepback are shown in figure 12. At Mach numbers below that for drag divergence ( $dC_D/dM = 0.10$ ) the effect of wing section on drag was similar to that measured at low speeds. At lift coefficients corresponding to the low-drag range for the 64A sections, the wings employing these sections usually had less drag at all angles of sweepback than the 4-digit wings except at supercritical speeds where the 4-digit wings

usually had less drag. The 64A wings had less drag than the 4-digit wings at practically all lift coefficients at Mach numbers of 0.80 and 0.83 for  $40^\circ$  of sweepback; at Mach numbers of 0.83, 0.86, and 0.88 for  $45^\circ$  of sweepback; and at Mach numbers of 0.88, 0.90, and 0.92 for  $50^\circ$  of sweepback. These effects are shown to best advantage in figure 13 which shows the lift-drag ratios of the various wings as a function of lift coefficient. It is believed that the drag advantages of the 64A wings at these particular Mach numbers stem from the separation phenomenon previously mentioned in the discussion of the pitching-moment characteristics. The higher lift-drag ratios of the 4-digit wings when compared with those for the 64A wings at some subcritical Mach numbers (Mach number of 0.80 at  $45^\circ$  of sweepback, for example) were probably a result of deterioration of the model surface which would affect the drag characteristics of the 64A wings more adversely than those of the 4-digit wings.

The effect of Mach number on drag coefficient at several lift coefficients is shown in figure 17 for the wings with  $40^\circ$ ,  $45^\circ$ , and  $50^\circ$  of sweepback. Drag divergence usually occurred at slightly higher Mach numbers for the 4-digit wings than for the 64A wings. However, at the Mach numbers of drag divergence and at the same angle of sweepback the 64A wings usually had lower drag than the 4-digit wings. The Mach numbers for drag divergence and the corresponding drag coefficients are shown for the wings at the various angles of sweepback in the following table:

$C_L$	$\Lambda = 40^\circ$				$\Lambda = 45^\circ$				$\Lambda = 50^\circ$			
	$M_{div}$		$C_{Ddiv}$		$M_{div}$		$C_{Ddiv}$		$M_{div}$		$C_{Ddiv}$	
	4-digit	64A	4-digit	64A	4-digit	64A	4-digit	64A	4-digit	64A	4-digit	64A
0.20	0.89	0.88	0.0096	0.0096	0.93	0.92	0.0108	0.0096	----	0.94	----	0.0100
.40	.86	.84	.0160	.0153	.88	.86	.0165	.0147	0.92	.91	0.0202	.0189
.50	.83	.81	.0214	.0191	.84	.85	.0224	.0208	.87	.90	.0285	.0286

The large increases of the drag coefficient for drag divergence with increasing sweepback at the higher lift coefficients were due to flow separation over the outer portions of the wings.

Figure 18 shows the variation with Mach number of maximum lift-drag ratio and the lift coefficient for maximum lift-drag ratio. The data in this figure and in figure 13 indicate that at subcritical speeds, the 64A wings had higher maximum lift-drag ratios than the 4-digit wings; however, at supercritical speeds and at  $40^\circ$  and  $45^\circ$  of sweepback the 4-digit wings had slightly higher maximum lift-drag ratios than the wings with 64A sections. Decreases in maximum lift-drag ratio with increasing angle of sweepback occurred at subcritical speeds for both wings.

It is of interest to note that increasing wing sweepback had only small effect on the maximum lift-drag ratios of the 4-digit wings at a Mach number of 0.90. It would appear that as the sweepback was increased at this Mach number, the drag decrease due to the increase in the Mach number for drag divergence was nullified by the increase in induced drag resulting from the lower aspect ratios which accompanied the increase in sweepback.

### Flow Studies

In an attempt to gain some insight into the separation occurring on the wings as affected by wing section, wing plan form, and test conditions, tuft studies were made on the wings at  $40^{\circ}$  and  $50^{\circ}$  of sweepback. The results of these studies are presented in figures 19 and 20.

Inasmuch as the addition of tufts to the wing surfaces affected the flow on the wings, the differences in separation due to wing section as shown by the results of the flow studies are probably somewhat obscured. However, as anticipated, it was indicated that the 64A wings were more prone to the leading-edge type of separation than the 4-digit wings, although this type of separation occurred on both the 4-digit and the 64A wings at the highest angle of sweepback. At low speeds, separation of the flow on the wings usually occurred less uniformly on the 64A wings than on the 4-digit wings. At Mach numbers of 0.80 and 0.90 and at angles of attack less than about  $8^{\circ}$ , the flow studies show that the effects of shock-induced separation are predominant on the wings. At  $40^{\circ}$  of sweepback and at a Mach number of 0.80 (fig. 19(c)) less separation was evident on the 64A wing than on the 4-digit wing. This reduced amount of separation is obviously the reason for the superiority of the 64A wing over the 4-digit wing previously noted at this Mach number and angle of sweepback in the discussion of the force data. The flow phenomena responsible for this effect is not known. With  $50^{\circ}$  of sweepback and at Mach numbers of 0.80 and 0.90, little difference was indicated by the tufts in the flow characteristics of the wings.

Lift and pitching-moment data measured with the tufts on the wings are compared in figures 21 through 24 with the previous results with aerodynamically smooth wings. This comparison indicated that the addition of tufts affected transition on the wings under some test conditions in such a way that the effective Reynolds numbers of the wings were probably increased. It is significant that the maximum lift coefficients attained by both the 4-digit and the 64A wings at an angle of sweepback of  $40^{\circ}$ , a Mach number of 0.25, and a Reynolds number of 2 million (fig. 21) were increased by the addition of tufts to values approaching those measured at the same angle of sweepback at a Mach number of 0.165 and a Reynolds number of 8 million. The inflection lift coefficients for both wings with  $40^{\circ}$  of sweepback and a Reynolds number of 2 million were also increased at all

Mach numbers by the addition of tufts. Although the addition of tufts had a large effect on the wings at  $40^{\circ}$  of sweepback, they had only small effect on the lift and pitching-moment characteristics of the wings at  $50^{\circ}$  of sweepback.

#### CONCLUSIONS

A wind-tunnel investigation has been made of twisted and cambered wings which were identical in all respects except wing section to compare the effects of 4-digit and 64A chordwise distributions of thickness upon the longitudinal aerodynamic characteristics of the wings. The wings were tested at angles of sweepback of  $40^{\circ}$ ,  $45^{\circ}$ , and  $50^{\circ}$ . The following conclusions were indicated:

1. At low speeds, the lift coefficient at which static longitudinal instability first became manifest was higher for the wings with 4-digit sections than for the wings with 64A sections.
2. This effect of section was inconsistent with increasing Mach number. For Mach numbers near 0.80 and a wing sweepback of  $40^{\circ}$ , the lift coefficient for static instability was higher for the wing with 64A sections than for the 4-digit wing.
3. Increasing the angle of wing sweepback resulted in decreases in the lift coefficient at which the abrupt longitudinal instability occurred, as would be predicted by simple sweep theory. At high Mach numbers this effect was larger for the wings with 64A sections than for the wings with 4-digit sections.
4. The wings with 4-digit sections had higher lift-curve slopes at lift coefficients greater than about 0.4 and higher maximum lifts than the corresponding wings with 64A sections.
5. At subcritical speeds and at lift coefficients corresponding to the low-drag range for the 64A section, the wings employing these sections usually had less drag and higher lift-drag ratios than the wings with 4-digit sections. However, at higher lift coefficients and at supercritical speeds, the wings with 4-digit sections generally had less drag.

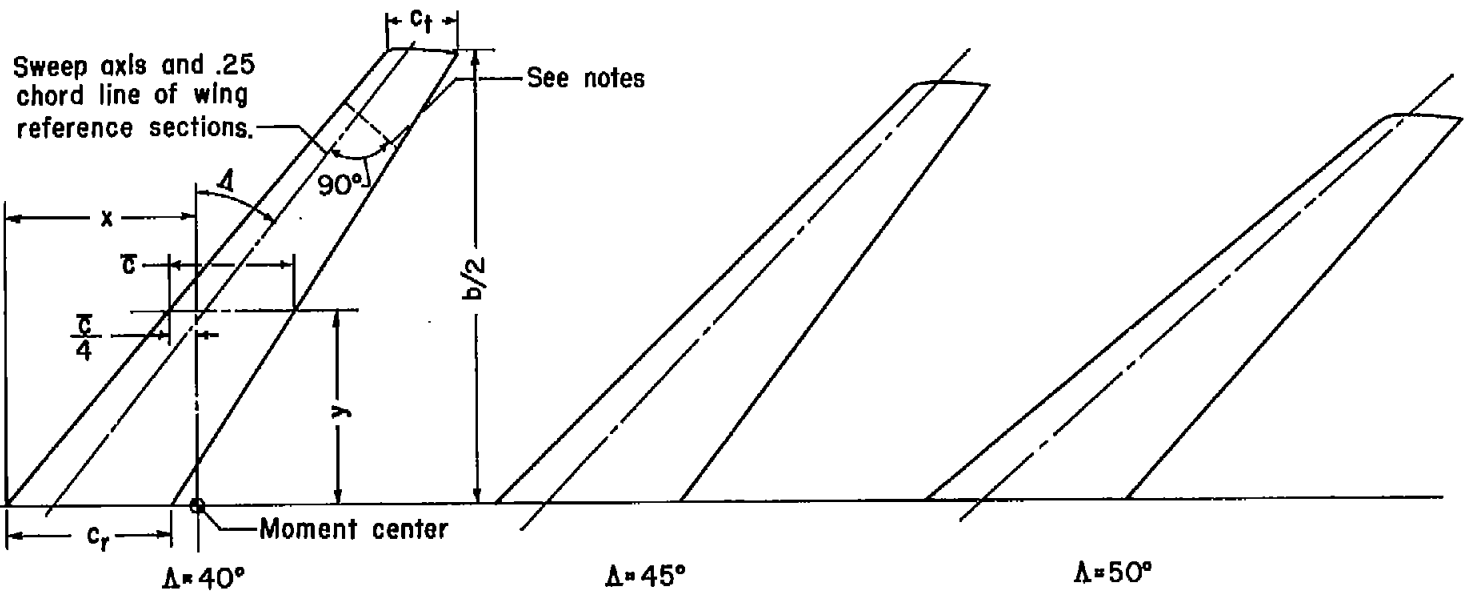
Ames Aeronautical Laboratory  
National Advisory Committee for Aeronautics  
Moffett Field, Calif., June 18, 1954

## REFERENCES

1. Edwards, George G., Tinling, Bruce E., and Ackerman, Arthur C.: The Longitudinal Characteristics at Mach Numbers up to 0.92 of a Cambered and Twisted Wing Having  $40^{\circ}$  of Sweepback and an Aspect Ratio of 10. NACA RM A52F18, 1952.
2. Summers, James L., and Treon, Stuart L.: The Effects of Amount and Type of Camber on the Variation With Mach Number of the Aerodynamic Characteristics of a 10-Percent-Thick NACA 64A-Series Airfoil Section. NACA TN 2096, 1950.
3. Nitzberg, Gerald E., Crandall, Stewart M., and Polentz, Perry P.: A Preliminary Investigation of the Usefulness of Camber in Obtaining Favorable Airfoil-Section Drag Characteristics at Supercritical Speeds. NACA RM A9G20, 1949.
4. Schneider, William C.: A Comparison of the Spanwise Loading Calculated by Various Methods With Experimental Loadings Obtained on a  $45^{\circ}$  Sweptback Wing of Aspect Ratio 8 at a Reynolds Number of  $4.0 \times 10^6$ . NACA RM L51G30, 1952.
5. Herriot, John G.: Blockage Corrections for Three-Dimensional-Flow Closed-Throat Wind Tunnels, With Consideration of the Effect of Compressibility. NACA Rep. 995, 1950. (Formerly NACA RM A7B28)
6. Sivells, James C., and Salmi, Rachel M.: Jet-Boundary Corrections for Complete and Semispan Swept Wings in Closed Circular Wind Tunnels. NACA TN 2454, 1951.
7. Jones, Robert T.: Effects of Sweep-Back on Boundary Layer and Separation. NACA Rep. 884, 1947.
8. Shibata, Harry H., Bandettini, Angelo, and Cleary, Joseph: An Investigation Throughout the Subsonic Speed Range of a Full-Span and a Semispan Model of a Plane Wing and of a Cambered and Twisted Wing, All Having  $45^{\circ}$  of Sweepback. NACA RM A52D01, 1952.

16

NACA RM A54F18



Wing	A	$\lambda$	$b/2$	$c_r$	$c_t$	$\bar{c}$	x	y	S/2	$a_r$ for $\alpha = 0^\circ$
a	7.00	0.4	54.610	22.290	8.916	16.558	25.348	23.404	5.917	$0^\circ$
b	6.03	0.4	50.408	23.900	9.560	17.755	27.755	21.604	5.857	$-0.05^\circ$
c	5.04	0.4	45.823	25.982	10.393	19.301	30.127	19.639	5.788	$-0.10^\circ$

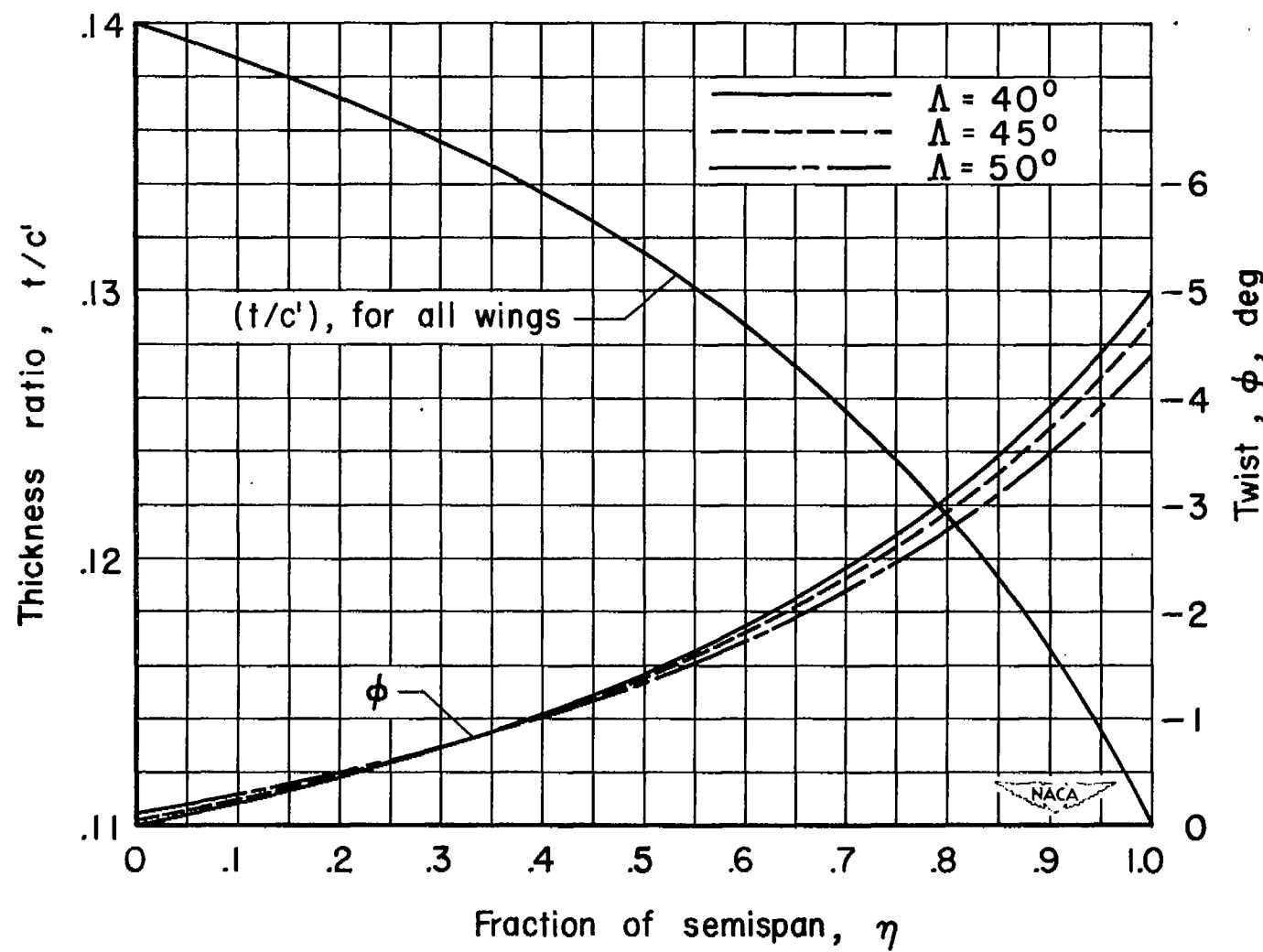


Notes:

- (1) Wing sections perpendicular to sweep axis have NACA 00XX or 64 A 0XX thickness distributions combined with an NACA  $\alpha = 0.8$  (modified) mean line,  $c_t = 0.4$ .
- (2) All dimensions in inches and areas in square feet.

(a) Dimensional details.

Figure 1.- Geometry of the wings.



(b) Distribution of twist and thickness ratio.

Figure 1.- Concluded.

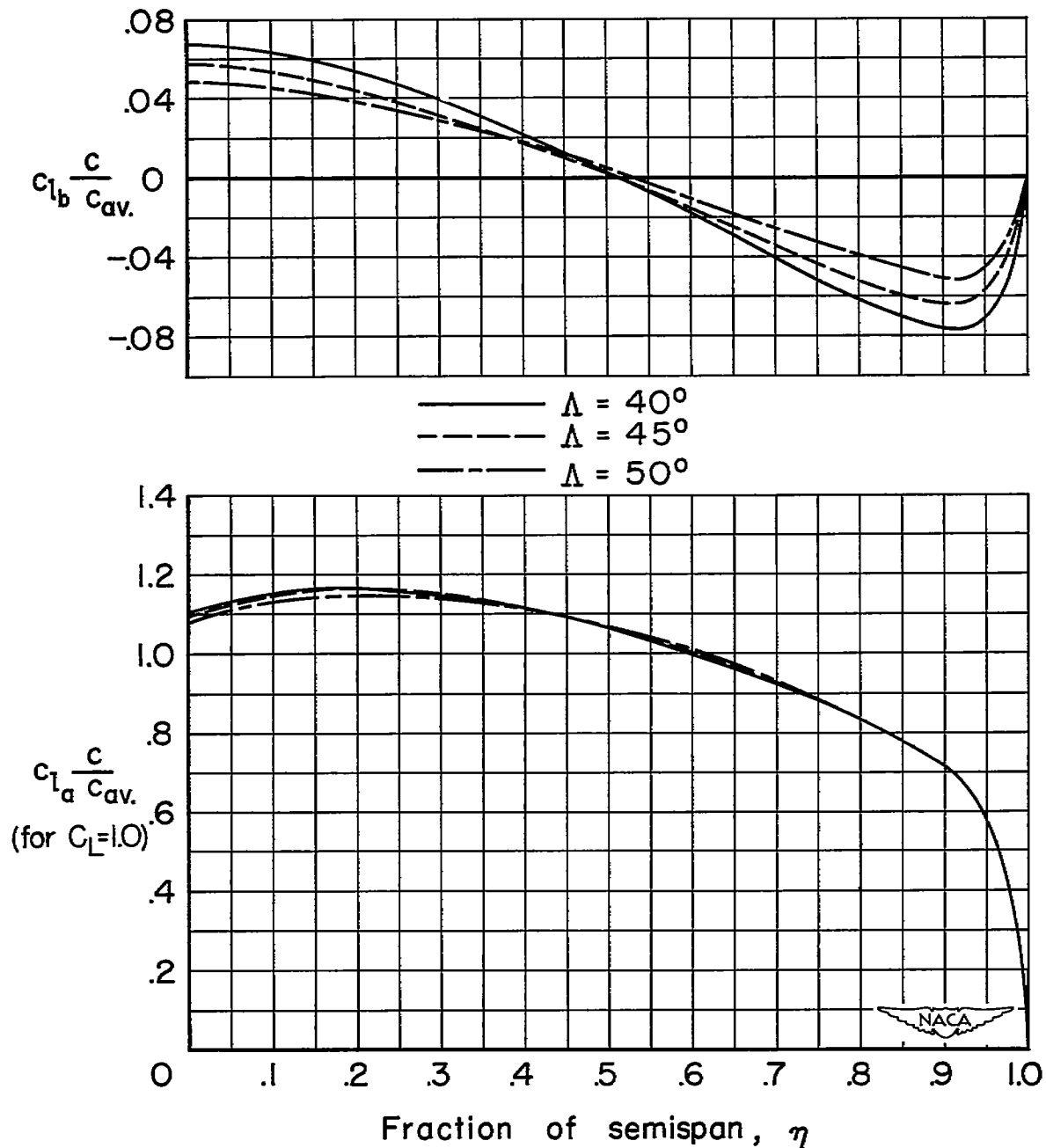
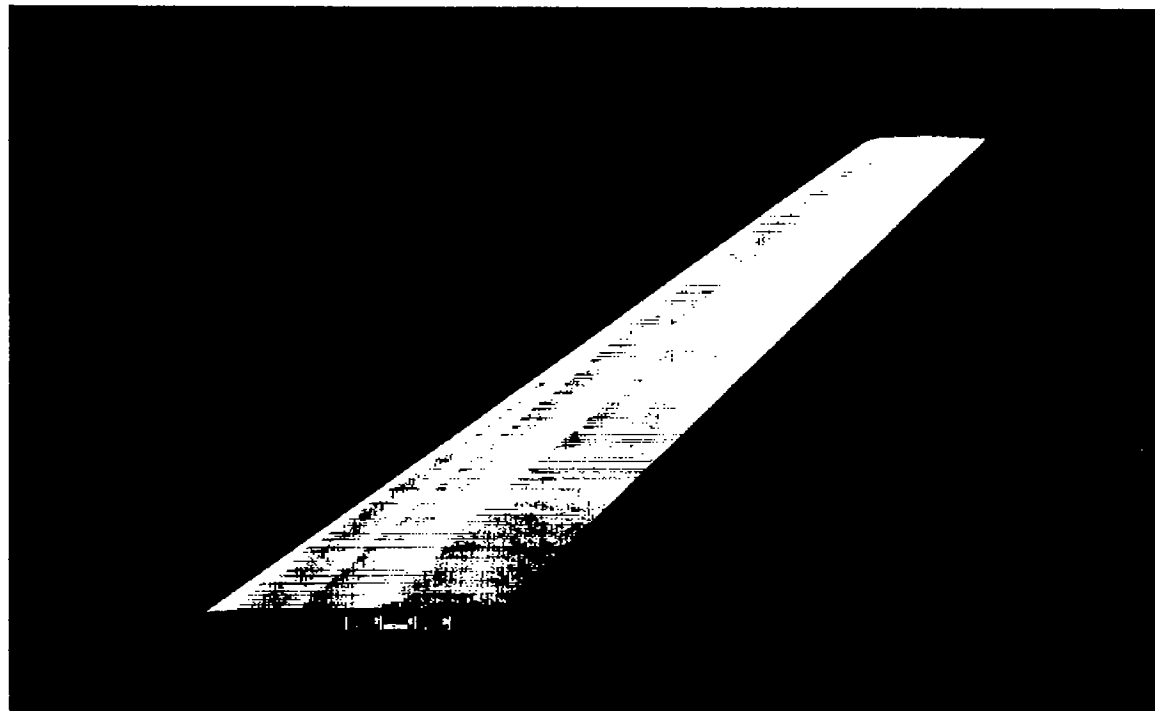


Figure 2.- The variations with sweepback of the theoretical spanwise distribution of  $c_l(c/c_{av})$  for basic and additional loading calculated by the Falkner 1x19 method.



A-18932

Figure 3.- Photograph of one of the models at  $50^{\circ}$  of sweepback.

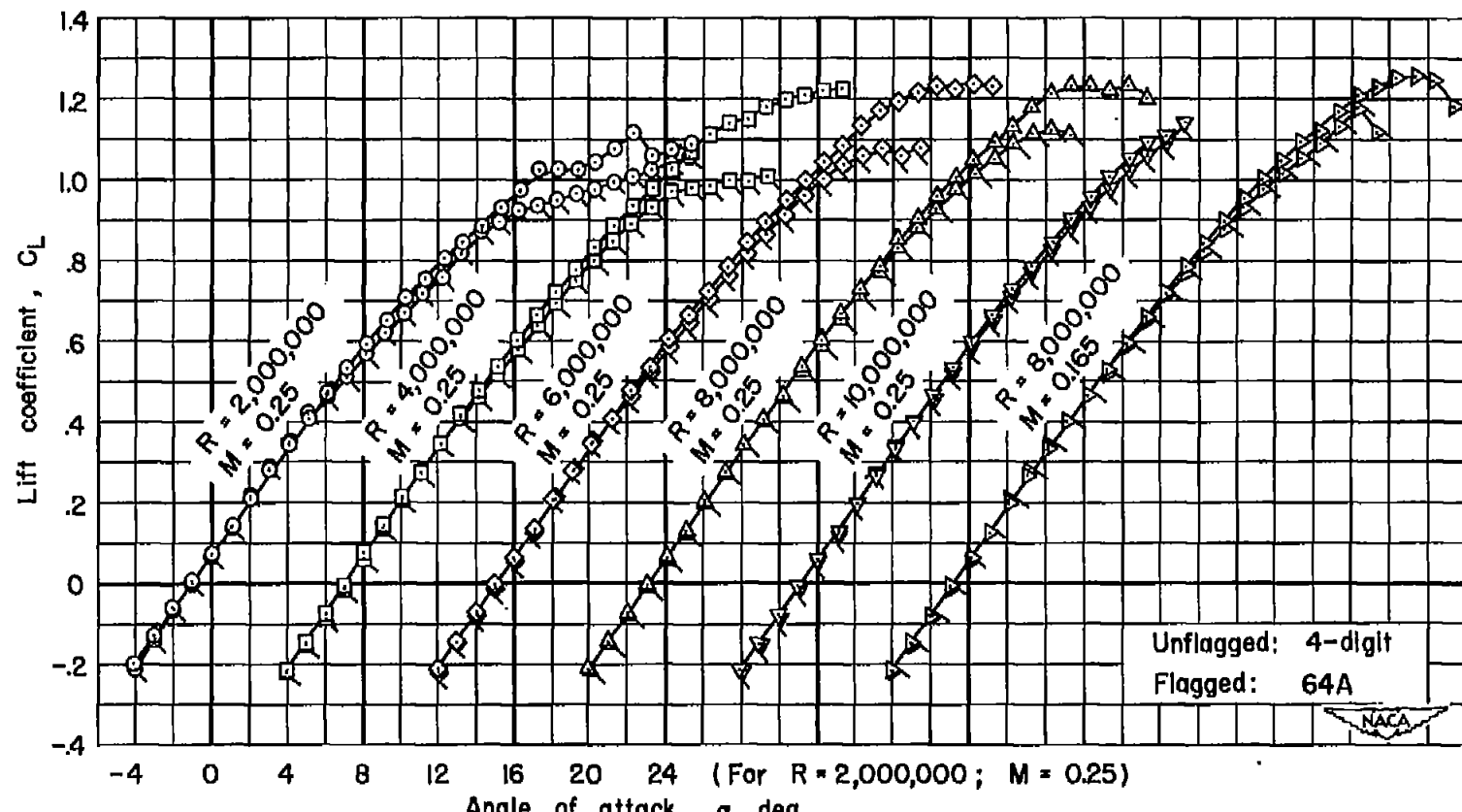
(a)  $\Lambda = 40^\circ$ 

Figure 4.- The effect of wing section at low speed and at several Reynolds numbers on the lift characteristics of the wing.

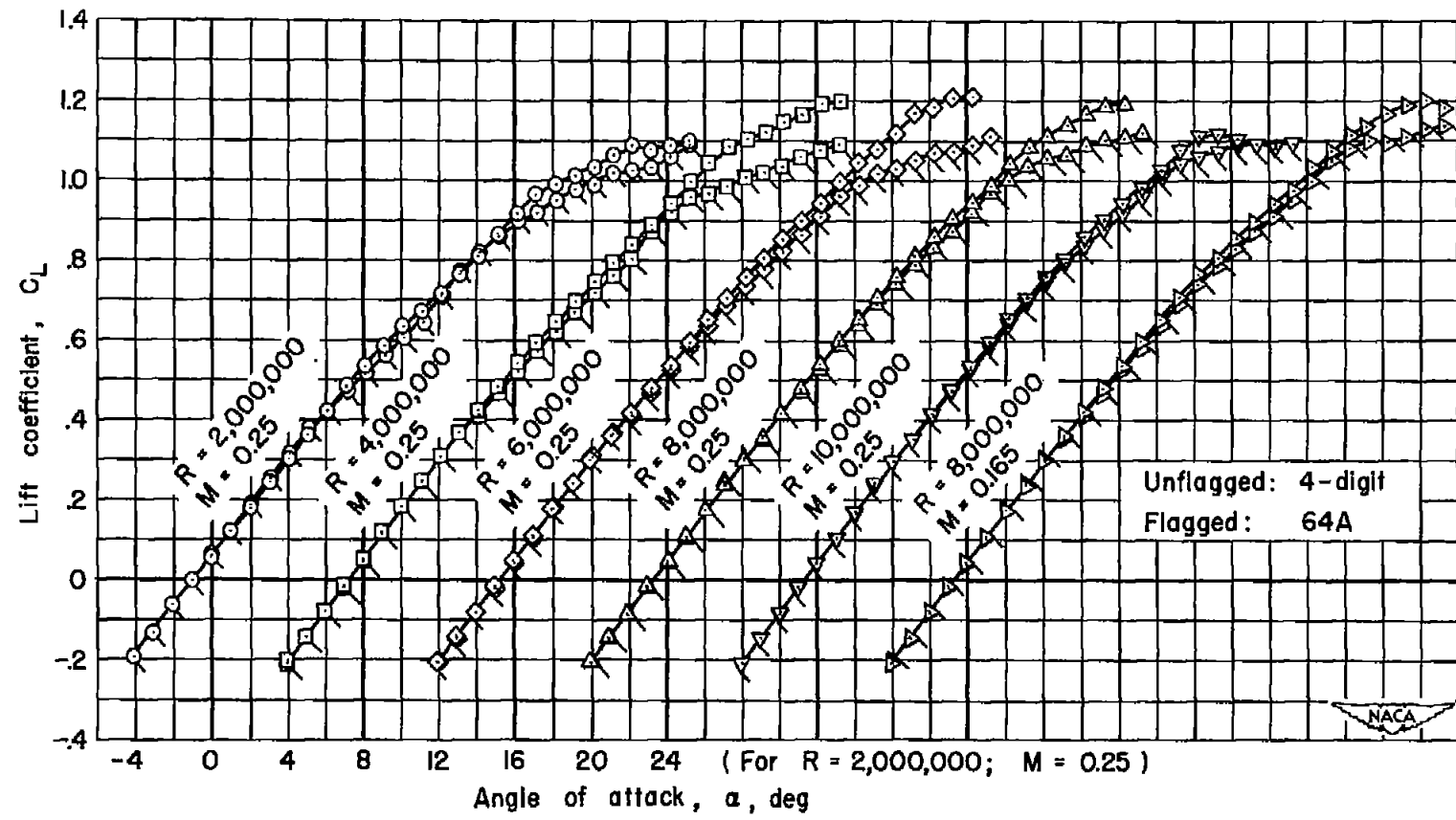


Figure 4.- Continued.

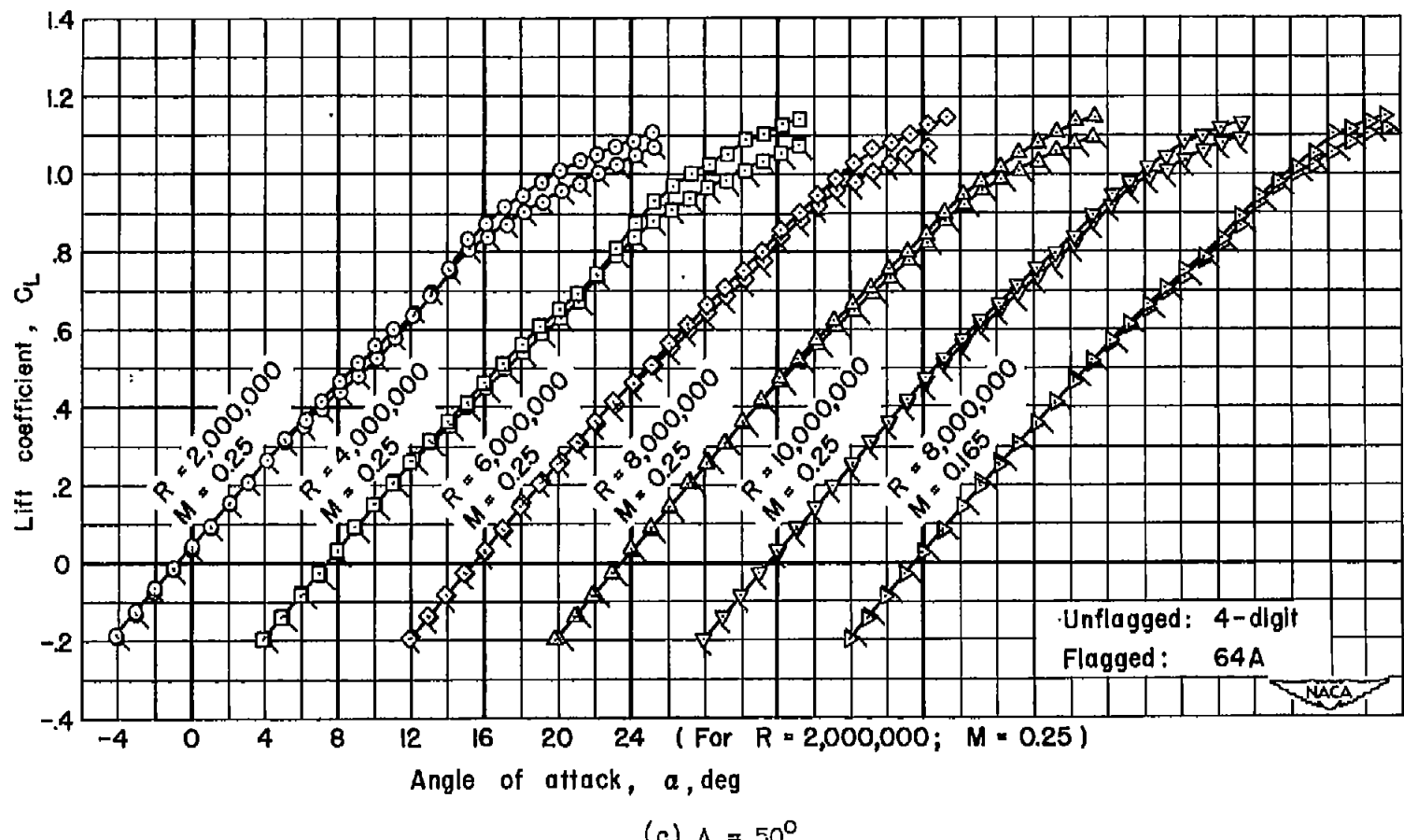


Figure 4.- Concluded.

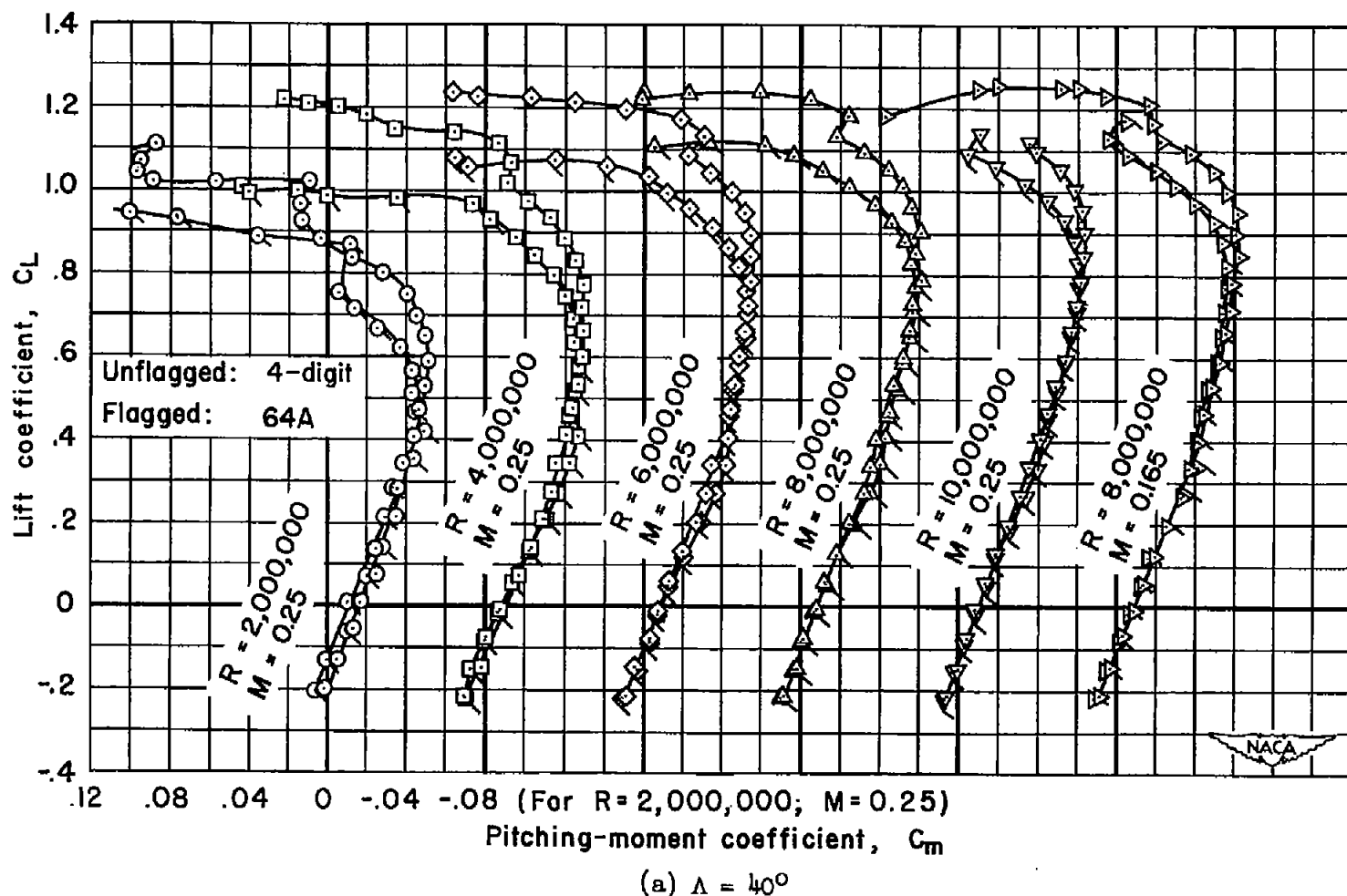


Figure 5.- The effect of wing section at low speed and at several Reynolds numbers on the pitching-moment characteristics of the wings.

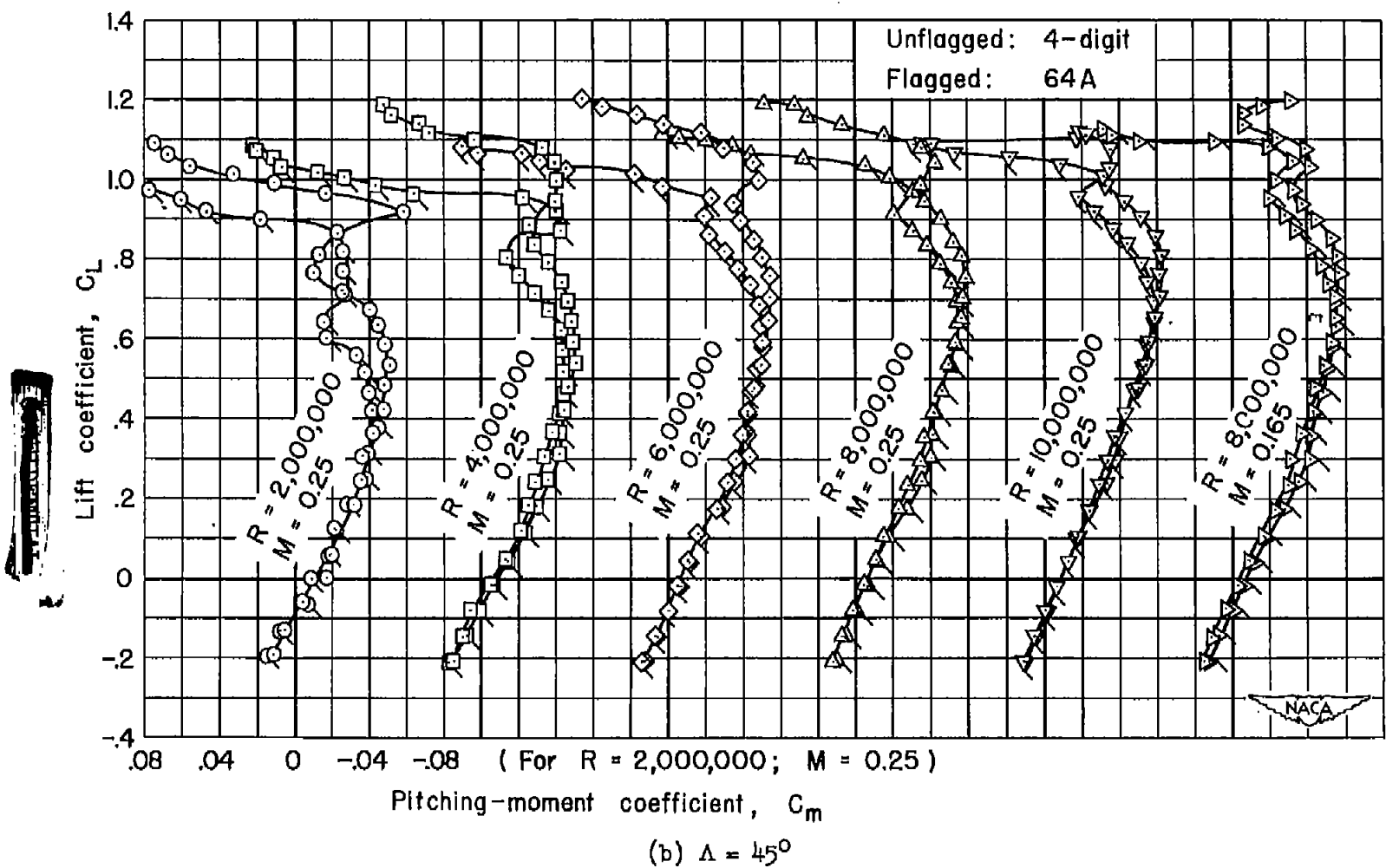


Figure 5.- Continued.

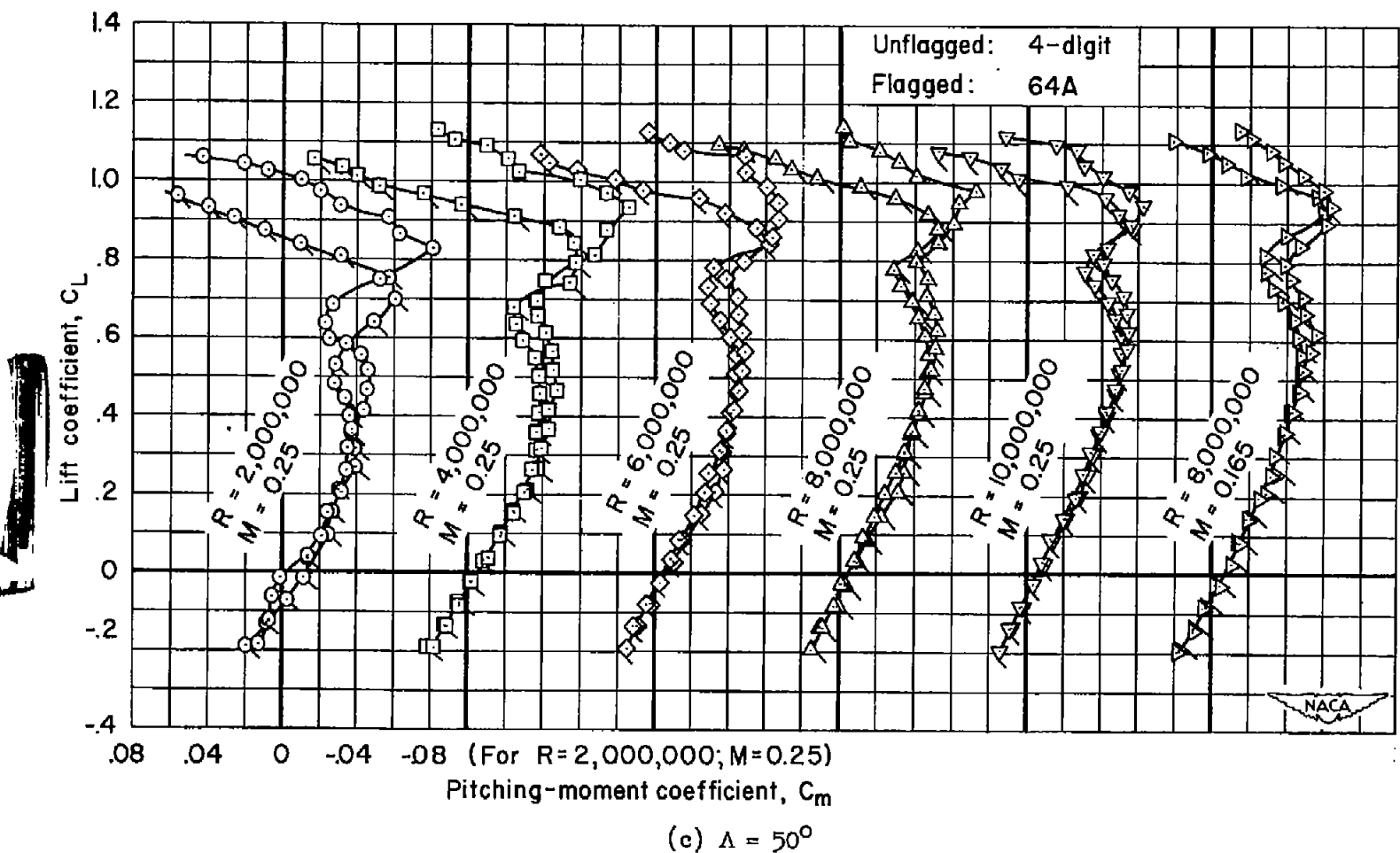


Figure 5.- Concluded.

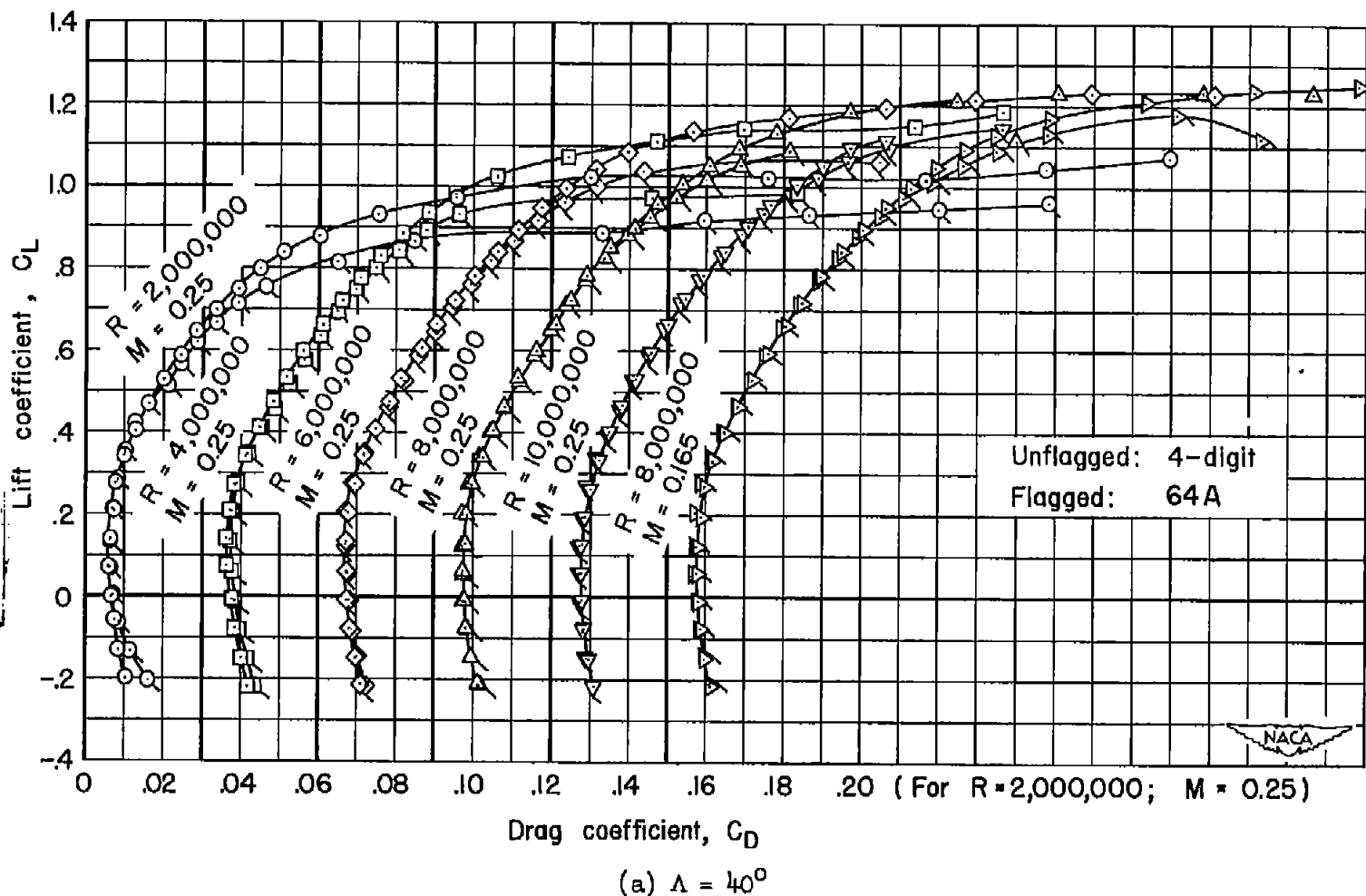


Figure 6.- The effect of wing section at low speed and at several Reynolds numbers on the drag characteristics of the wings.

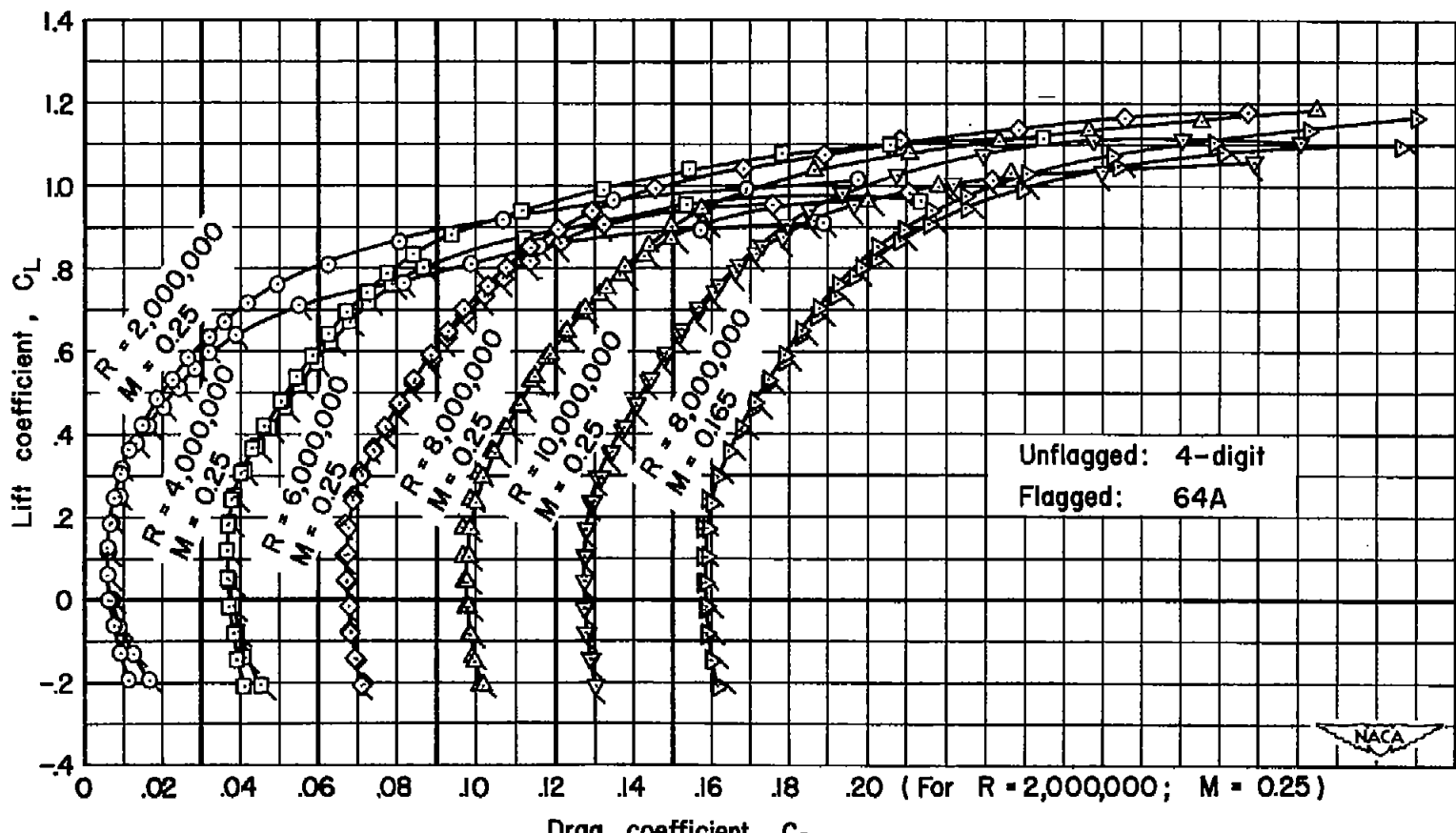
(b)  $\Lambda = 45^\circ$ 

Figure 6.- Continued.

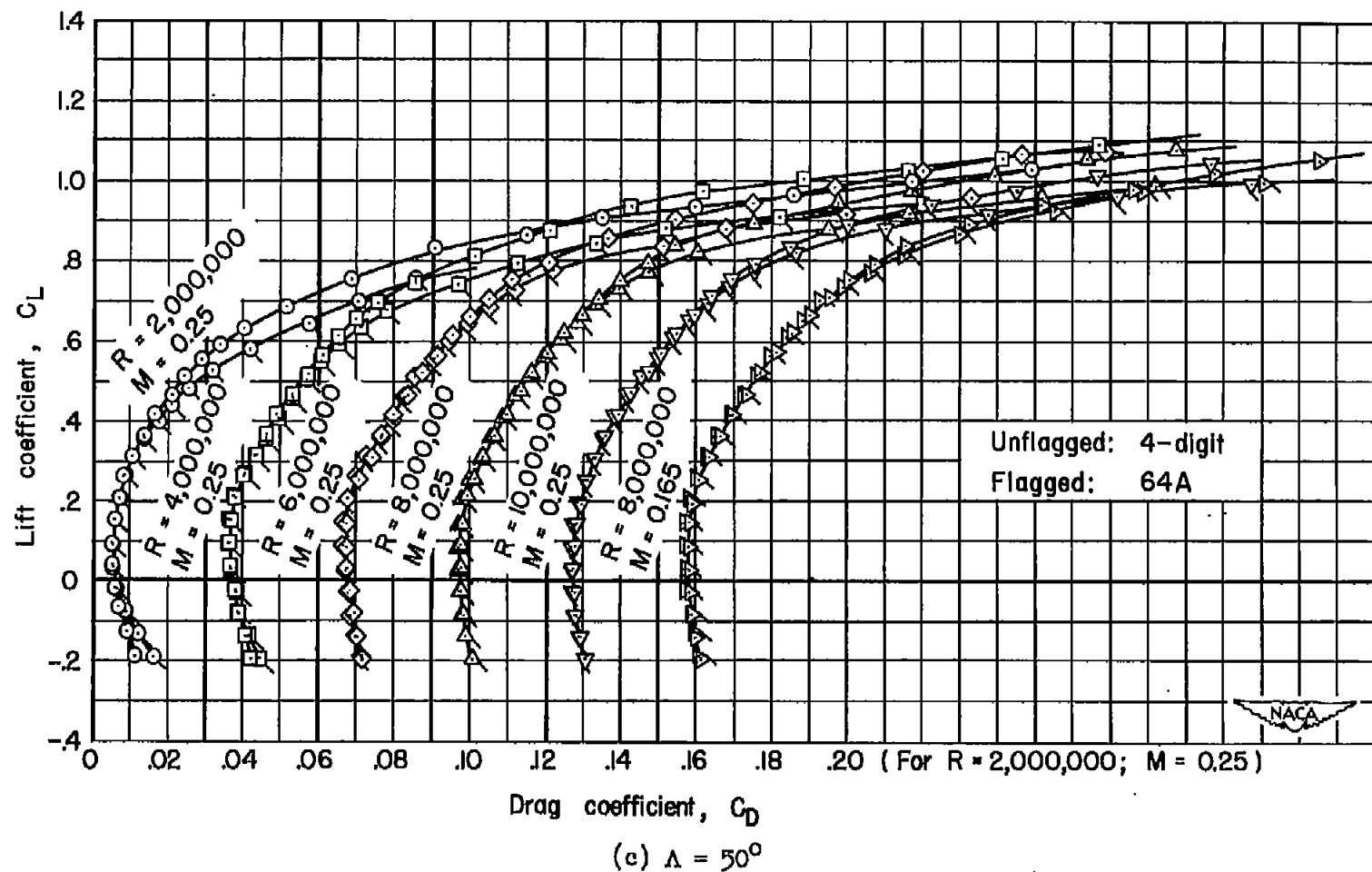


Figure 6.- Concluded.

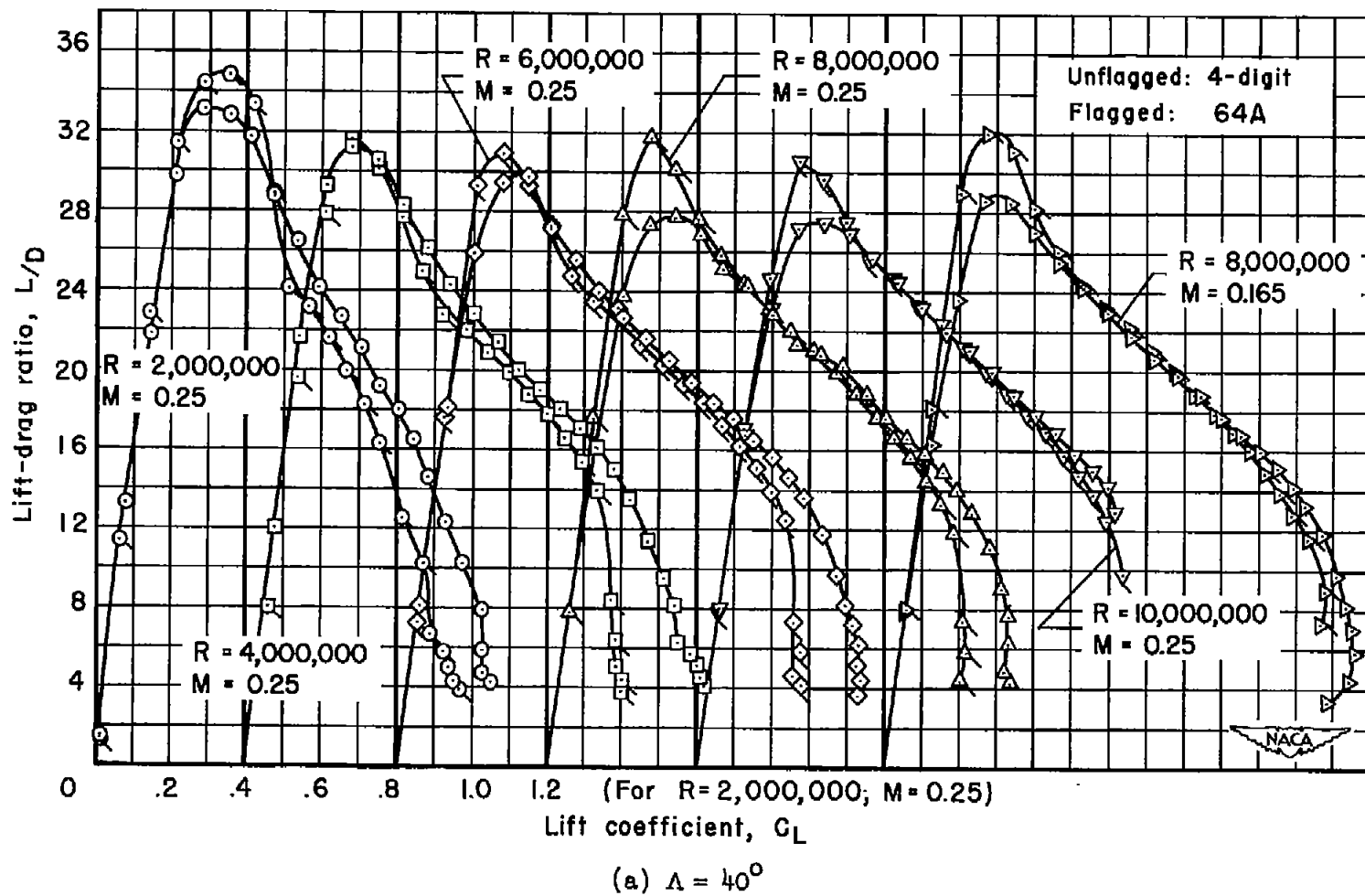


Figure 7.- The effect of wing section at low speed and at several Reynolds numbers on the lift-drag ratios of the wings.

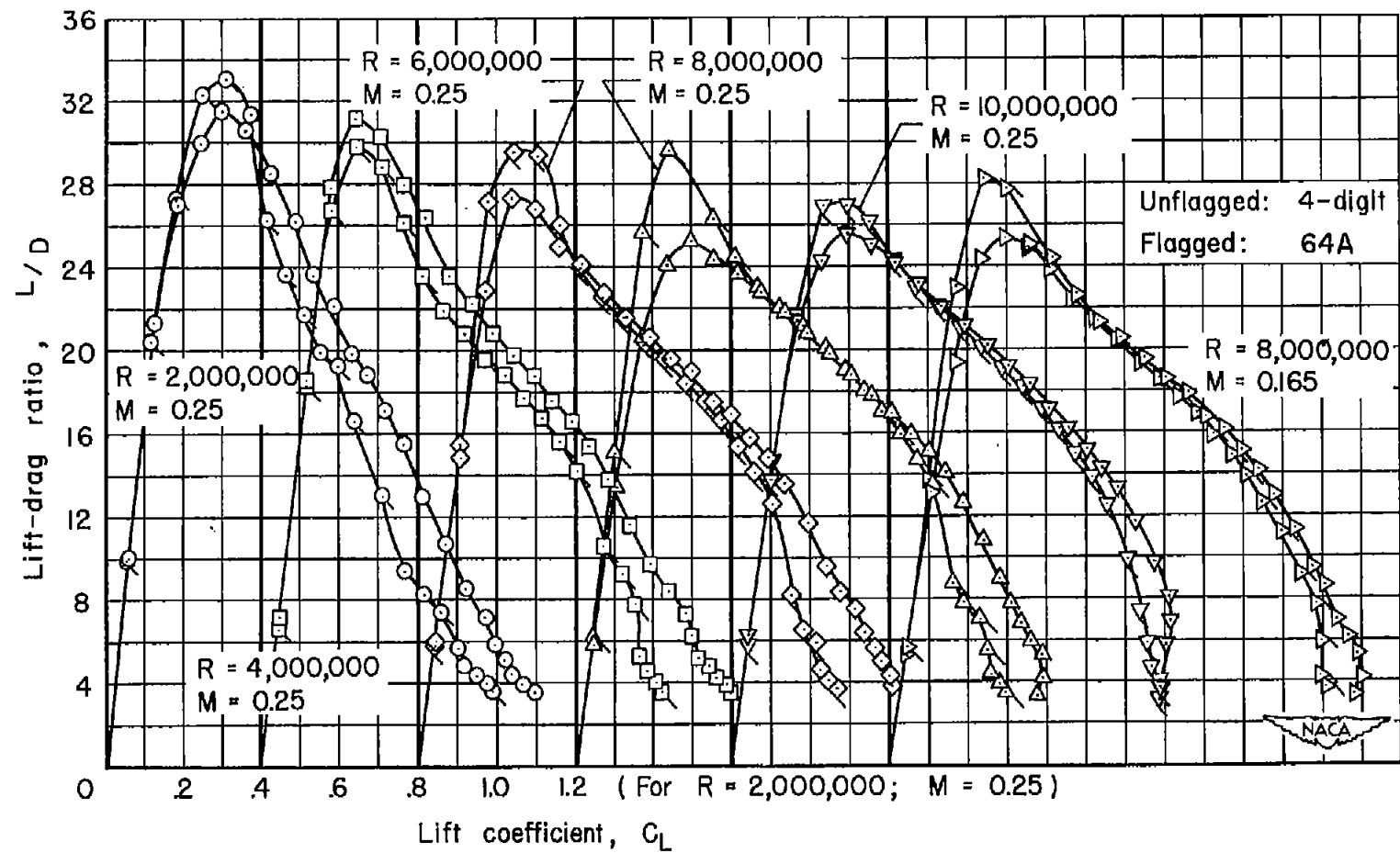
(b)  $\Lambda = 45^\circ$ 

Figure 7.- Continued.

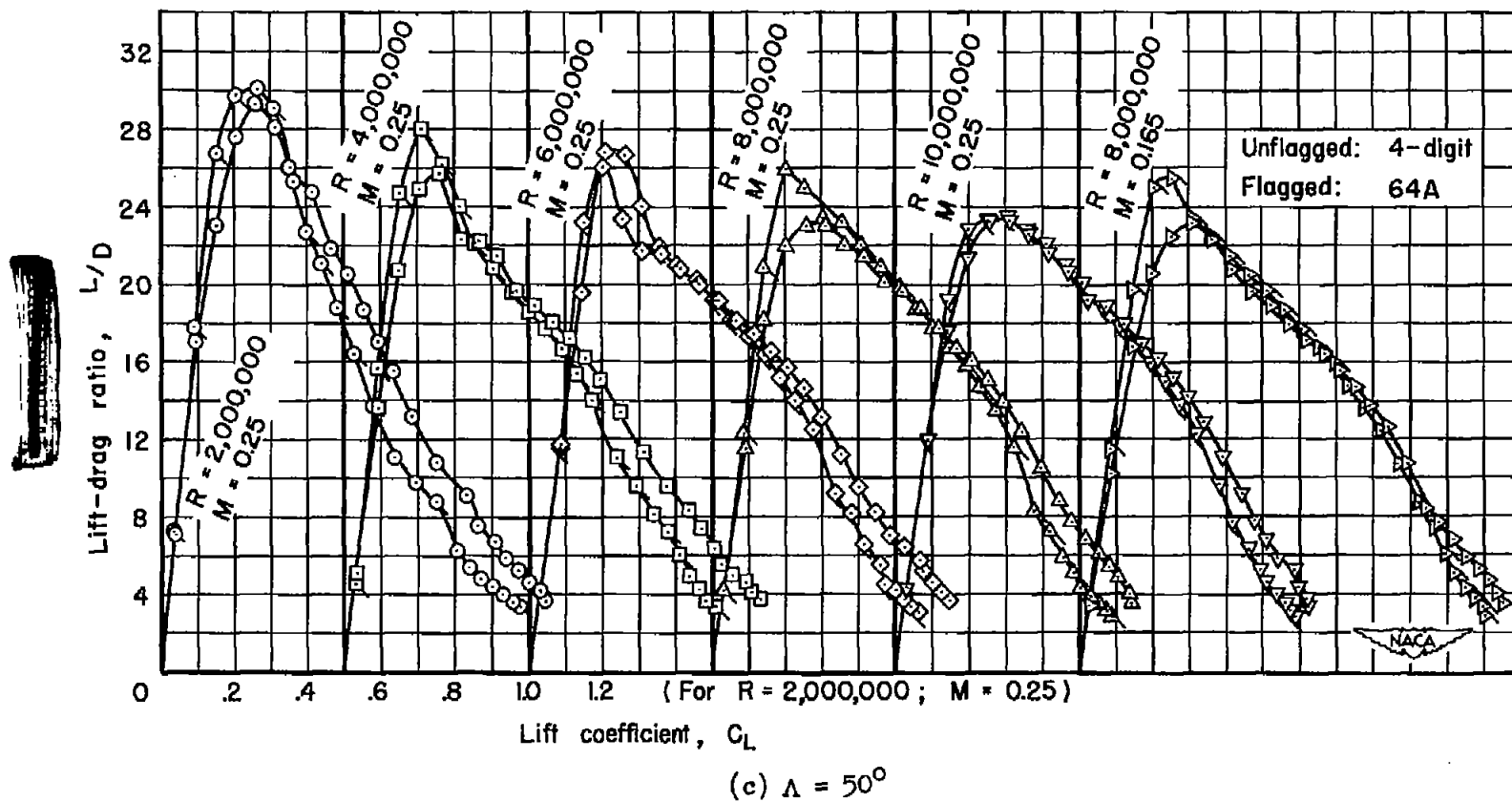


Figure 7.- Concluded.

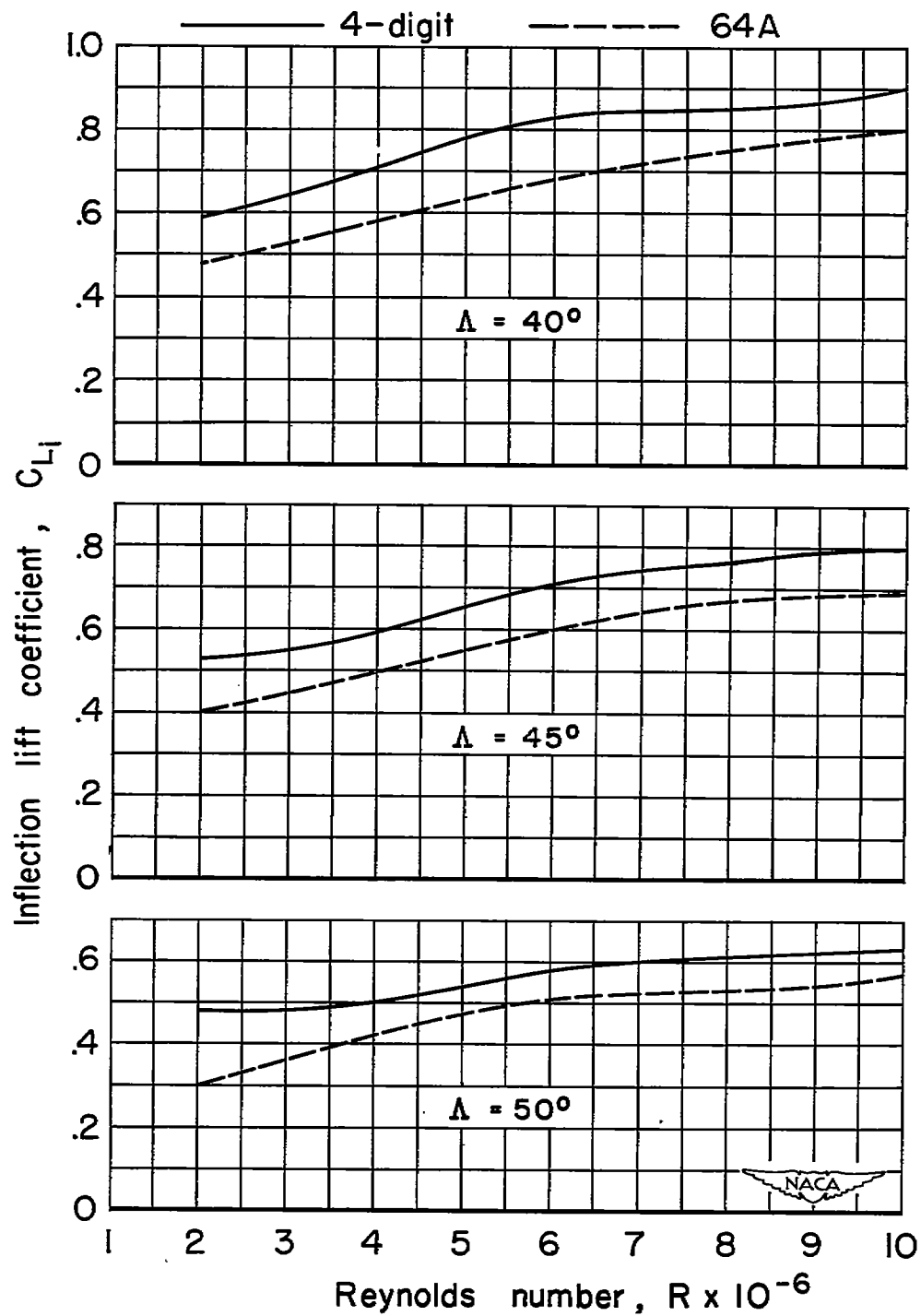


Figure 8.- The variation with Reynolds number of the inflection lift coefficients of the wings at several angles of sweepback;  $M = 0.25$ .

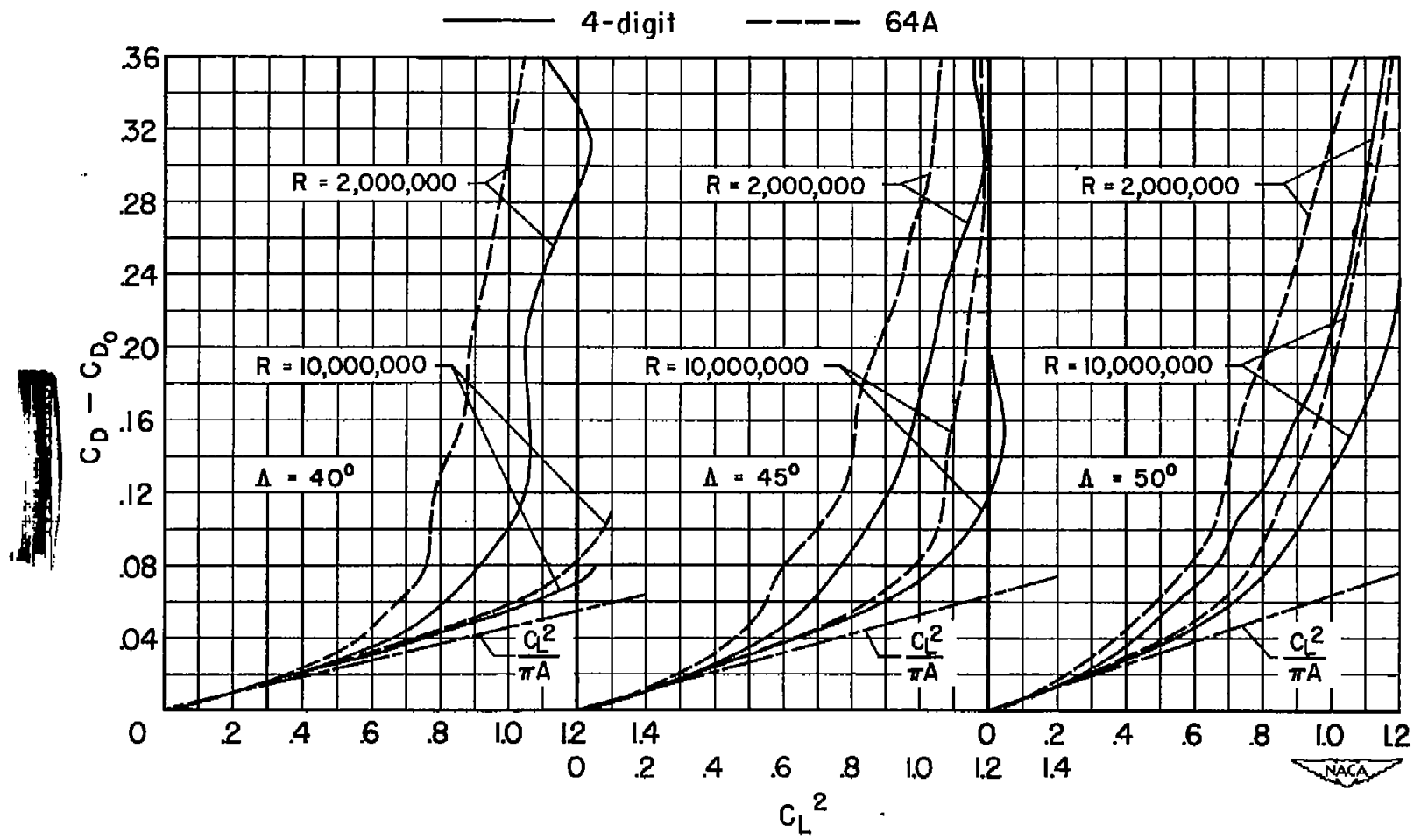


Figure 9.- The variation of drag due to lift with lift coefficient squared at several angles of sweepback and at Reynolds numbers of 2,000,000 and 10,000,000;  $M = 0.25$ .

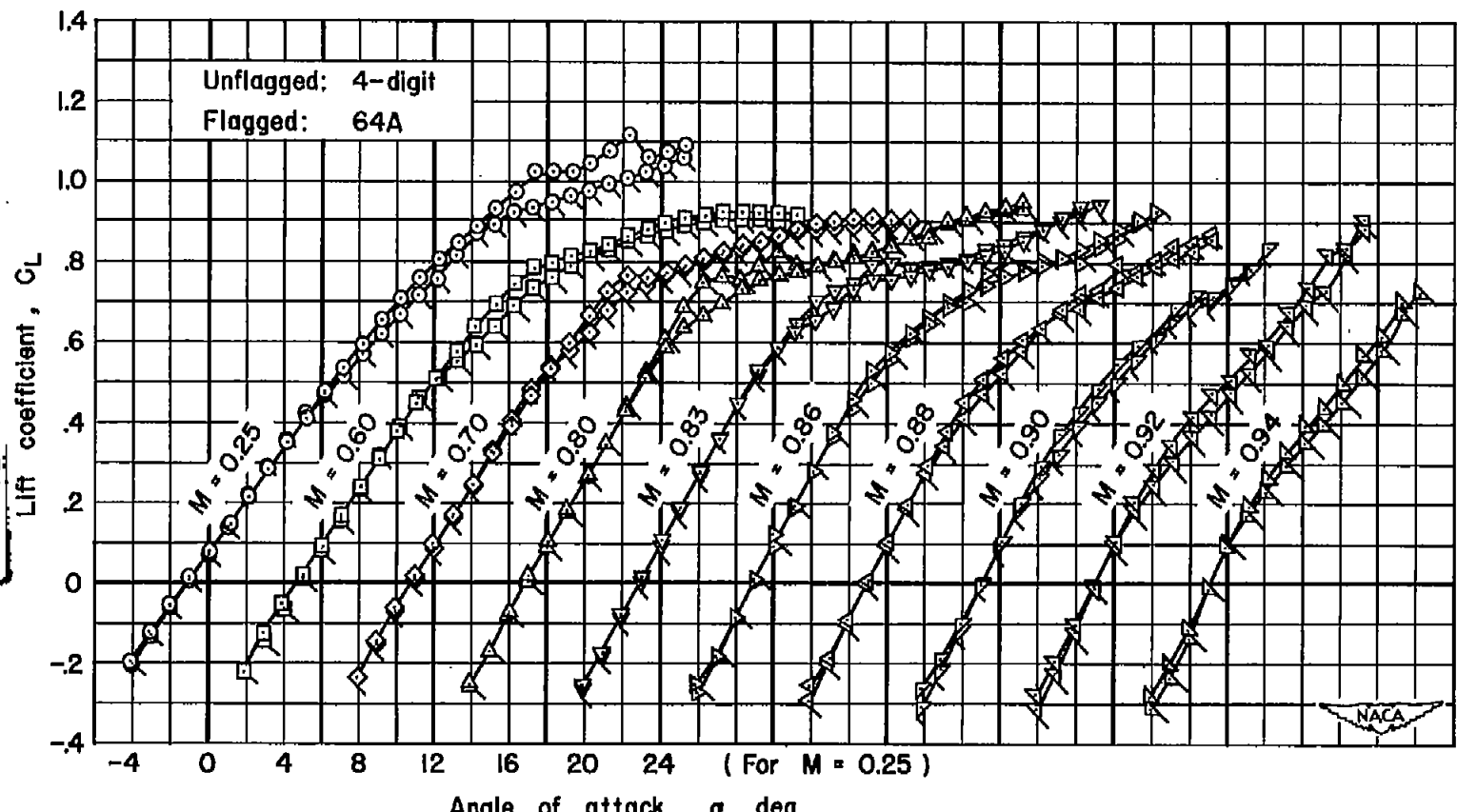
(a)  $\Lambda = 400$ 

Figure 10.- The effect of wing section at several Mach numbers on the lift characteristics of the wings;  $R = 2,000,000$ .

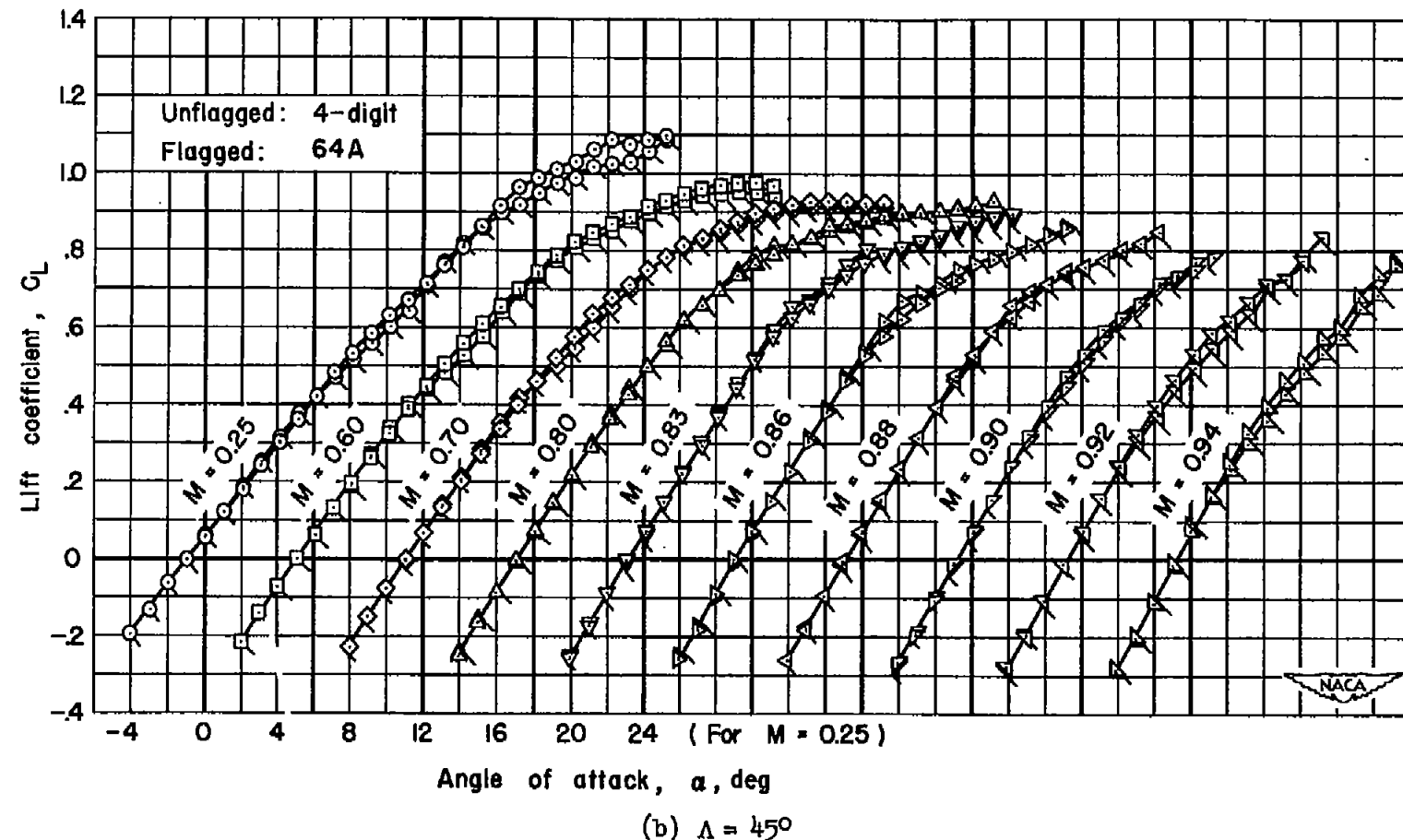


Figure 10.- Continued.

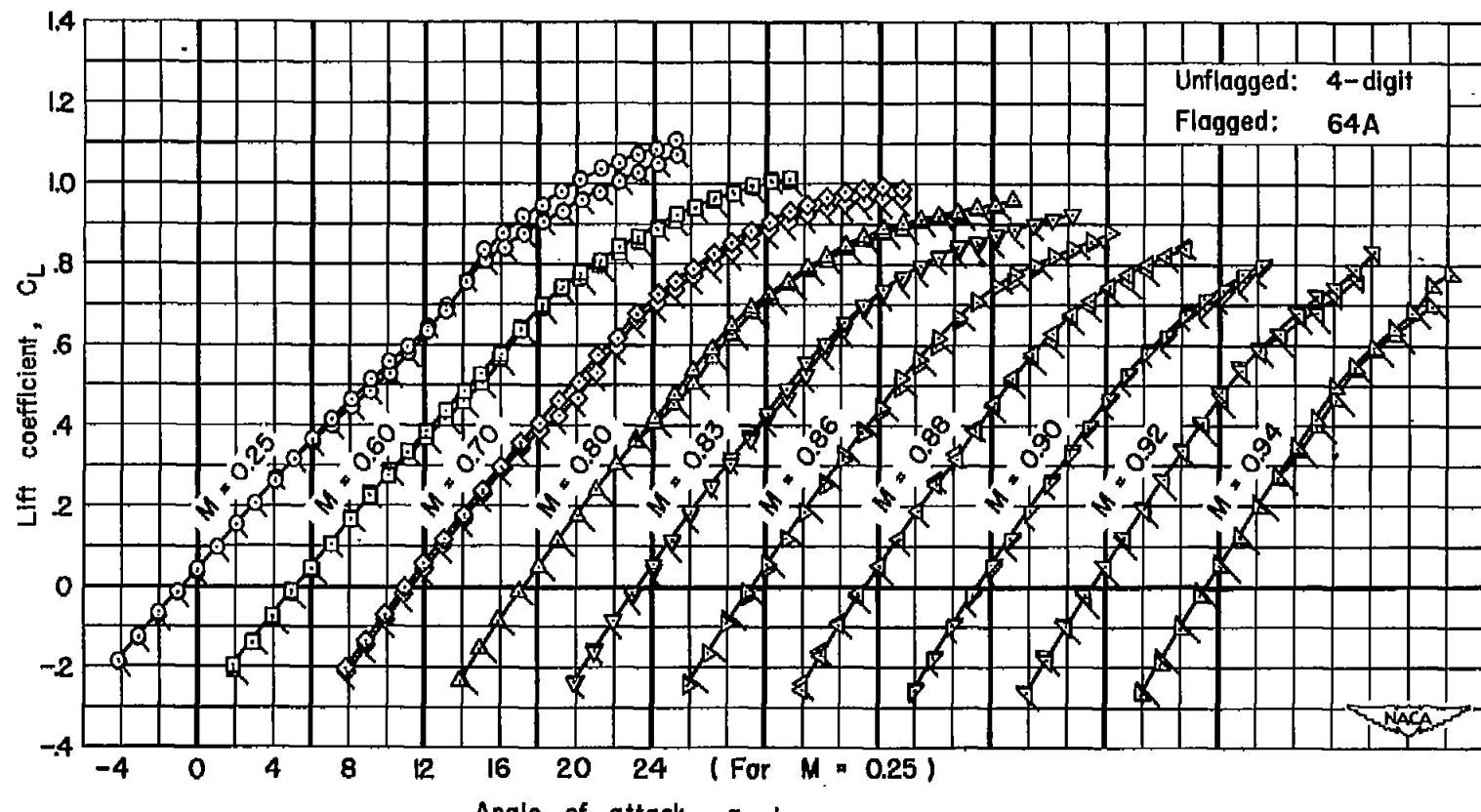
(c)  $\Delta = 50^\circ$ 

Figure 10.- Concluded.

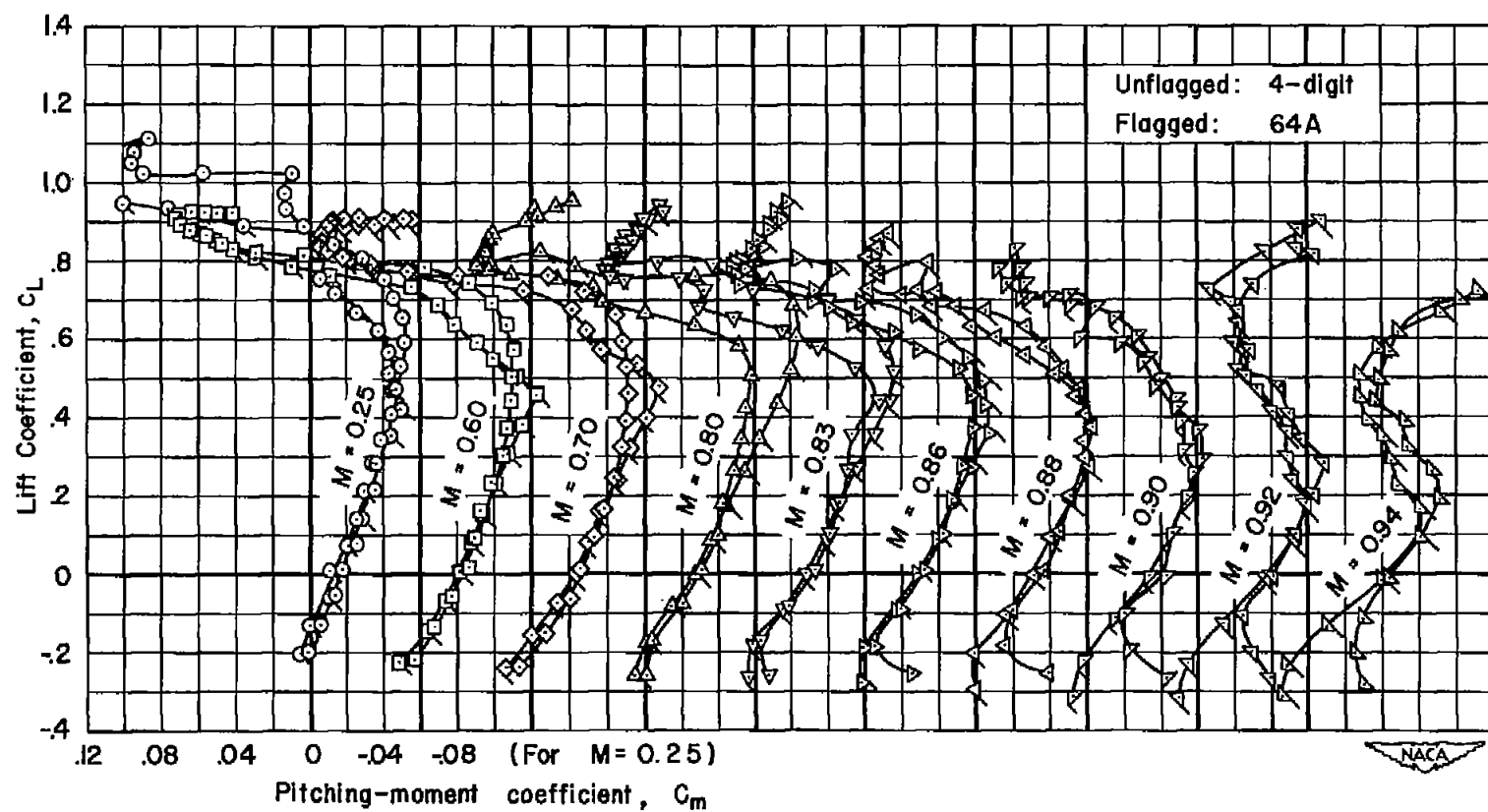
(a)  $\Lambda = 40^\circ$ 

Figure 11.- The effect of wing section at several Mach numbers on the pitching-moment characteristics of the wings;  $R = 2,000,000$ .

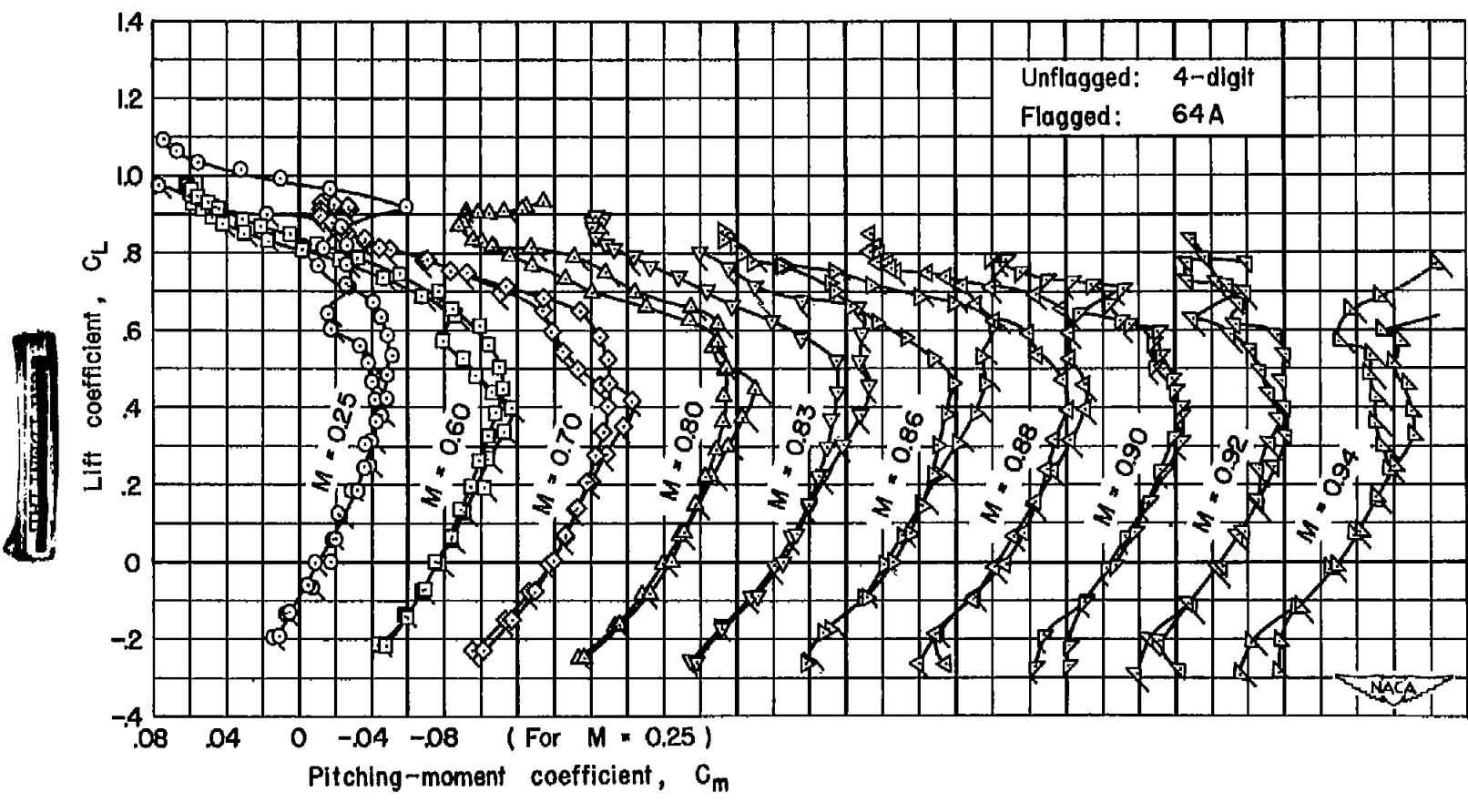


Figure 11.- Continued.

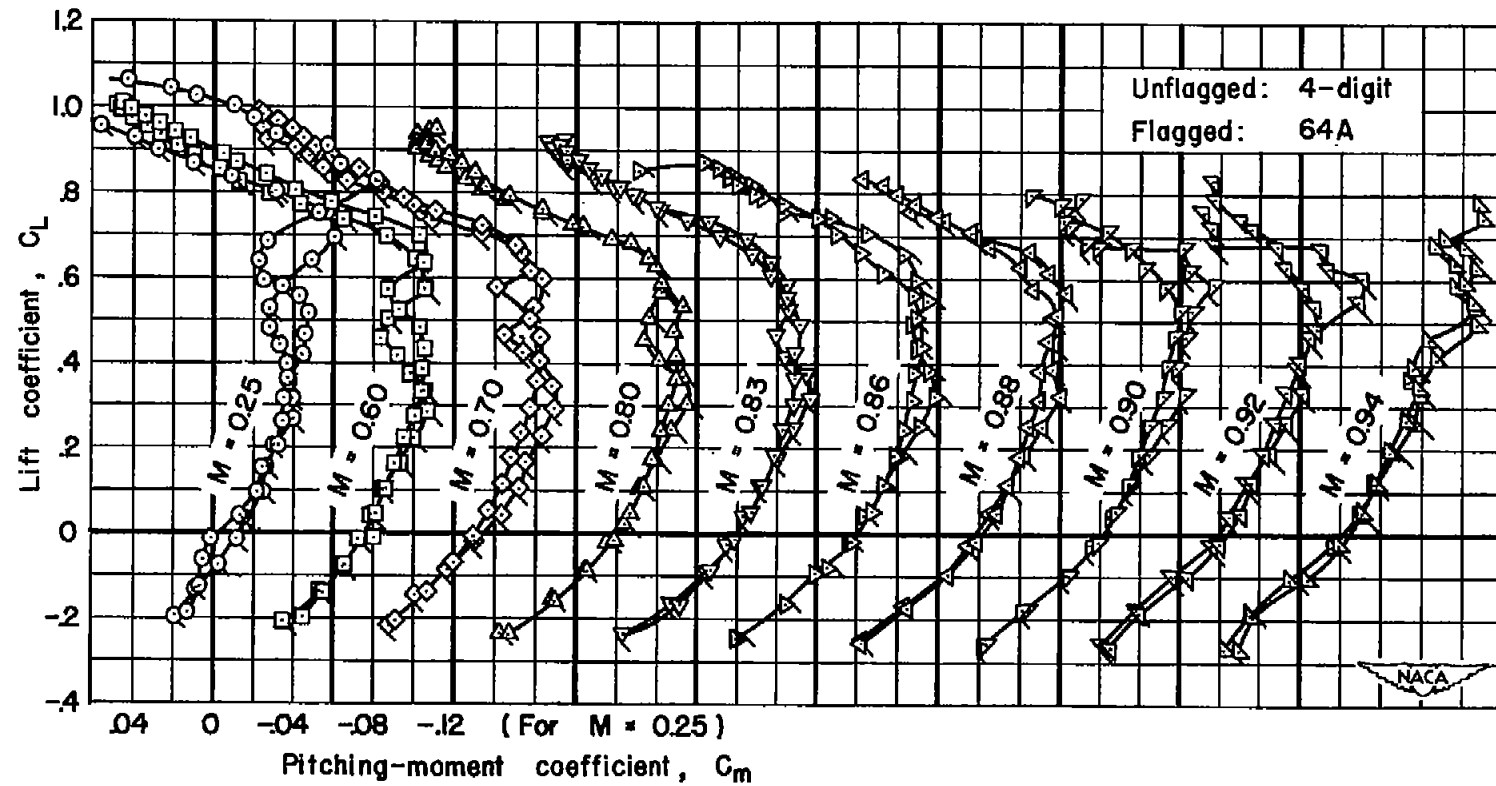
(c)  $\alpha = 50^\circ$ 

Figure 11.- Concluded.

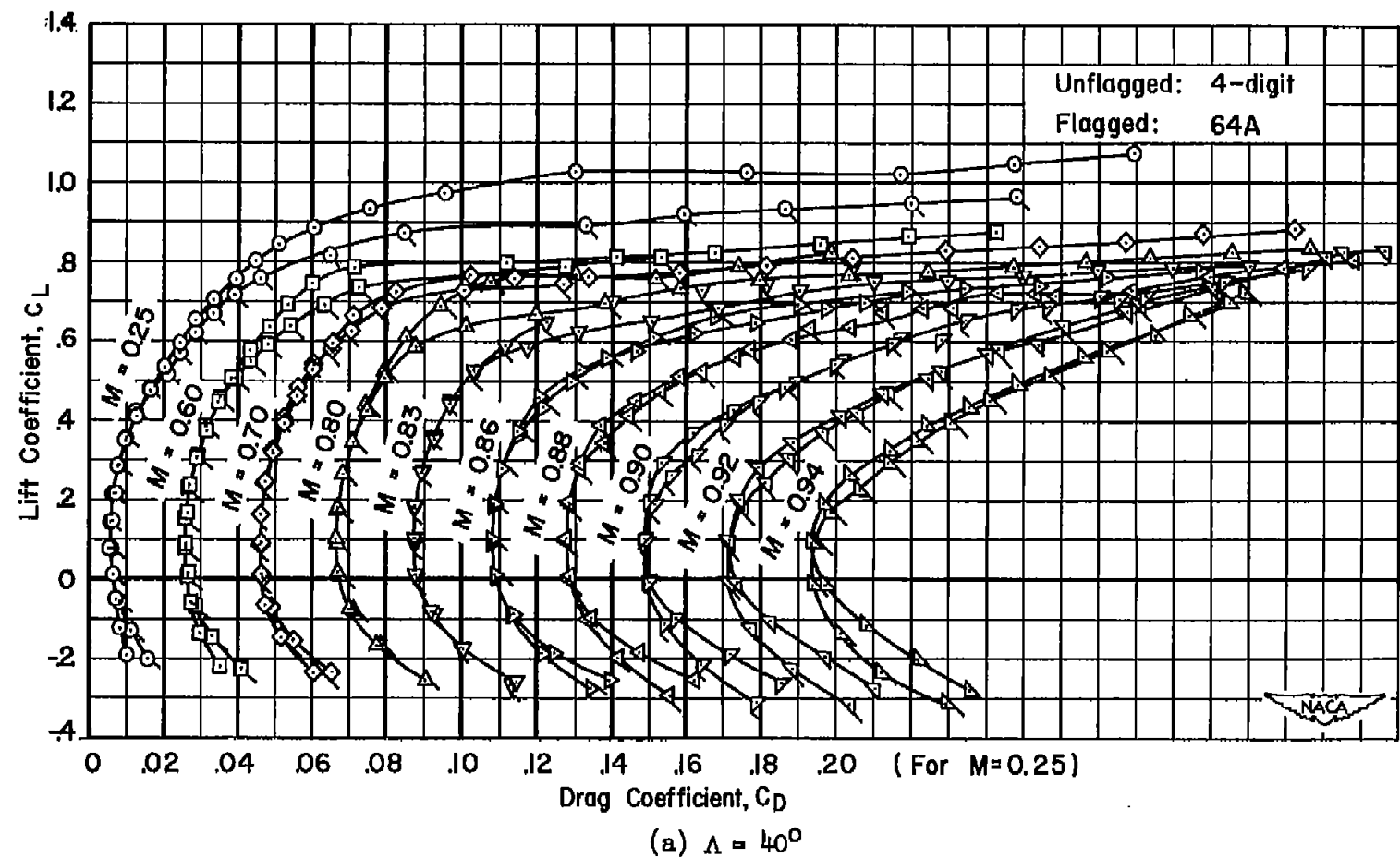


Figure 12.- The effect of wing section at several Mach numbers on the drag characteristics of the wings;  $R = 2,000,000$ .

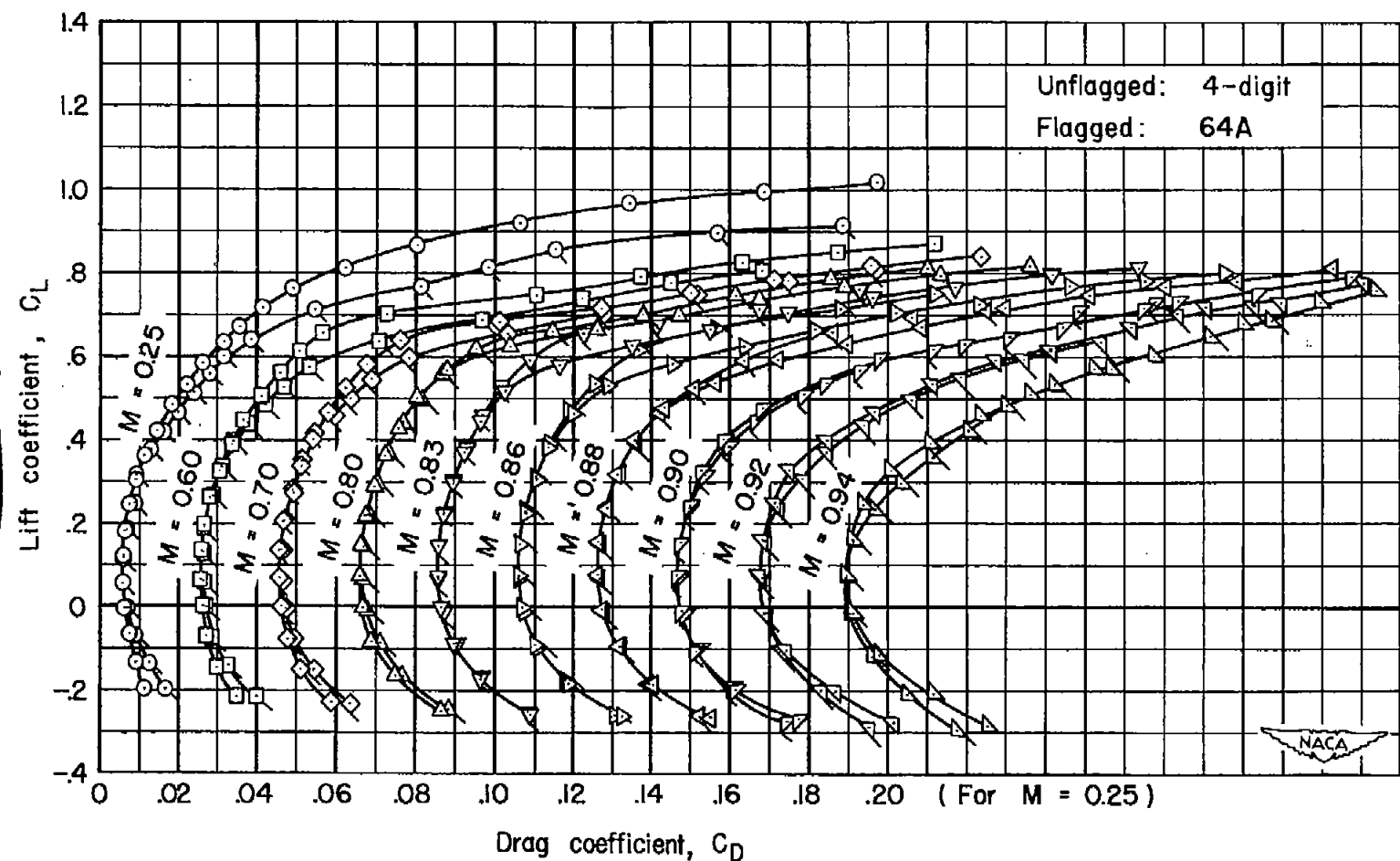
(b)  $\Delta = 45^\circ$ 

Figure 12.- Continued.

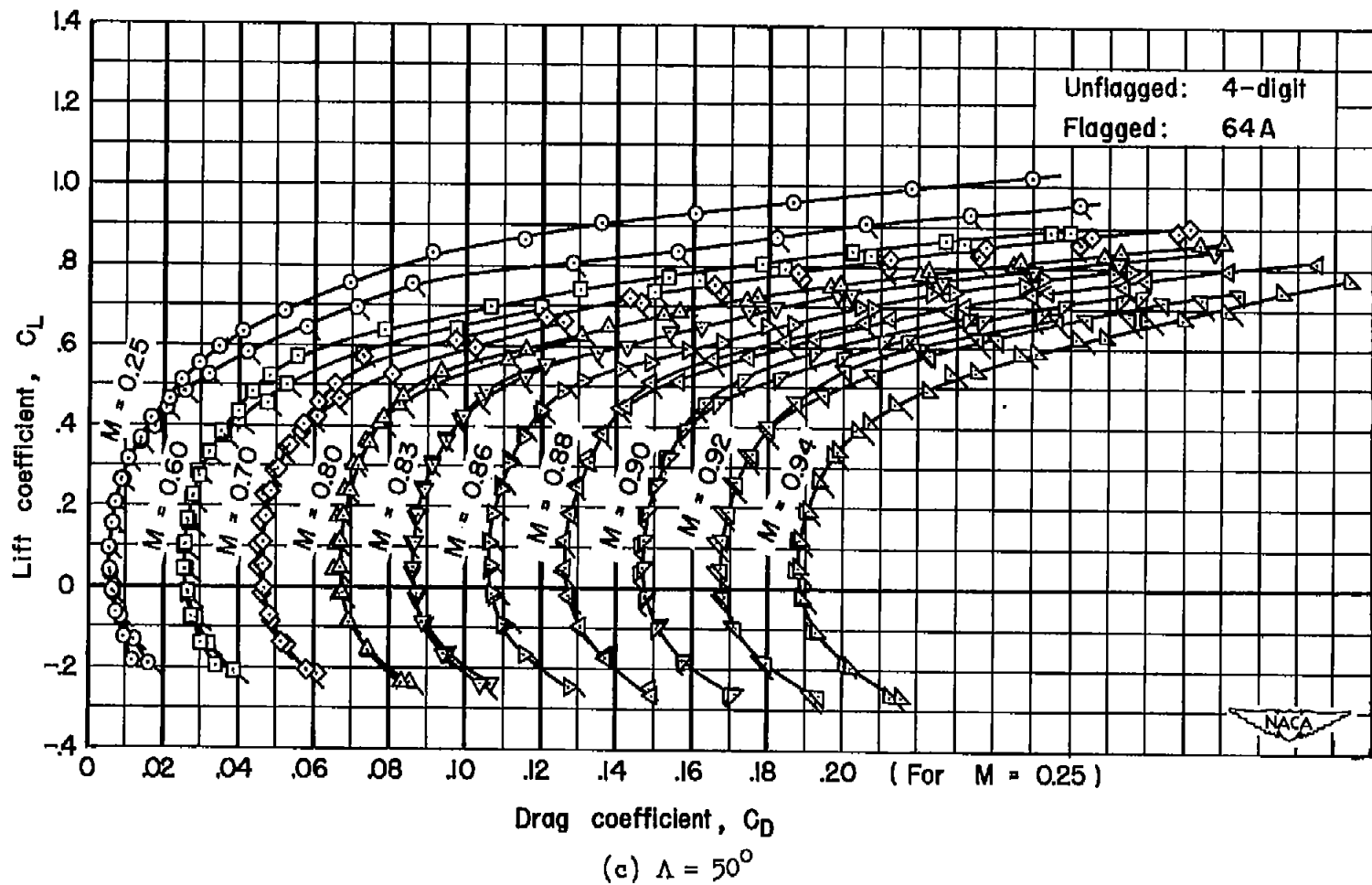


Figure 12.-- Concluded.

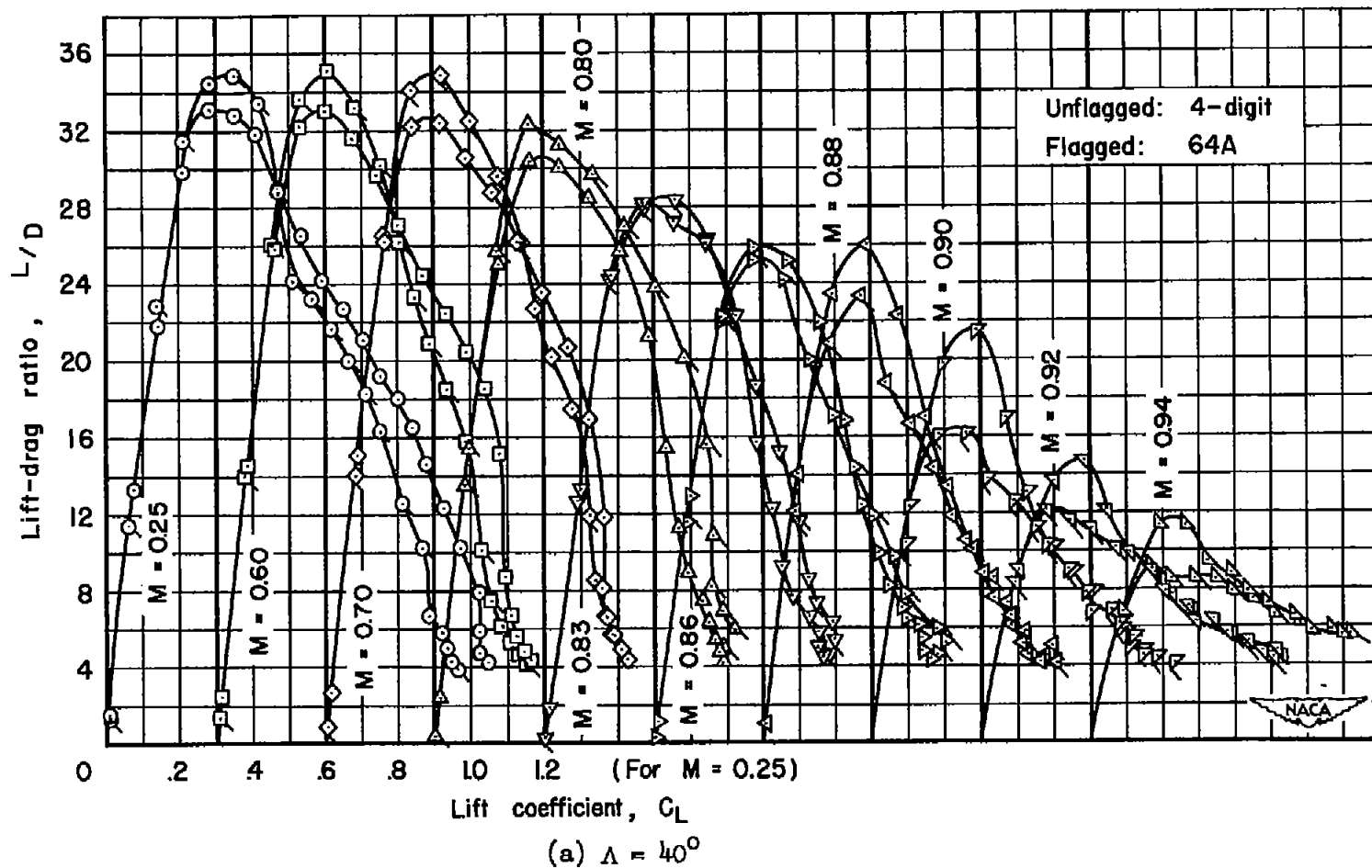


Figure 13.- The effect of wing section at several Mach numbers on the lift-drag characteristics of the wings;  $R = 2,000,000$ .

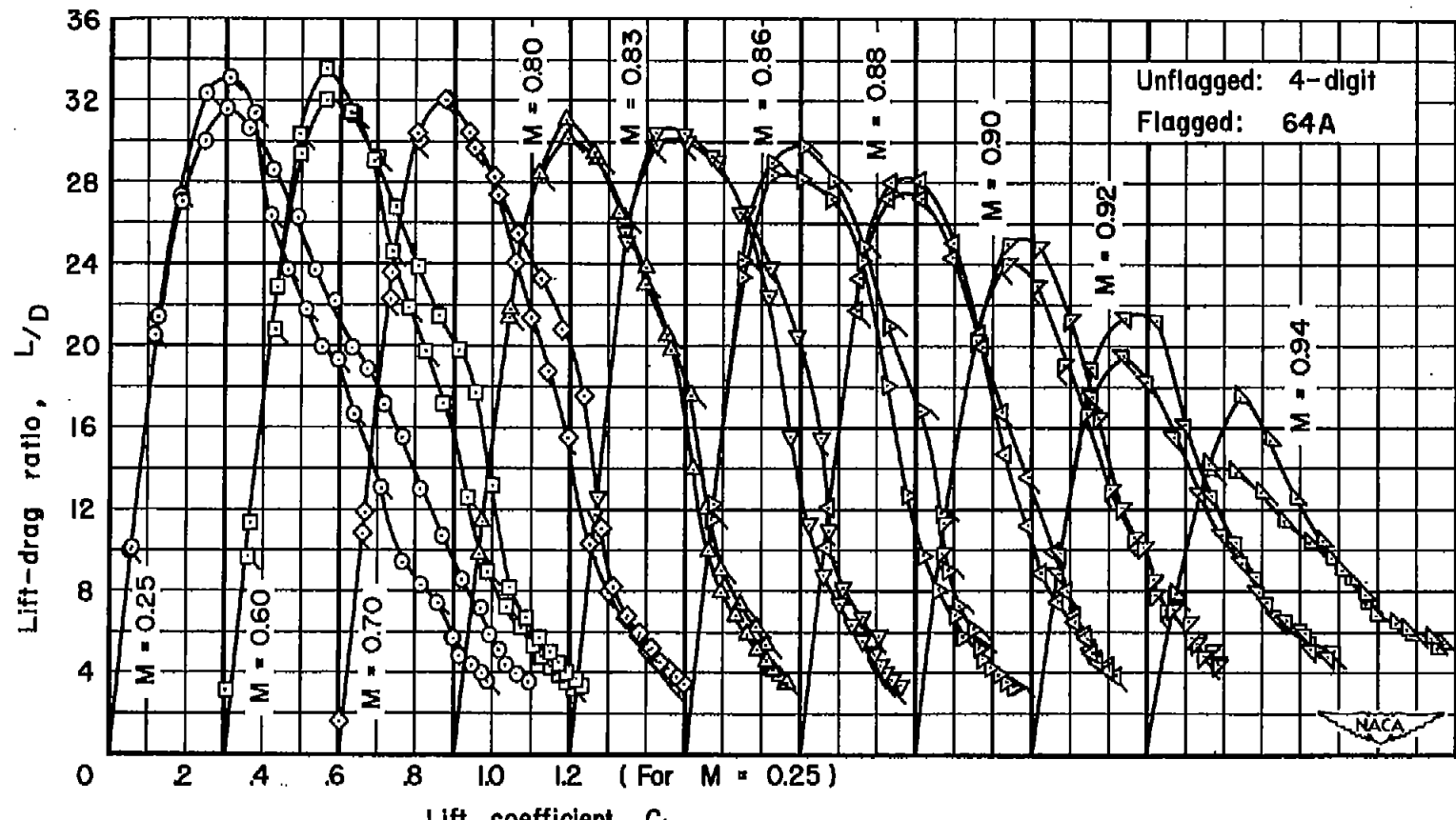
(b)  $\Delta = 45^\circ$ 

Figure 13.- Continued.

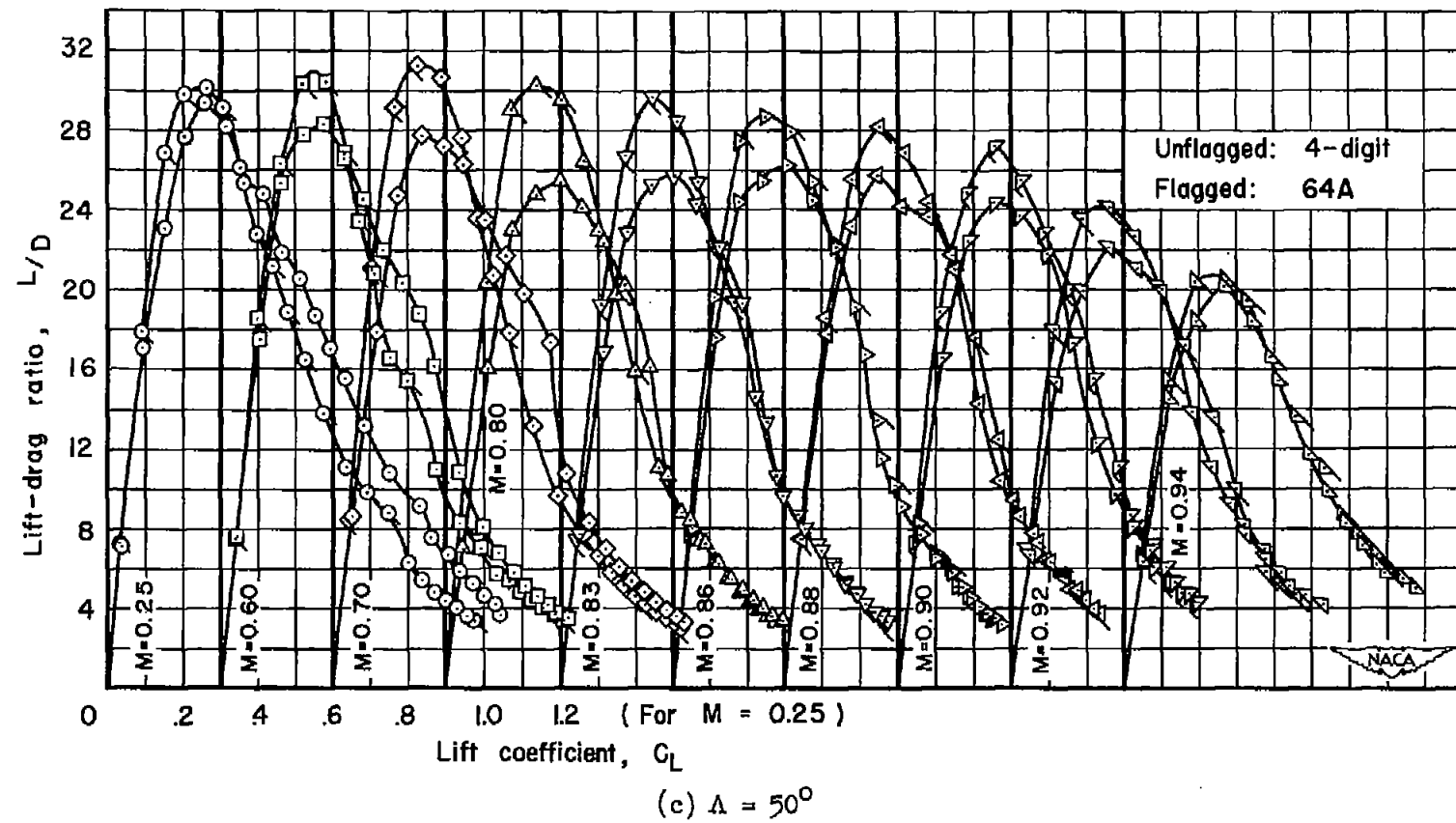


Figure 13.- Concluded.

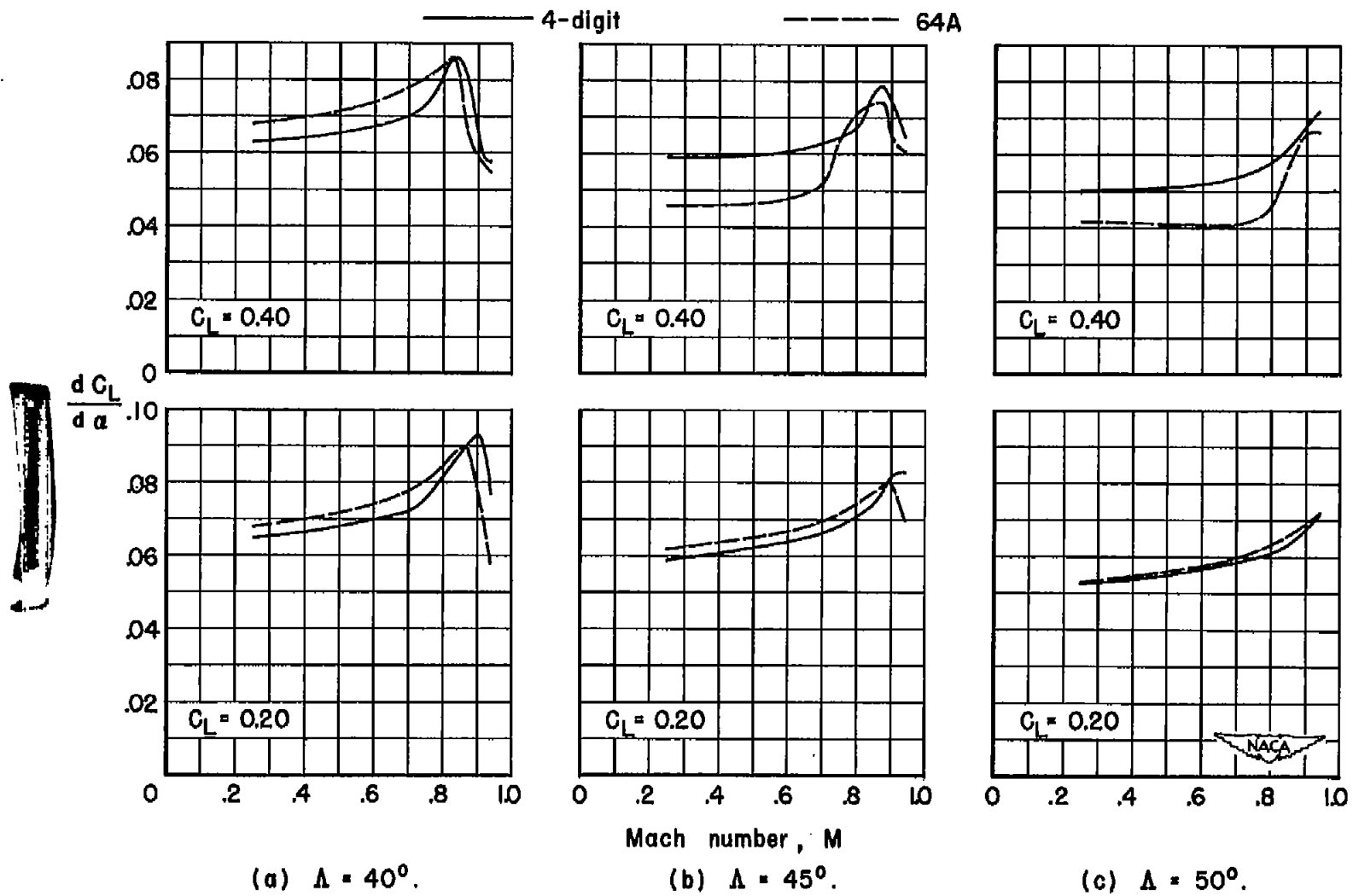


Figure 14.- The variation with Mach number of the lift-curve slopes of the wings at constant lift coefficients and several angles of sweepback;  $R = 2,000,000$ .

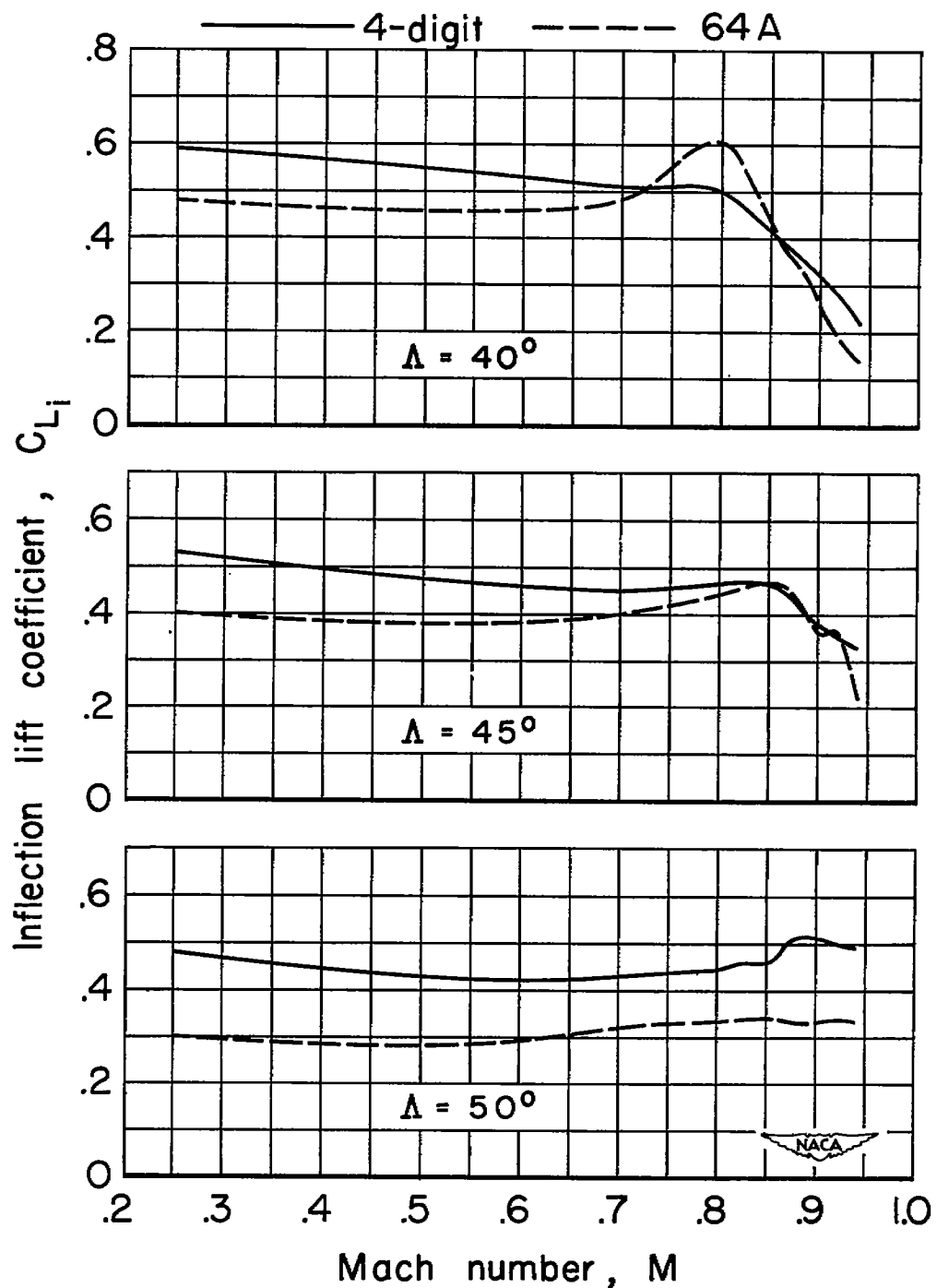


Figure 15.- The variation with Mach number of the inflection lift coefficients of the wings at several angles of sweepback;  
 $R = 2,000,000$ .

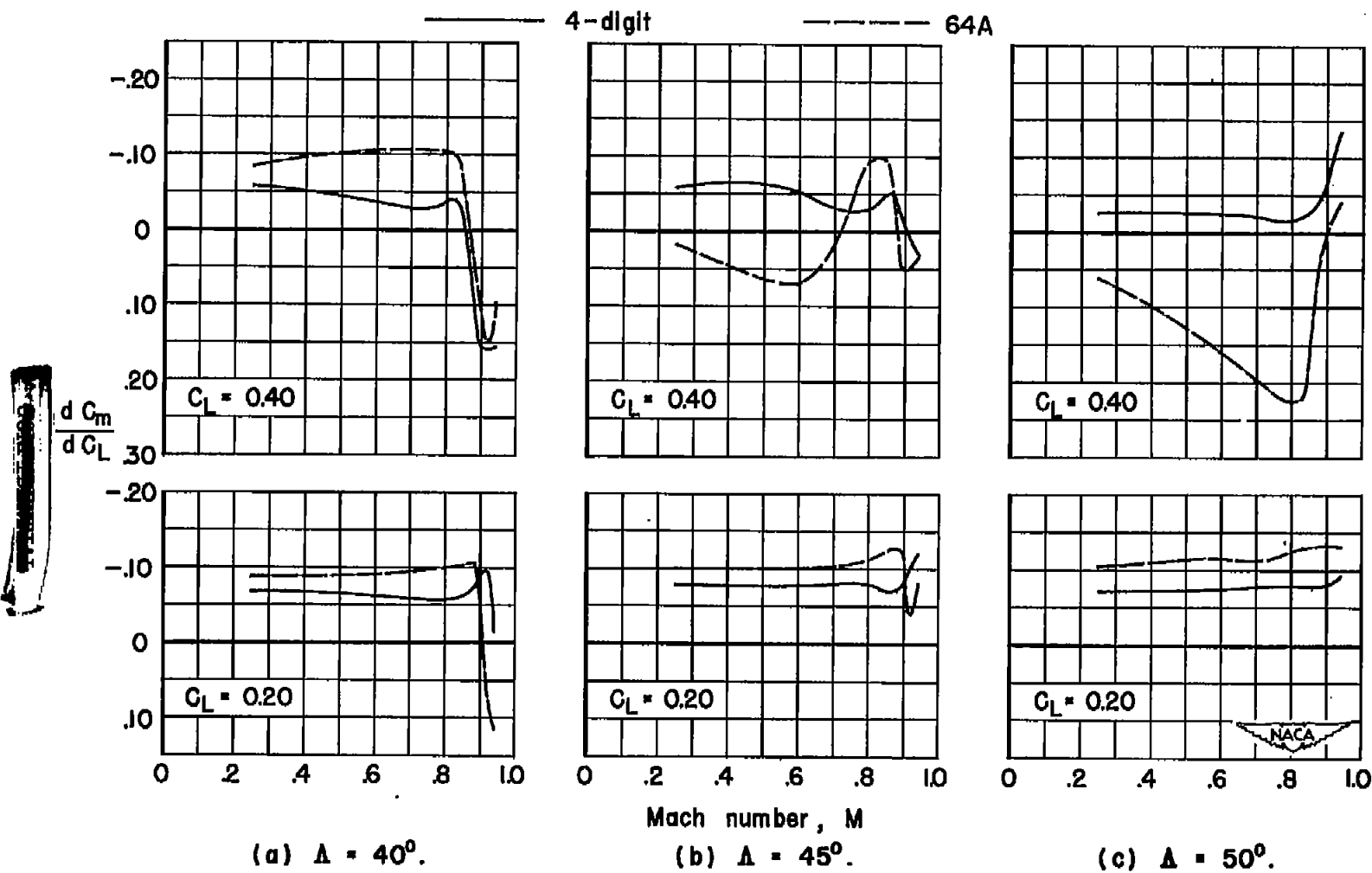


Figure 16.- The variation with Mach number of the pitching-moment-curve slopes of the wings at constant lift coefficients and several angles of sweepback;  $R = 2,000,000$ .

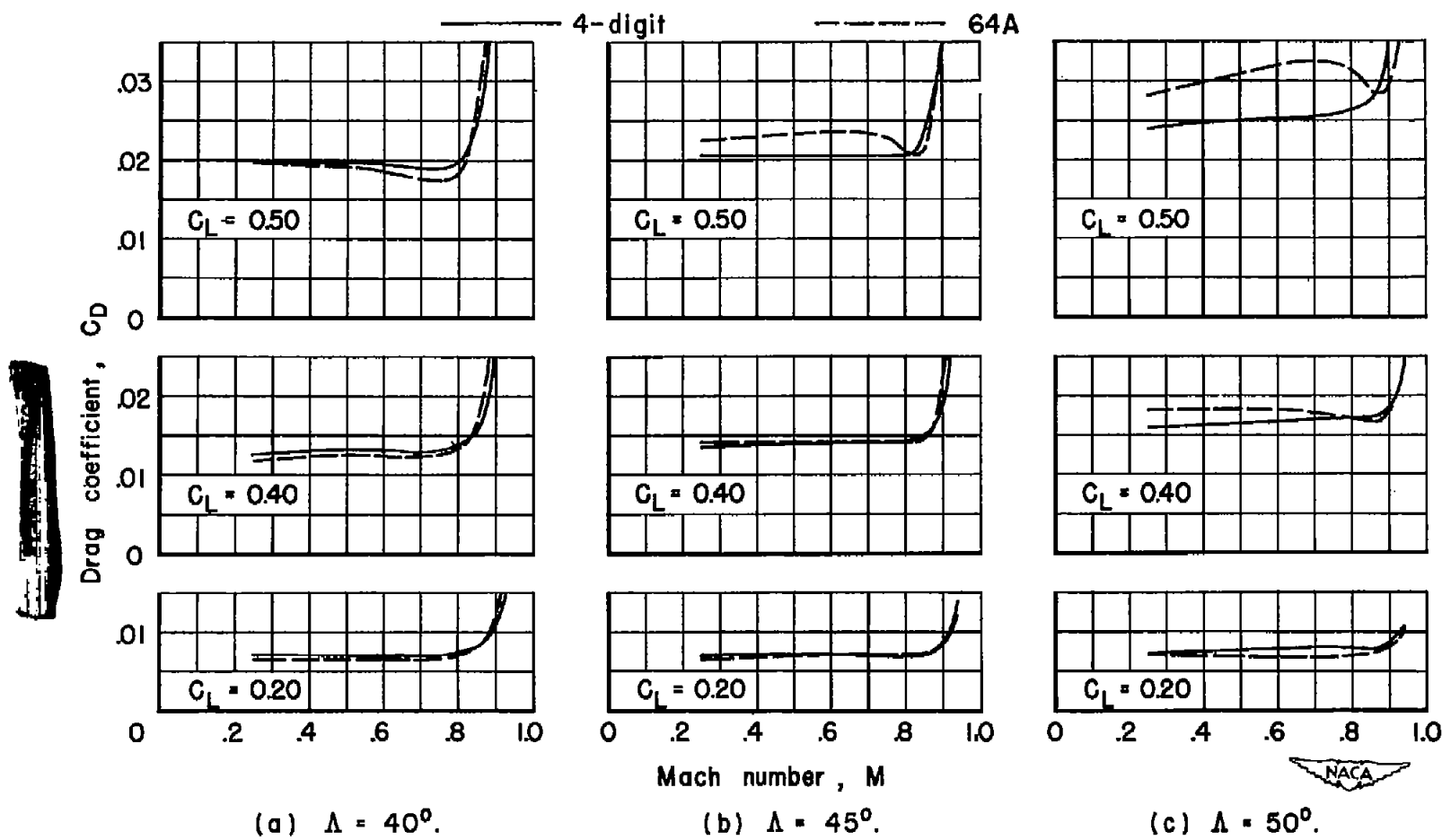


Figure 17.- The variation with Mach number of the drag coefficients of the wings at constant lift coefficients and several angles of sweepback;  $R = 2,000,000$ .

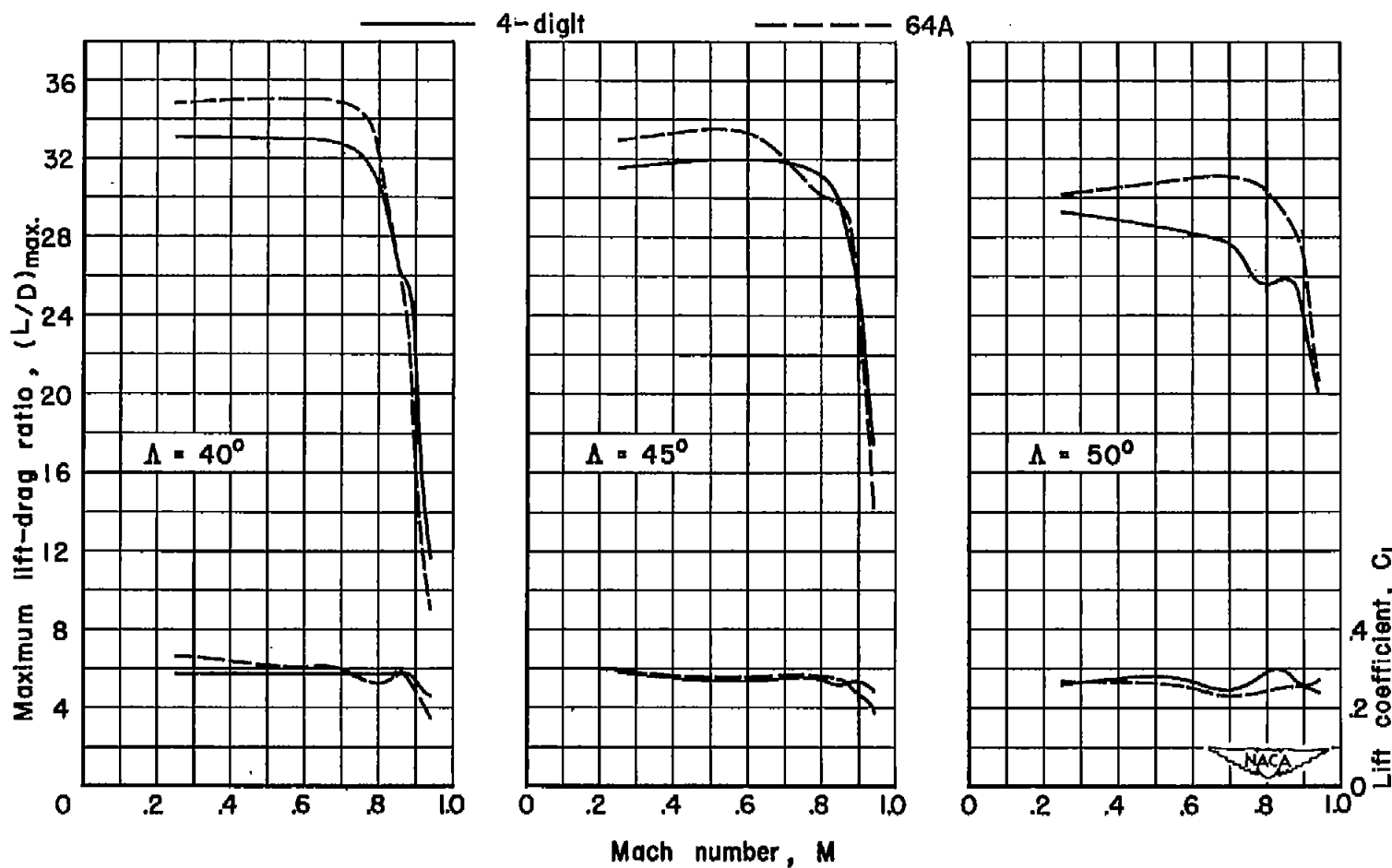
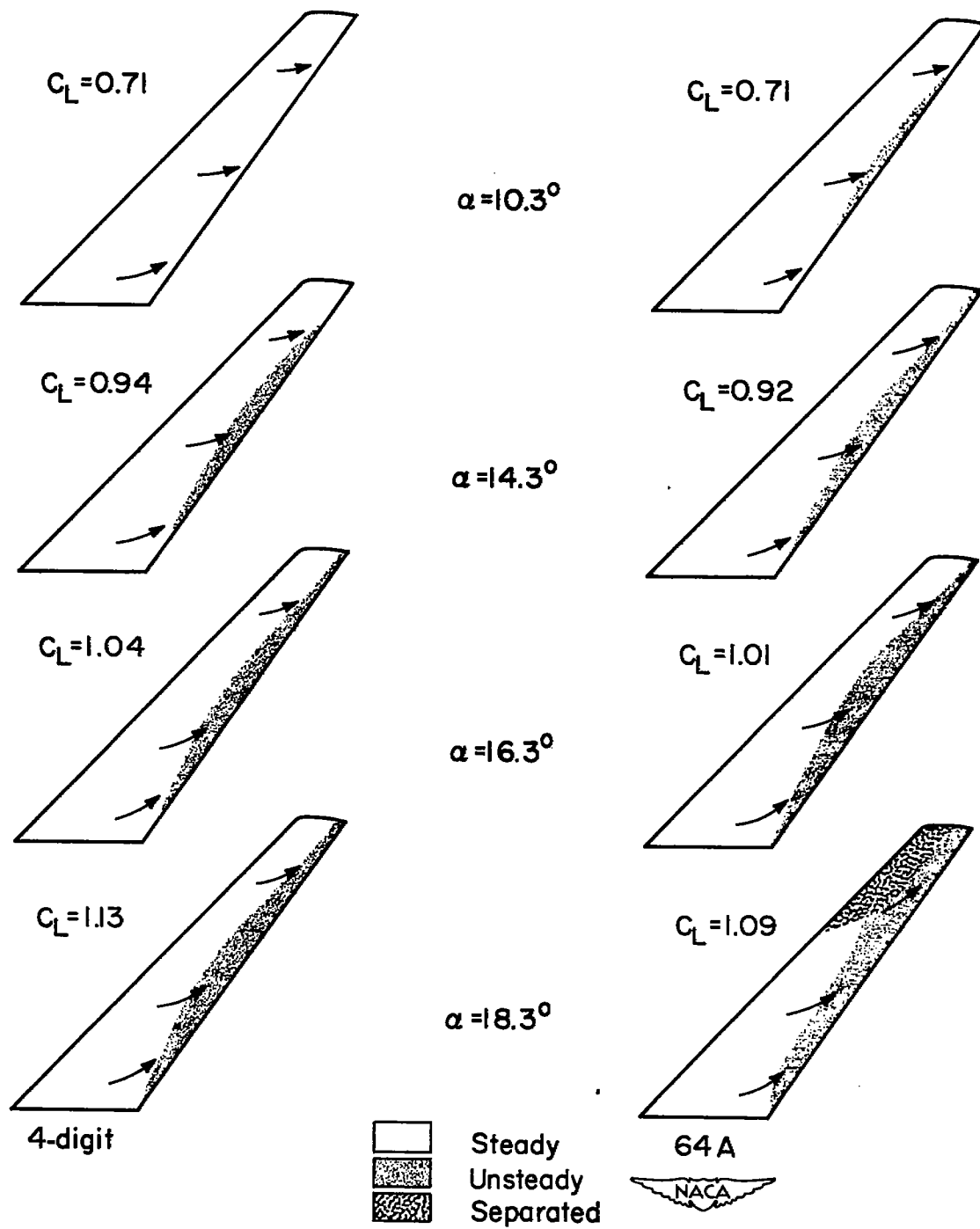


Figure 18.- The variation with Mach number of the maximum lift-drag ratios and the lift coefficients for maximum lift-drag ratios of the wings at several angles of sweepback;  $R = 2,000,000$ .



(a)  $M = 0.165; R = 8,000,000$

Figure 19.- Flow studies on the wings with 40° of sweepback.

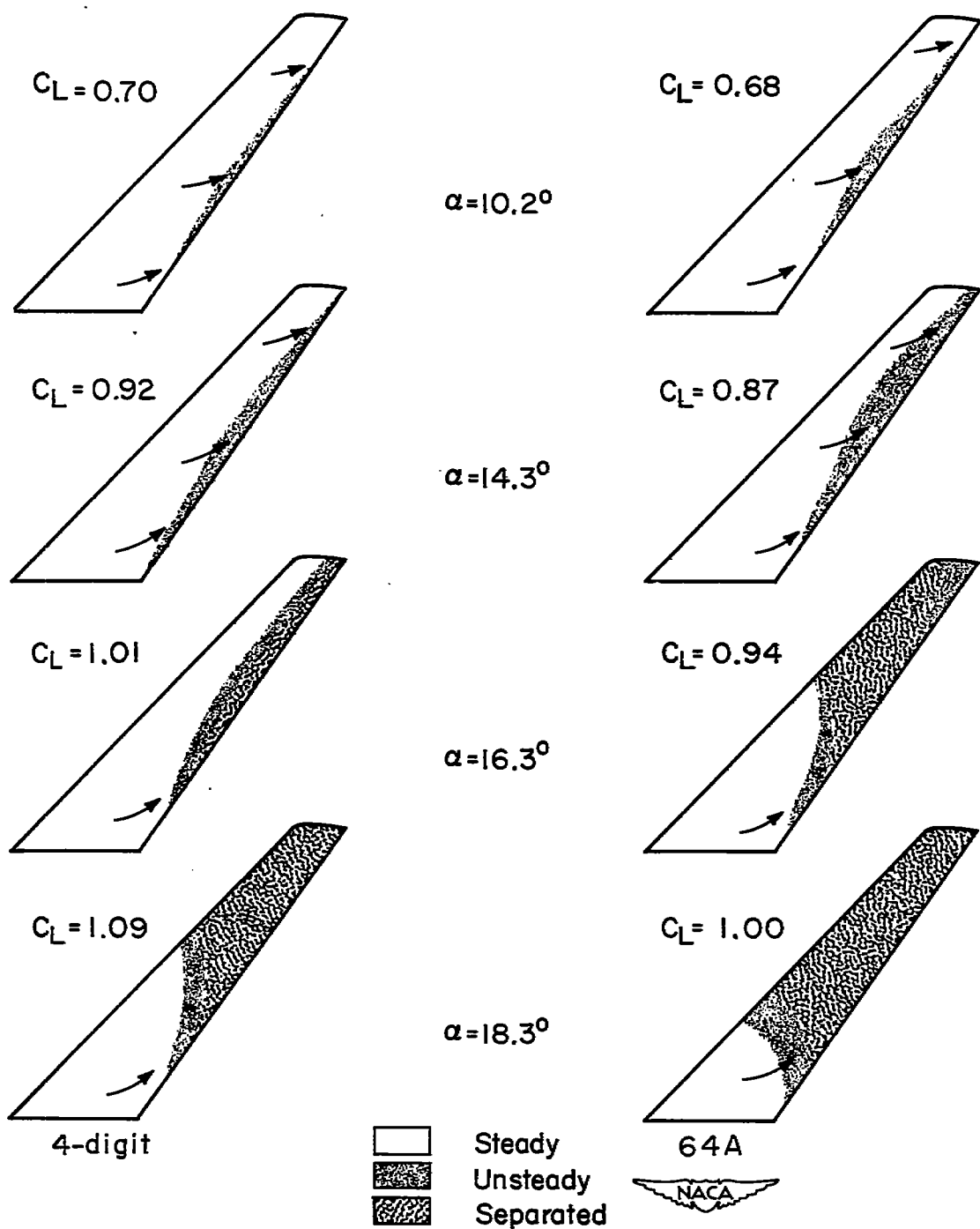
(b)  $M = 0.25; R = 2,000,000$ 

Figure 19.- Continued.

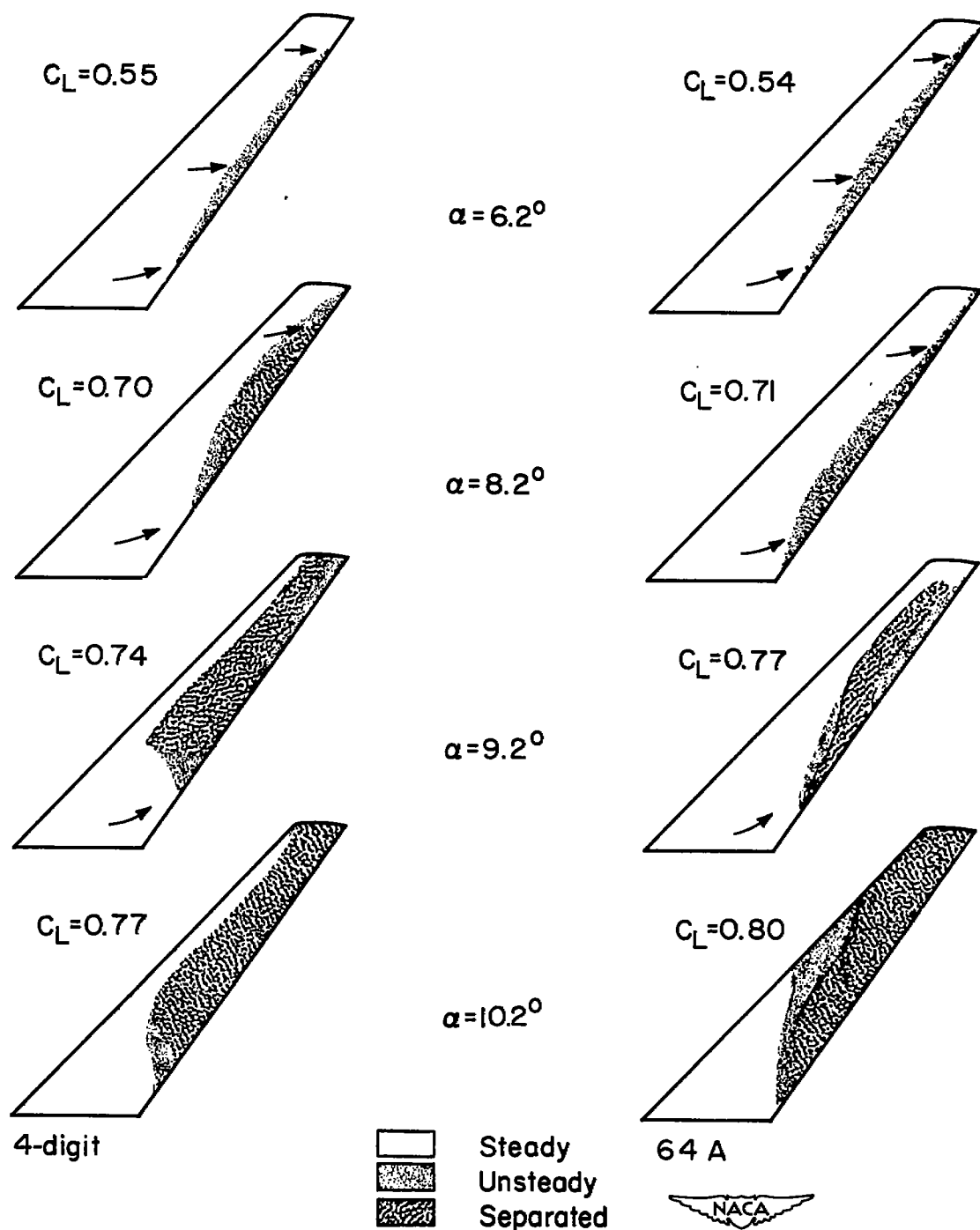
(c)  $M = 0.80; R = 2,000,000$ 

Figure 19.- Continued.

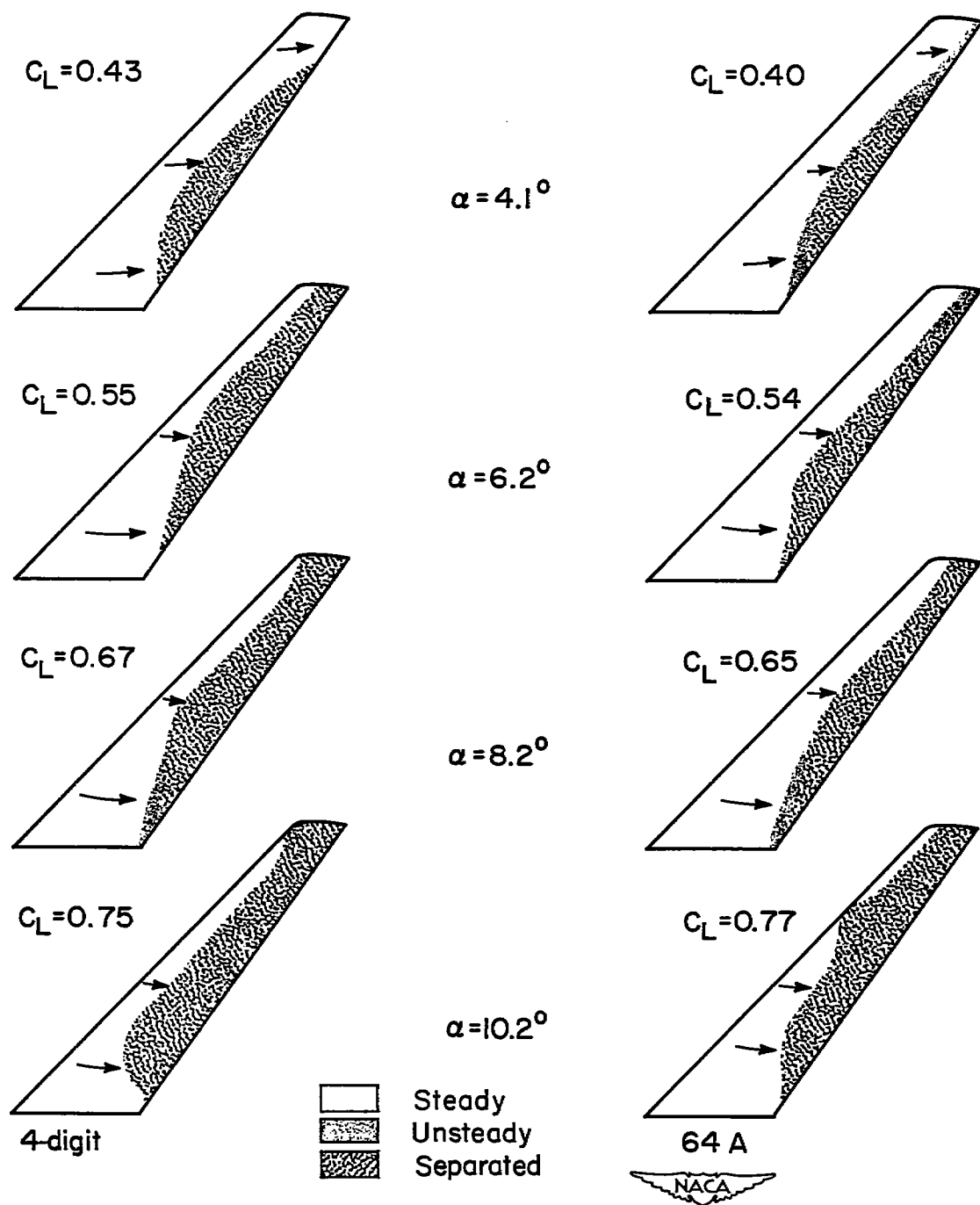
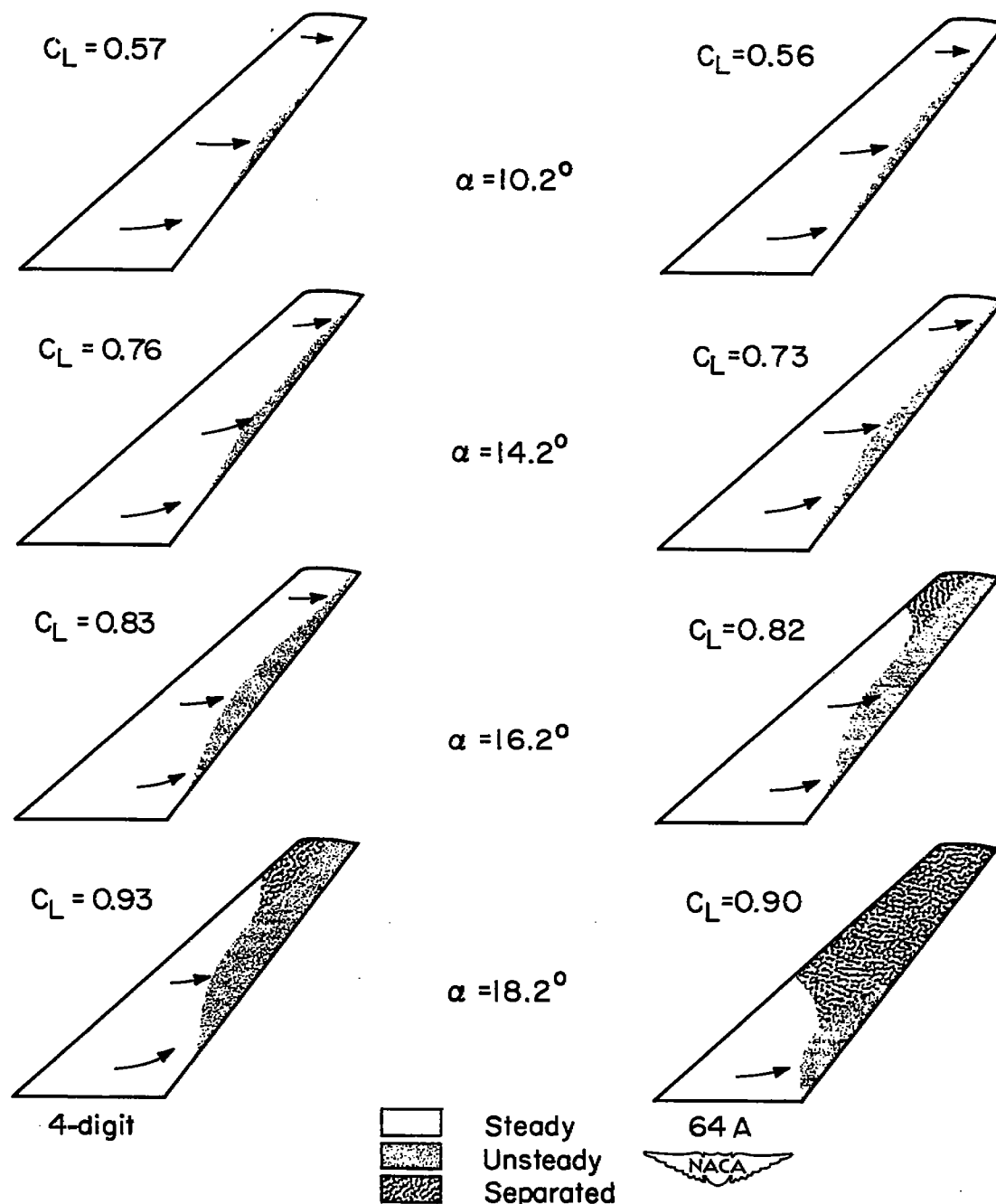
(a)  $M = 0.90; R = 2,000,000$ 

Figure 19.- Concluded.



(a)  $M = 0.165; R = 8,000,000$

Figure 20.- Flow studies on the wings with  $50^\circ$  of sweepback.

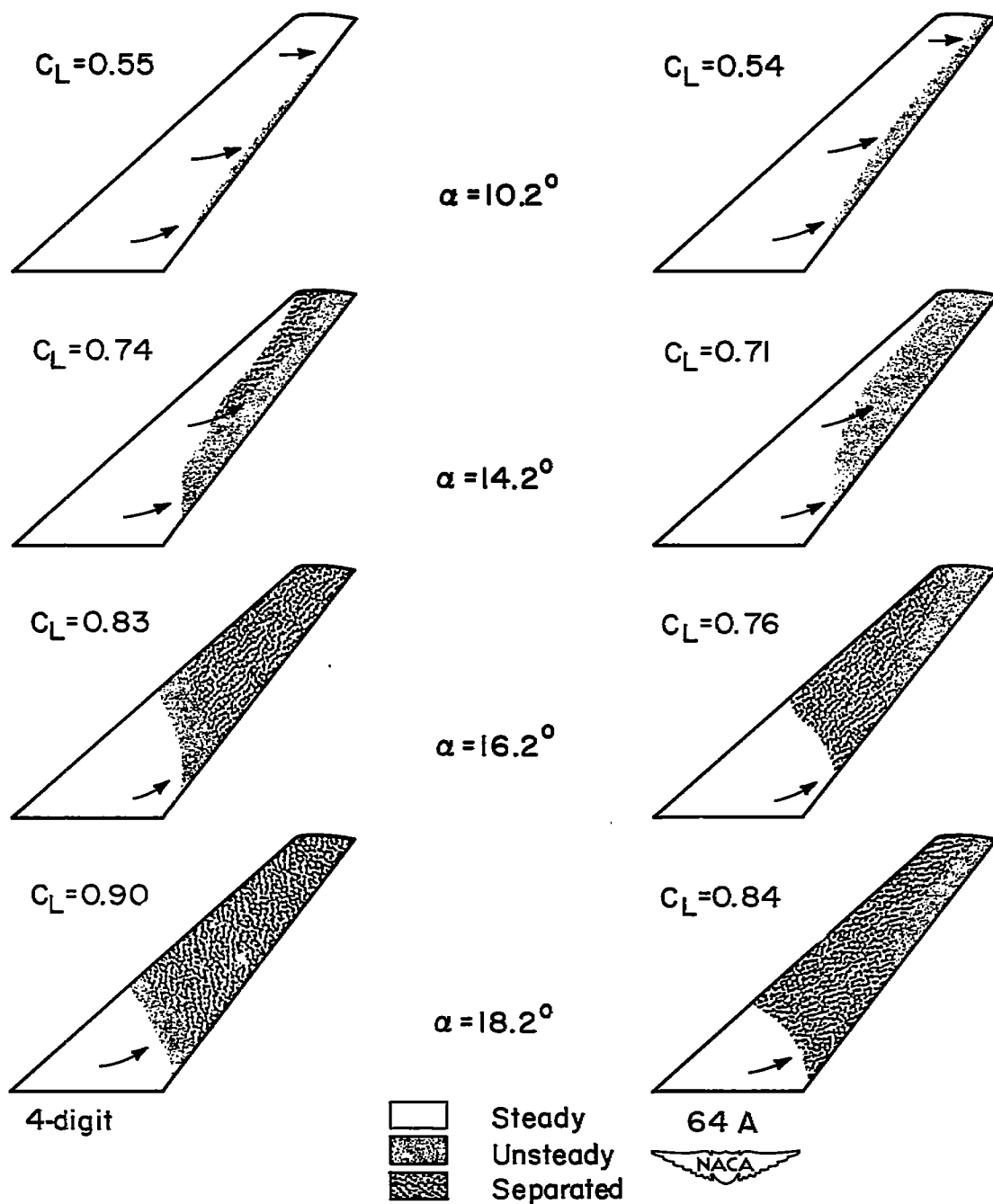
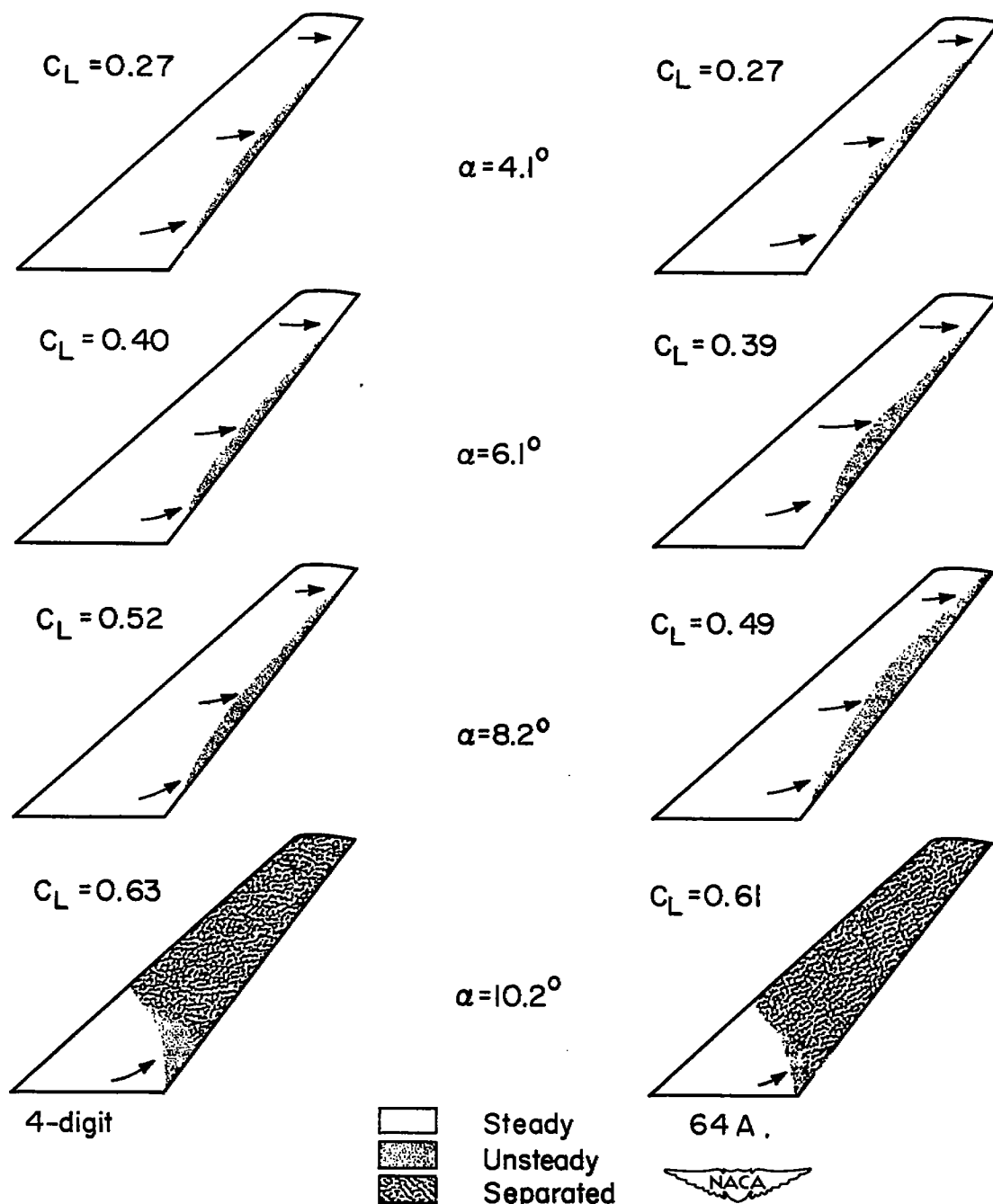
(b)  $M = 0.25; R = 2,000,000$ 

Figure 20.- Continued.



(c)  $M = 0.80$ ;  $R = 2,000,000$

Figure 20.- Continued.

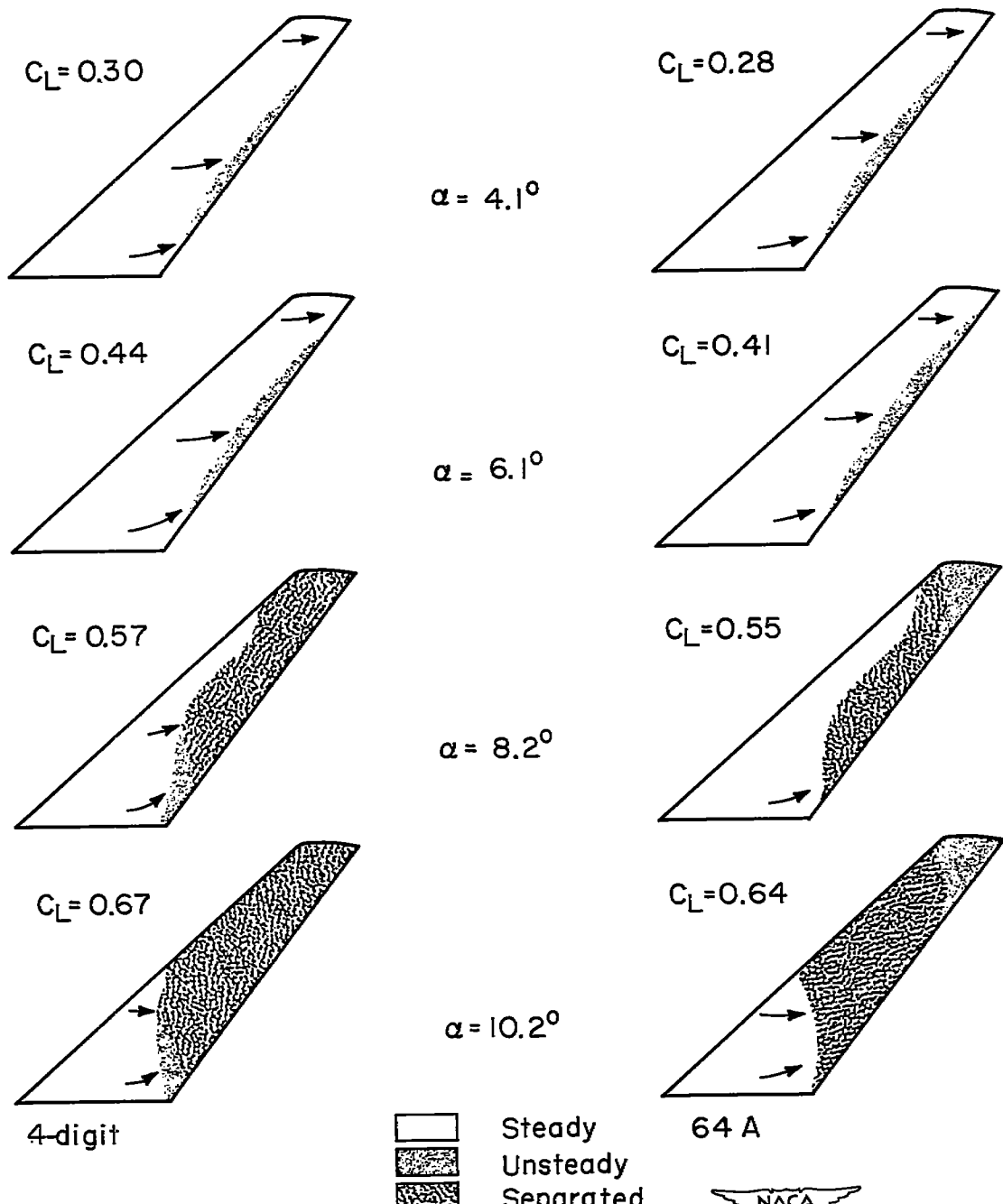
(d)  $M = 0.90$ ;  $R = 2,000,000$ 

Figure 20.- Concluded.

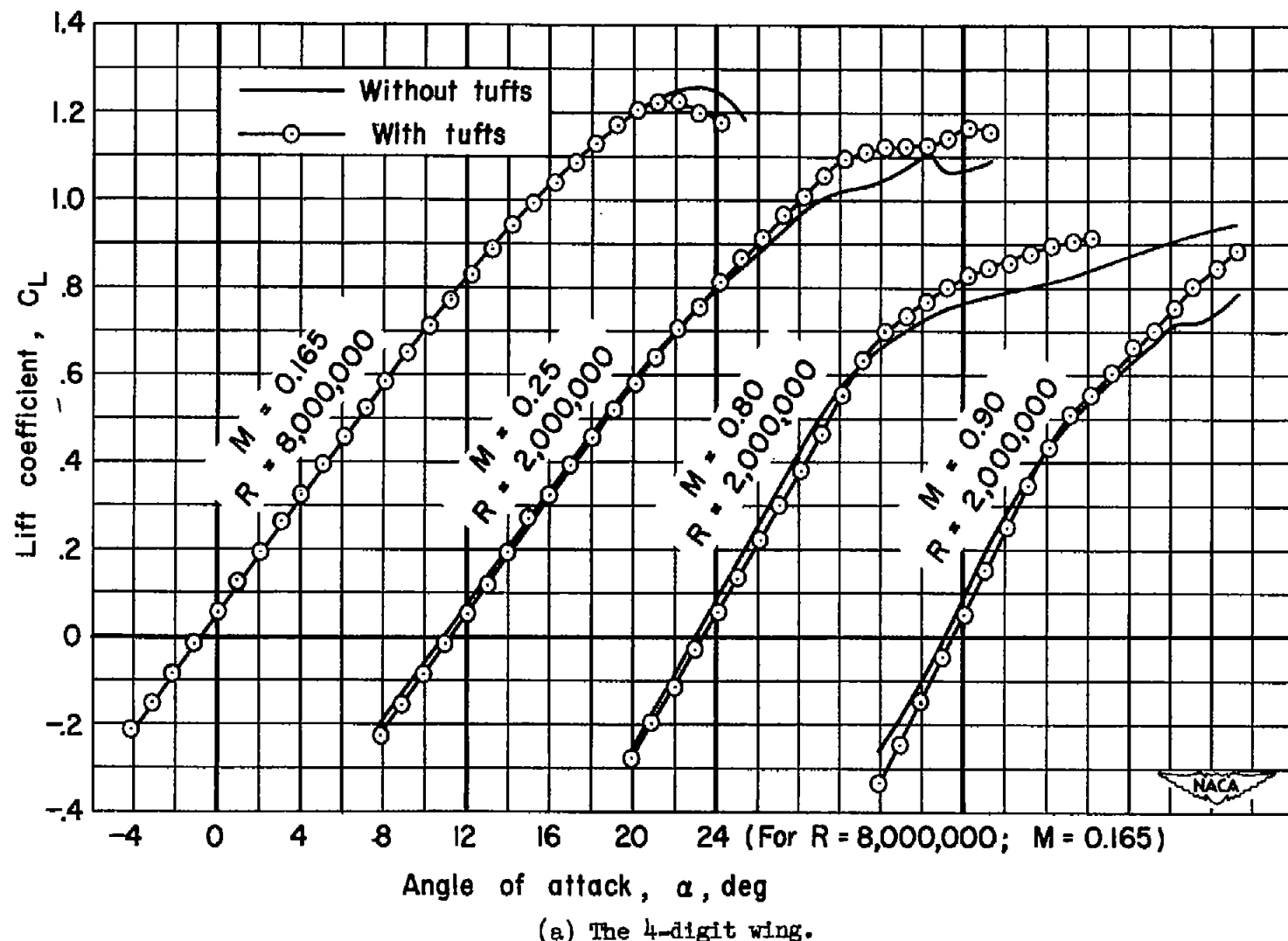


Figure 21.- The effect of tufts upon the lift characteristics of the wings with 40° of sweepback.

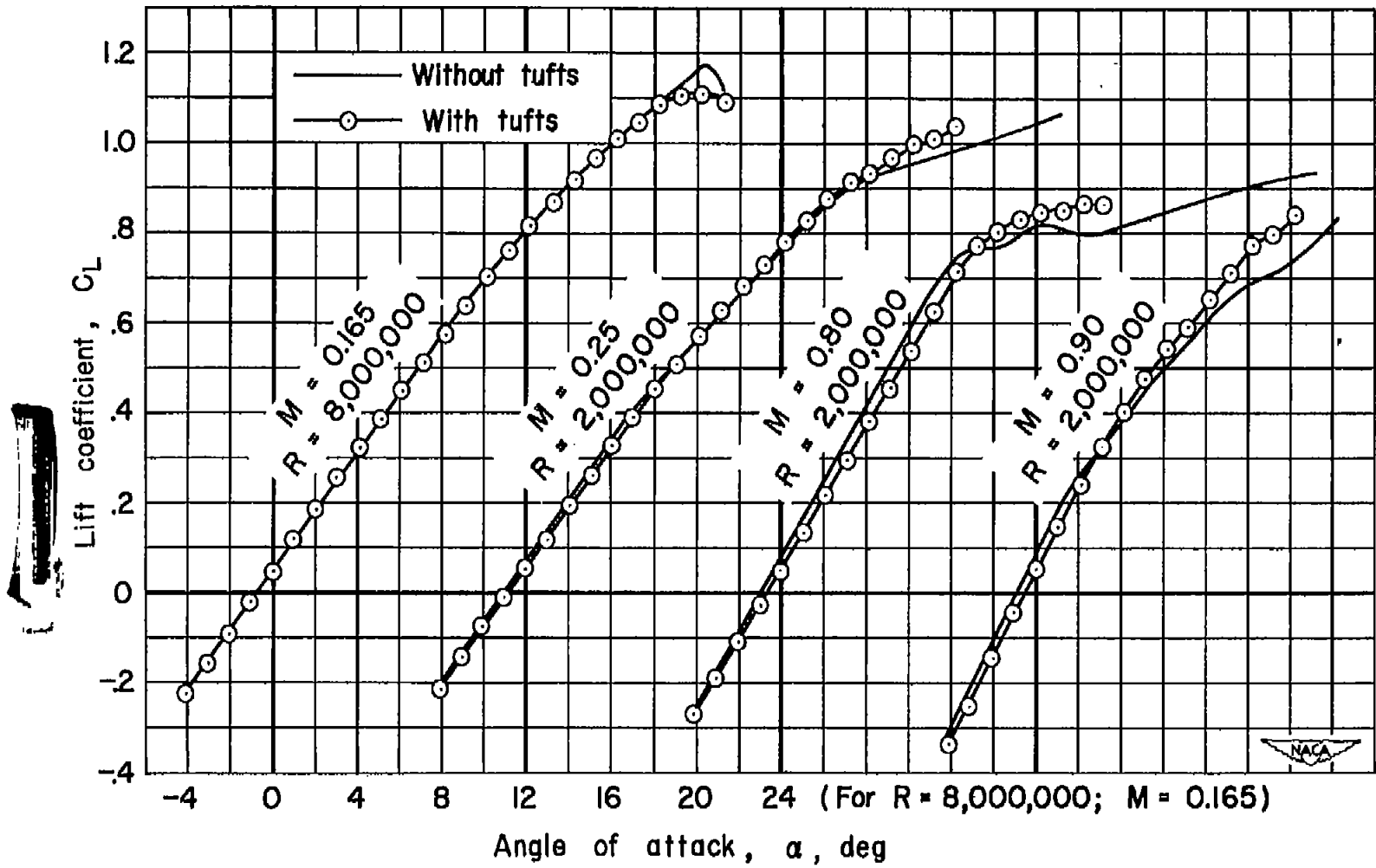
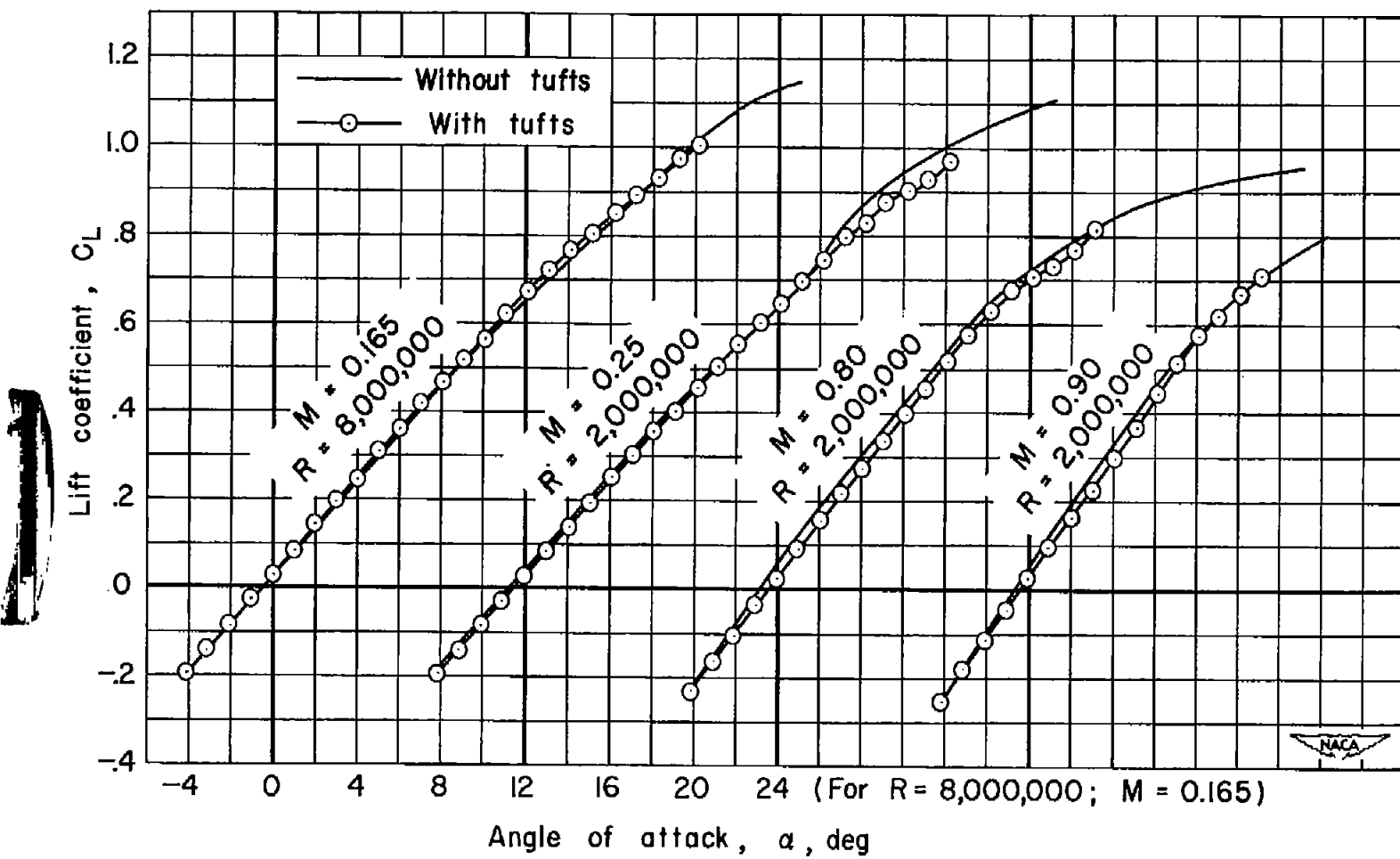
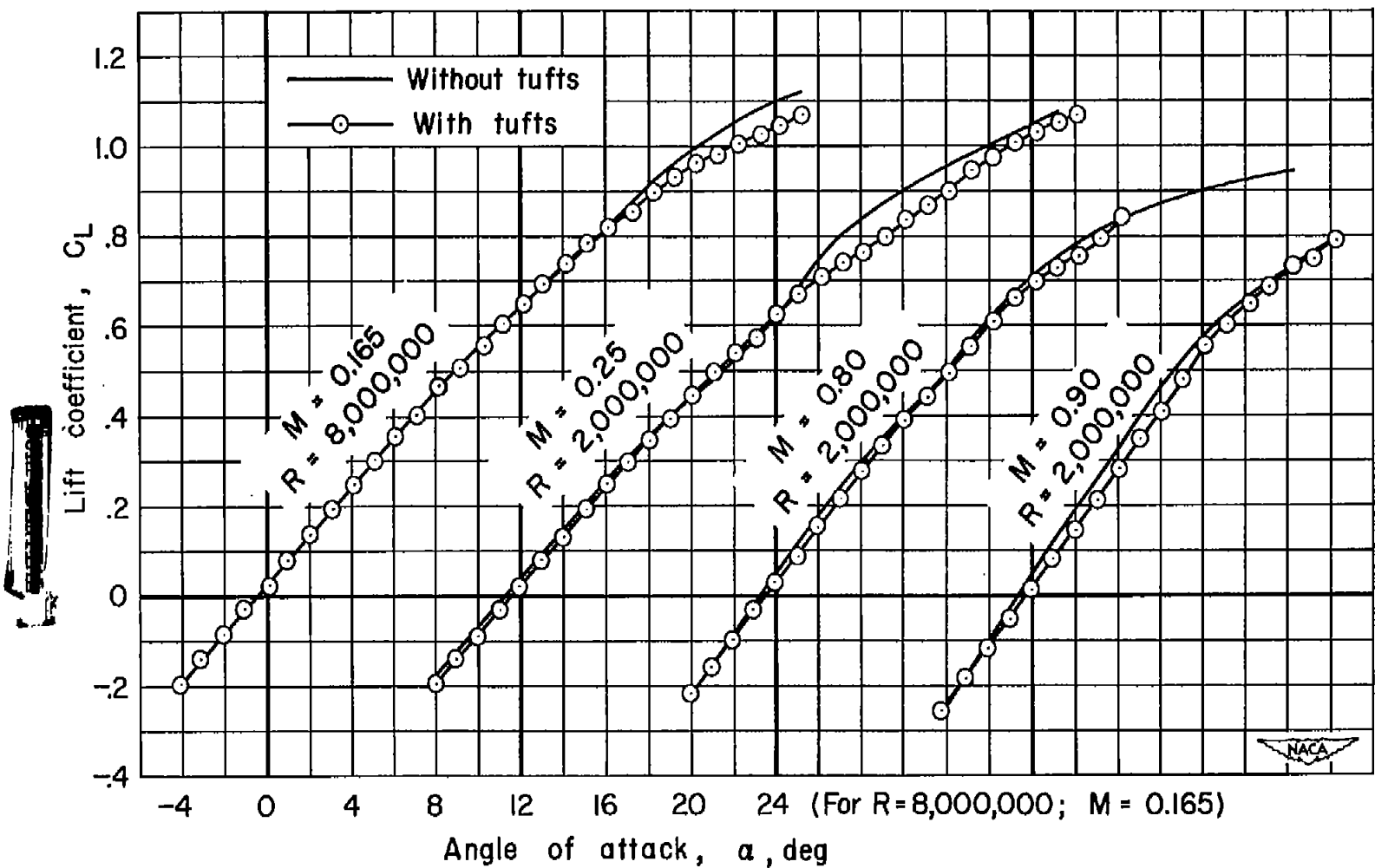


Figure 21.- Concluded.



(a) The 4-digit wing.

Figure 22.- The effect of tufts upon the lift characteristics of the wings with  $50^\circ$  of sweepback.



(b) The 64A wing.

Figure 22.- Concluded.

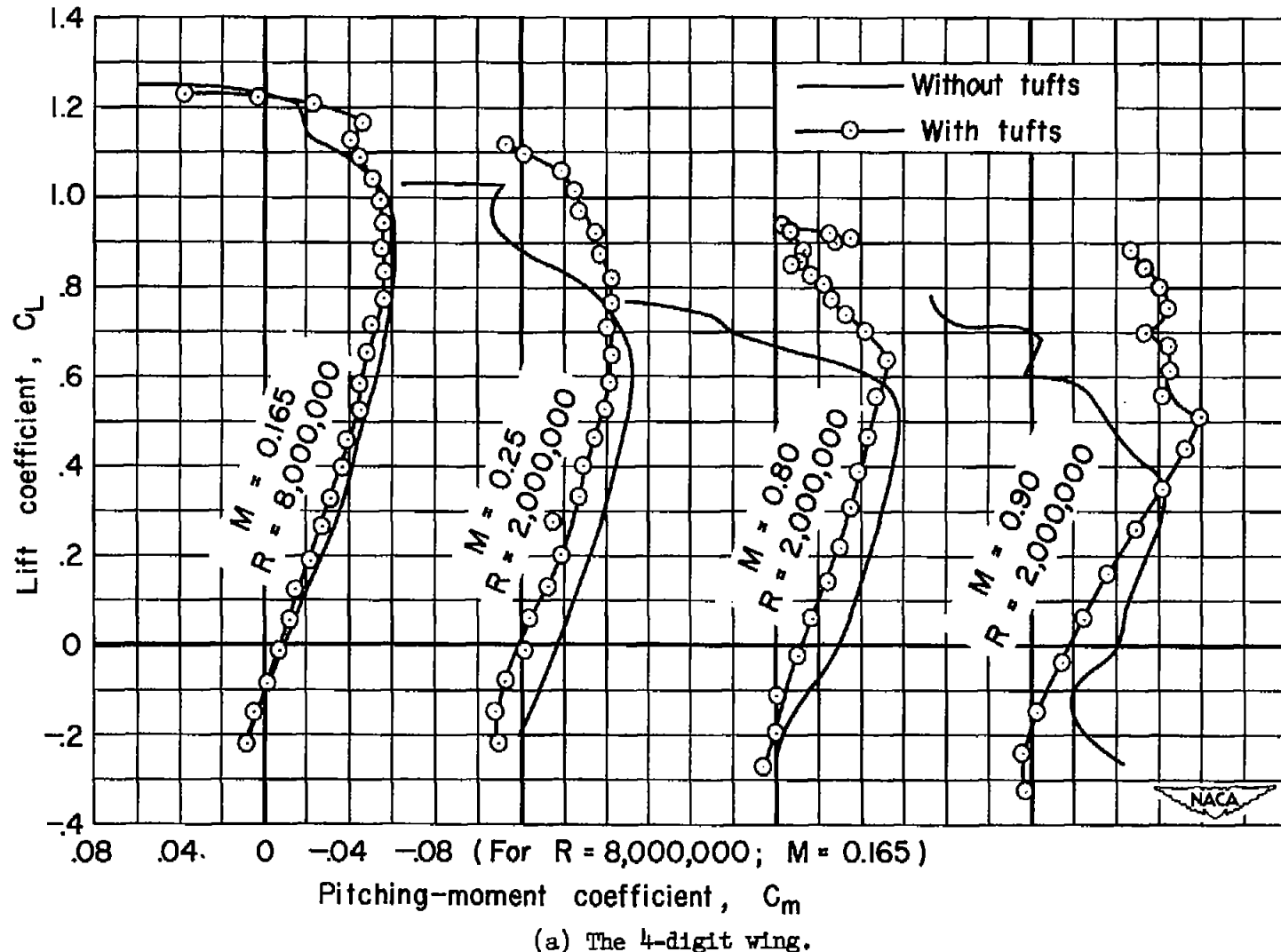
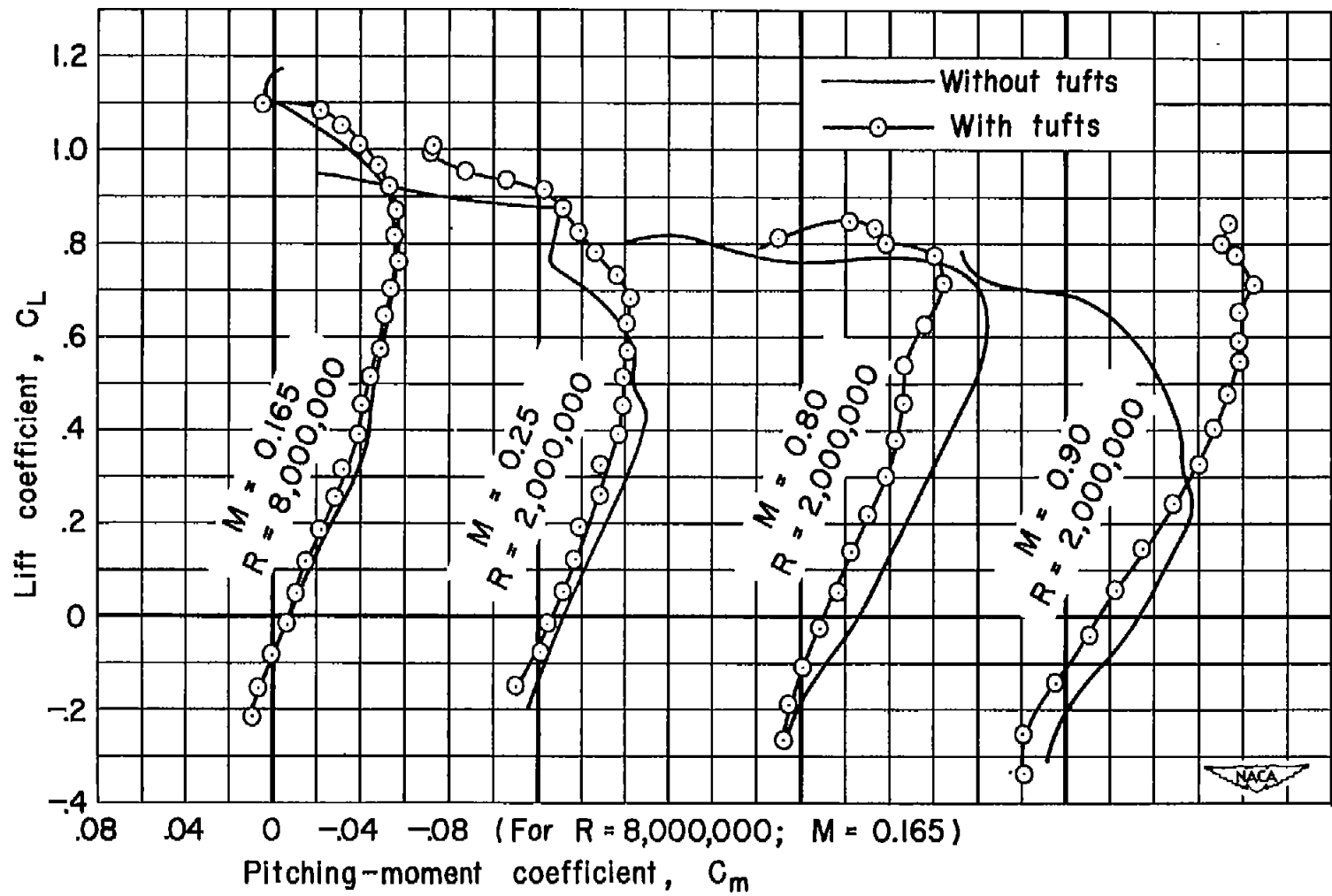
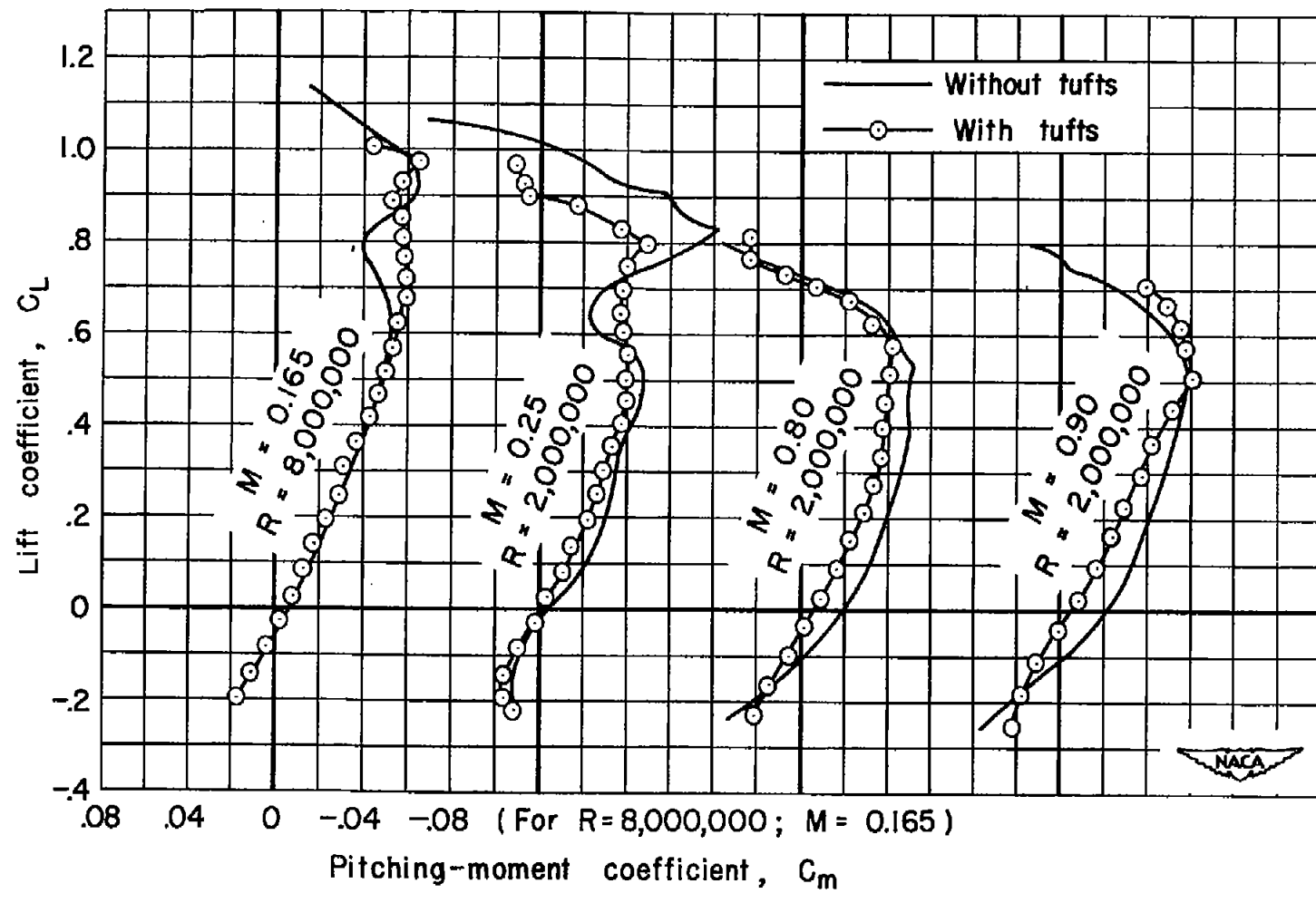


Figure 23.- The effect of tufts upon the pitching-moment characteristics of the wings with  $40^\circ$  of sweepback.



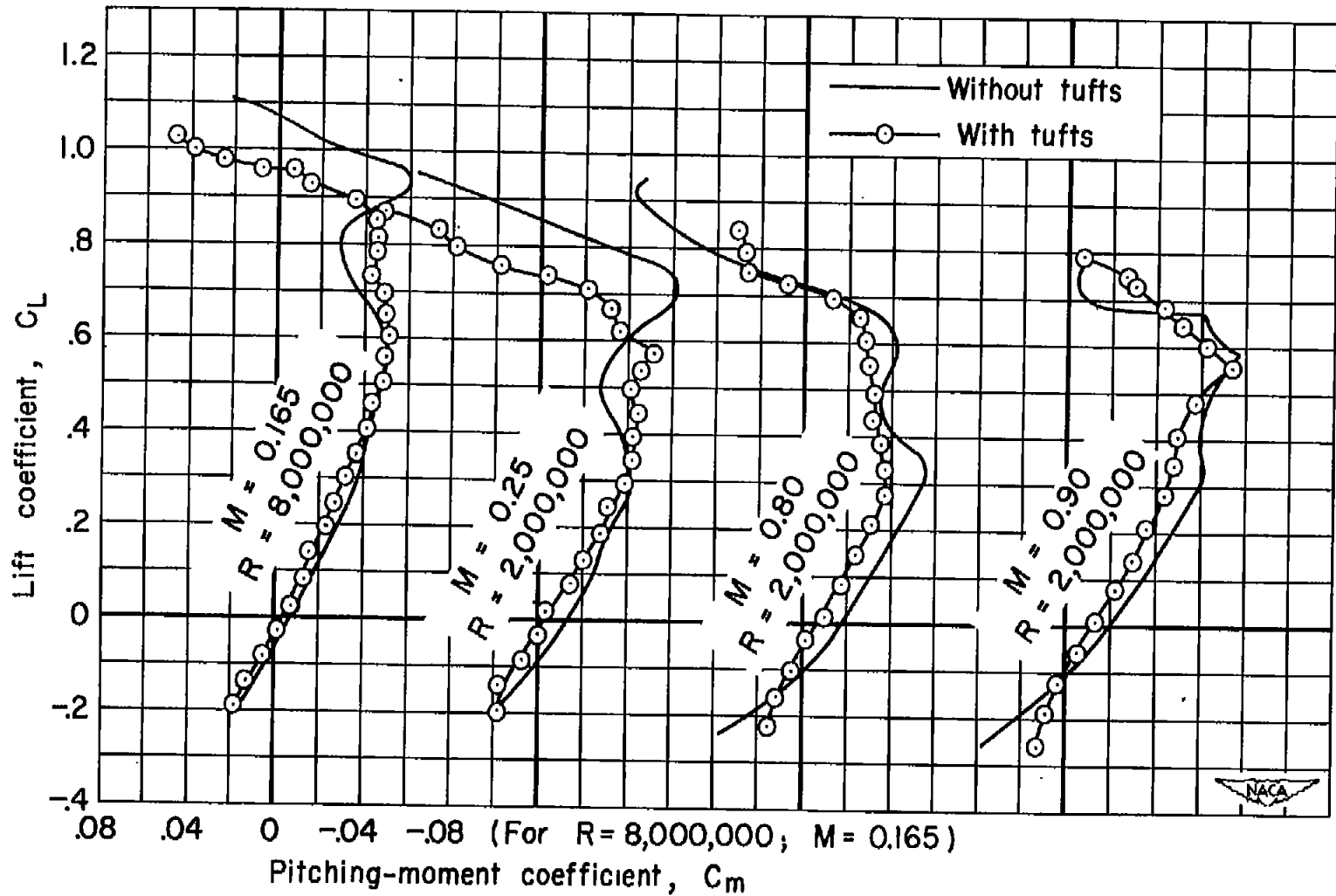
(b) The 64A wing.

Figure 23.- Concluded.



(a) The 4-digit wing.

Figure 24.- The effect of tufts upon the pitching-moment characteristics of the wings with  $50^\circ$  of sweepback.



(b) The 64A wing.

Figure 24.- Concluded.

LANGLEY RESEARCH CENTER



3 1176 01359 8090

**DO NOT REMOVE SLIP FROM MATERIAL**

**Delete your name from this slip when returning material to the library.**

NASA Langley (Rev. Dec. 1991)

**RIAD N-75**